Title
Characterizing Senescence in Astrocytes and its Effect on Neurons

Author
Limbad, Chandani Bhupendrabhai

Publication Date
2017

Peer reviewed|Thesis/dissertation

Characterizing Senescence in Astrocytes and its Effect on Neurons

By

Chandani Bhupendrabhai Limbad

A dissertation submitted in partial satisfaction of the

requirements for the degree of

Doctor of Philosophy

in

Comparative Biochemistry

in the

Graduate Division

of the

University of California, Berkeley

Committee in charge:

Professor Judith Campisi, Chair
Professor Fenyong Liu
Professor Andreas Stahl
Professor Danica Chen

Spring 2017

Characterizing Senescence in Astrocytes and its Effect on Neurons

By

Chandani Bhupendrabhai Limbad

Abstract

Characterizing Senescence in Astrocytes and its Effect on Neurons

By

Chandani Bhupendrabhai Limbad

Doctor of Philosophy in Comparative Biochemistry

University of California, Berkeley

Professor Judith Campisi, Chair

Cellular senescence, characterized by a permanent cell cycle arrest and an inflammatory phenotype called the senescence-associated secretory phenotype (SASP), has been described during aging and various age-related diseases. Neurodegenerative diseases are a major part of age-related diseases. Cognitive decline has been shown to happen in diseases such as Alzheimer's (AD) and in cancer patients after chemotherapy or radiotherapy treatments. Even though there is a link between inflammation and neurodegenerative diseases, there is no in-depth analysis of senescence in the brain. Among various cell types in the brain, astrocytes represent the most abundant population. Astrocytes have proliferative capacity and are essential for neuron survival.

In this study, I first induced senescence in cultured human primary astrocytes using X- irradiation, and determined that astrocytes exhibit various senescence markers including p16, SASP, and downregulation of LMNB1 and HMGB1. Interestingly, as it was particular to senescent (SEN) astrocytes, we detected a downregulation of a specific family of genes, coding for glutamate and potassium transporters, both at the RNA and protein levels. Further we performed unbiased RNA-seq study on non-senescent (NS) and SEN astrocytes to determine the pathways specifically affected in astrocytes. RNA-seq data showed that almost 50% of the genes were upregulated and 50% of the genes were downregulated in SEN astrocytes compared to NS astrocytes. RNA-seq data also confirmed the downregulation of glutamate and potassium transporters upon senescence. These genes are essential for normal astrocyte function in order to maintain homeostasis of neurotransmitter glutamate, potassium ion and water transport, and the strong decrease in their expression in senescent astrocytes suggest a key role of senescence in various brain pathologies.

Further, I performed co-culture assays of neurons and astrocytes in the presence, or the absence, of glutamate to determine whether SEN astrocytes trigger glutamate toxicity and lead to neuronal death. The results showed that SEN astrocytes indeed produced neuronal death in the presence of glutamate.

Then, I analyzed senescence in ten different regions of the mouse brain. For this study, I used six different age groups of C57BL/6 wild type (WT) mice, starting from 2 months to 22 months. Using real-time PCR, I determined variations in the expression of p16, SASP factors, and LMNB1 across the different regions of the mouse brains. The expression of p16 and several SASP factors was upregulated in most of the brain regions during aging.

I also investigated the presence of senescent cells after X-irradiation in vivo in the mouse brain, and detected an upregulation of p16 and SASP expression in brain samples after irradiation. These data suggest that senescence induced in astrocytes may fuel an inflammatory microenvironment in the brain, which would lead to various brain pathologies, and may also lead to brain cancer recurrence after radiotherapy. To test for a potential role of senescence during neurodegenerative diseases, I used the J20 Alzheimer's disease (AD) mouse model. Real-time PCR results showed an upregulation of p16 and SASP factors in the hippocampus and cortex tissues of the J20 mice compared to wild-type (WT) controls. In addition, the hippocampus from J20 mice showed a downregulation of glutamate and potassium transporters in comparison with hippocampus from age-matched WT mice.

Together this project represents a comprehensive study of the senescent phenotype in astrocytes, either grown in culture or in a mouse brain. Overall these results show that senescence can affect the normal function of astrocytes and cause neuronal cell death. Various mouse models, including natural aging, radiation therapy and AD, are showing the presence of senescent cells and suggest a deleterious role of these cells. Therefore, these findings may open up novel ways to develop treatments for brain diseases.

Dedicated to my parents,

Mr. Bhupendrabhai Harilal Limbad and Mrs. Hansaben Bhupendrabhai Limbad

Contents

List of Figures

List of Tables

Nomenclature

AD	Alzheimer's disease
ALS	Amyotrophic lateral sclerosis
AQP4	Aquaporin-4
BBB	Blood–brain barrier
CM	Conditioned media
CXCL-1	Chemokine (C-X-C motif) ligand 1
CXCL-10	Chemokine (C-X-C motif) ligand 10
DAPI	4',6-diamidino-2-phenylindole
DDR	DNA damage response
DMSO	Dimethyl sulfoxide
DNA-SCARS	DNA segments with chromatin alterations reinforcing senescence
DOXO	Doxorubicin
EAAT1	Excitatory amino acid transporter 1
EAAT2	Excitatory amino acid transporter 2
ELISA	Enzyme-linked immunosorbent assay
GBM	Glioblastomas
GFAP	Glial fibrillary acidic protein
GLAST	GLutamate aspartate transporter

GLT-1	Glutamate transporter 1
GS (GLUL)	Glutamine synthetase
HMGB1	High mobility group box 1
IL-1B	Interleukin 1 beta
IL-6	Interleukin 6
IL-8	Interleukin 8
IR	Irradiation induced senescent samples
IR1 to IR21	Day 1 to Day 21 after irradiation
J20	hAPP transgenic mouse model for AD
Kir4.1	ATP-sensitive inward rectifier potassium channel 10
LMNB1	Lamin B1
MEFs	Mouse embryonic fibroblasts
MMP-3	Matrix metalloproteinase-3
NMDA	N-methyl-D-aspartate
NS	Non-senescent
P16	Cyclin-dependent kinase inhibitor 2A
P16-3MR	Trimodality reporter
PBS	Phosphate-buffered saline
PD	Parkinson's disease
RNA-Seq	RNA sequencing
RT-PCR	Reverse transcription polymerase chain reaction
SA-β-Gal	Senescence-associated beta-galactosidase
SASP	Senescence-associated secretory phenotype

SEN	Senescent
TGF-a	Transforming growth factor alpha
TMZ	Temozolomide
WT	Wild-type

Acknowledgments

I would like to express my heartfelt gratitude to all who have been part of my graduate school journey. First and foremost, I thank my mentor, Dr. Judith Campisi, for providing me an opportunity and support to work under her guidance to pursue the Ph.D. degree. Judy is an expert in the field of senescence and aging, to get trained under her guidance has been a very uplifting experience. Judy's knowledge, enthusiasm, and passion for science is extremely motivating. This journey has instilled me with tools and strength necessary for achieving my future goals. None of these would have been possible without Judy.

My sincere thanks to my thesis committee members, Dr. Fenyong Liu, Dr. Andreas Stahl, and Dr. Danica Chen for their incredible support and advice throughout my Ph.D. It was amazing to realize how much they cared about my progress and success. I would also like to thank Dr. Sangwei Lu for being on my qualifying exam committee. Such knowledgeable and compassionate mentors have kept me focused on my goal. I am extremely thankful to the Department of Comparative Biochemistry at University of California, Berkeley for the most rewarding experience in my academic progress.

Getting a Ph.D. from one of the world's top university was my dream. Today, when I am finishing my Ph.D. from UC Berkeley; it feels surreal. It would not have been possible without the support of my family, friends and most importantly Dr. Pierre Desprez. Pierre has been a boss, a mentor, a colleague, a guide but above all, he is like a father figure. Pierre has helped me to nurture my career in the USA by giving me continuous guidance since 2009 till date. Specifically for Ph.D., right from the beginning he helped me to strengthen and prepare my application for Ph.D. admission, he introduced me to Judy and now at the end he did final edits on my thesis. Thus has been his support! How incredible is that! I feel lucky to know such a wonderful person. I also want to thank Dr. Sean McAllister, who has taken out time to give me advice whenever I needed. Thank you so much for those selfless and very much needed advices.

Friends, the building blocks of my life, this journey would have been impossible without any of you. My whole NYC club (Jagruti Chaudhari, Shruti Nayak, Parita Patel, Jinal Patel, Jigar Patel, Archit Patel), Minal Patel, Aruna Kumavat, Ira Tyagi, Anna Desai, Reetika Jain, Neha Mehta, Priyanka Khemka– each of you have been an important wheel so that I was able to roll on this journey and finally reached the destination! Cannot thank you enough for being there any day any time! Special thanks to my lab buddy, Fatouma Alimirah. Thank you so much for continuous motivation and all your help whenever I needed. Thank you for those long phone calls, dinners till midnights and your incredible friendship. I would also like to thank a senior classmate at UC Berkeley, Chun-Han Lin, for sharing his experience every semester, which made my journey smoother. I would like to thank lab members, Michael Velarde, Su Liu and Chisaka Kuehnemann, for always making the lab lively place to work together.

My family members, especially, Trupti Parmar, Maitrayi Pithadiya, Dipti Parmar, Nitin Limbad, Hitaxi Pthadiya, Ashok Pithadiya, Ankita Limbad, Vaishali Limbad, are my real strength. It is not possible to verbalize all the support you provided for this long journey. I must have done some magnificent Karmas to be part of this family! My Ph.D. belongs to you.

And above all are my parents, Mr. Bhupendrabhai Limbad and Mrs. Hansaben Limbad. My parents are the simplest, down to earth yet intellectually very modern and wonderful people. Despite any financial challenges or being surrounded by conservative society, they have given me wings to fly free and achieve my dreams. My mother has been a constant source of strength and love. I derive my patience and perseverance from my mother. My father always taught us, " Nishaan Chuk Maaf, Pan Nahi Maaf Nichu Nishaan", (a Gujarati proverb), meaning, "It's ok if you miss the higher goal, but never set lower goals". He taught us to dream big and work hard with honesty. I strive to follow these principles and hope to continue them with my parent's blessings.

Chapter 1: Introduction

1.1 What is senescence?

Cellular senescence was first identified by Hayflick et al. as an intrinsic process that halts the proliferation of normal cells (Hayflick 1965; Campisi 2005). Thus, cellular senescence refers to the essentially irreversible growth arrest that occurs when cells that can divide encounter oncogenic stress. With the possible exception of embryonic stem cells (Miura, Mattson, and Rao 2004), most division-competent cells, including some tumor cells, can undergo senescence when appropriately stimulated (Shay and Roninson 2004; Campisi and d'Adda di Fagagna 2007).

1.2 What causes cellular senescence?

There are many stimuli that induce senescence. Telomere erosion, the gradual loss of DNA at the ends of chromosomes (telomeres), leads to the limited growth of human cells in culture. Telomeric DNA is lost with each S phase because DNA polymerases are unidirectional and cannot prime a new DNA strand, resulting in loss of DNA near the end of a chromosome. In addition, most cells do not express telomerase, the specialized enzyme that can restore telomeric DNA sequences de novo (Harley, Futcher, and Greider 1990; Bodnar et al. 1998). The persistent DNA damage response (DDR) is generated by the eroded telomeres and genomic damage at nontelomeric sites, which initiates and maintains the senescence growth arrest (d'Adda di Fagagna et al. 2003; Takai, Smogorzewska, and de Lange 2003; Herbig et al. 2004; Nakamura et al. 2008; Rodier et al. 2009; Rodier and Campisi 2011). DNA double strand breaks are also one of the prominent senescence inducers ((Di Leonardo et al. 1994). In addition, compounds such as histone deacetylase inhibitors, which relax chromatin without physically damaging DNA, activate the DDR proteins ataxia telangiectasia mutated (ATM) and the p53 tumor suppressor (Bakkenist and Kastan 2003), and induce a senescence response (Ogryzko et al. 1996; Munro et al. 2004). Many strong mitogenic signals, such as those delivered by certain oncogenes or highly expressed pro-proliferative genes also lead to senescence (Serrano et al. 1997; Lin et al. 1998; Zhu et al. 1998; Dimri et al. 2000). Mitogenic signals can misfire replication origins and collapses replication fork, which can create DNA damage and a persistent DDR (Bartkova et al. 2006; Di Micco et al. 2006; Mallette, Gaumont-Leclerc, and Ferbeyre 2007).

Senescence can also occur without detectable DDR signaling or significant telomere erosion by loss of the PTEN tumor suppressor, a phosphatase that counteracts pro-proliferative/pro-survival kinases (Alimonti et al. 2010). In addition, ectopic expression of the cyclin-dependent kinase inhibitors (CDKis) such as p21WAF1 and p16INK4a, cause senescence without an obvious DDR (McConnell et al. 1998; Rodier et al. 2009). Other than these stimuli, a cell culture stress can also lead to senescence for which the natural and in vivo equivalents are unknown (Ramirez et al. 2001). These stresses include inappropriate substrata, serum and oxidative stress (Fusenig and Boukamp 1998; Yaswen and Stampfer 2002; Parrinello et al. 2003).

1.3 Markers of senescence

There are no specific marker or hallmark of senescence identified thus far for the senescent state. Senescent cells are different than quiescent or terminally differentiated cells. However, since there is not one specific marker for senescence, the identification of senescent cells is not straightforward. There is a combination of markers, which together are assigned to identify senescent cells (Figure 1) but interestingly not all the senescent cells express all possible senescence markers.

Following are the combination of markers to identify senescent cells:

- Permanent growth arrest that cannot be reversed by known physiological stimuli.
- Increase in size, sometimes enlarging more than twofold relative to the size of non-senescent counterparts (Hayflick 1965).
- Expression of the senescence-associated B-galactosidase (SA-β-gal) (Dimri et al. 1995), which partly reflects the increase in lysosomal mass (Lee et al. 2006).
- Expression of p16INK4a, which is not commonly expressed by quiescent or terminally differentiated cells (Alcorta et al. 1996; Hara et al. 1996; Serrano et al. 1997; Brenner, Stampfer, and Aldaz 1998; Stein et al. 1999).
- DNA segments with chromatin alterations reinforcing senescence (DNA-SCARS).
- Secretion of growth factors, proteases, cytokines, and other factors that have potent autocrine and paracrine activities (Acosta et al. 2008; Coppe et al. 2008; Coppe et al. 2010; Kuilman et al. 2008). This secretome is named the senescence-associated secretory phenotype (SASP).

Interestingly, even though permanent growth arrest is a marker of senescent cells, when these cells do not express the CDKi p16INK4a, they are capable of resuming growth after genetic interventions that inactivate the p53 tumor suppressor (Beausejour et al. 2003). However, there is no evidence that spontaneous p53 inactivation occurs in senescent cells in culture or in vivo. The p16INK4a tumor suppressor is induced by culture stress and as a late response to telomeric or intrachromosomal DNA damage (Brenner, Stampfer, and Aldaz 1998; Robles and Adami 1998; Ramirez et al. 2001; te Poele et al. 2002; Jacobs and de Lange 2004; Le et al. 2010). In some cells, p16INK4a causes formation of senescence-associated heterochromatin foci (SAHF), which silence critical pro-proliferative genes (Narita et al. 2003). It has been published that in mice and humans p16INK4a expression increases with age, which leads to the reduction in progenitor cell number that occurs in multiple tissues during aging (Zindy et al. 1997; Nielsen et al. 1999; Krishnamurthy et al. 2004; Ressler et al. 2006; Liu et al. 2009; Janzen et al. 2006; Krishnamurthy et al. 2006; Molofsky et al. 2006). Cells that senesce with persistent DDR signaling express persistent nuclear foci, termed DNA segments with chromatin alterations reinforcing senescence (DNA-SCARS). These foci contain activated DDR proteins, including phospho-ATM and phosphorylated ATM/ataxia telangiectasia and Rad3 related (ATR) substrates (d'Adda di Fagagna et al. 2003; Herbig et al. 2004; Rodier et al. 2009), and are distinguishable from transient damage foci (Rodier and Campisi 2011). DNA-SCARS include dysfunctional telomeres or

telomere dysfunction–induced foci (TIF) (d'Adda di Fagagna et al. 2003; Takai, Smogorzewska, and de Lange 2003; Herbig et al. 2004; Kim et al. 2004).

1.4 Senescence in aging

Positive effects of senescence and SASP (Figure 1.2)

Senescence was initially considered as a tumor-suppressive mechanism (Hayflick 1965), and this aspect has been very well studied in the past several decades. However, other than tumor-suppression, any other beneficial aspect of senescence was not investigated until recent years.

Another aspect includes the role of senescent cells in facilitating tissue repair. Acute liver injury leads hepatic stellate cells to proliferate and produce extracellular matrices to repair the damage. After the damage is repaired, these stellate cells undergo senescence. If some of the cells continue to proliferate instead of undergoing senescence, they produce excessive extracellular matrix (ECM) leading to tissue fibrosis. This has been shown in mice lacking senescence effectors (Krizhanovsky et al, 2008). Thus the senescence response in liver injury prevents liver fibrosis. This effect of senescence is critically dependent on the matrix metalloproteinases (MMP) that comprise part of the SASP (Krizhanovsky et al. 2008). p53-dependent senescence program in hepatic stellate cells is necessary during chronic liver damage in order to prevent liver fibrosis and cirrhosis. If this program is ablated, it leads to reduced survival and enhanced transformation of adjacent epithelial cells into hepatocellular carcinoma (Lujambio et al. 2013).

In addition to hepatic fibrosis, the senescence response and the SASP are important for wound healing (Jun and Lau 2010; Demaria et al. 2014). In response to cutaneous wounds, fibroblasts and endothelial cells undergo senescence in a CCN1-dependent manner (Jun and Lau 2010). Senescence facilitates wound closure by inducing myofibroblast differentiation through the secretion of platelet-derived growth factor AA (PDGF-AA) (Demaria et al. 2014). As mentioned earlier, p16INK4a is a marker of senescent cells. In the PDGF-AA-dependent wound closure model, if p16INK4a-positive senescent cells are eliminated using transgenic mice, it delays the wound closure. The p16-3MR transgenic mouse model has a trimodel transgene under the p-16 promoter that allows the tracking and the elimination of senescent cells in vivo. The topical treatment of recombinant PDGF-AA rescues the delayed wound closure and induces myofibroblast differentiation in the absence of senescent cells (Demaria et al. 2014). This model is discussed again in the chapter focused on the use of various mouse models (Chapter 4).

Furthermore, senescent cells have the capability to recruit immune cells, such as natural killer (NK) cells, to kill tumor cells (Ventura et al. 2007; Xue et al. 2007). The SASP factors are critical to recruit NK cells to eliminate malignant cells (Iannello et al. 2013). In addition to malignant cells, immune cells attracted by the SASP also remove nearby damaged cells (Krizhanovsky et al. 2008). Premalignant senescent hepatocytes in mice have the ability to induce T-cell-mediated adaptive immune response. These cells secrete chemokines and cytokines that promote immune-mediated clearance

(senescence surveillance), which requires an intact CD4. However, these premalignant senescent hepatocytes promote the development of hepatocellular carcinomas in case of impaired immune surveillance (Kang et al. 2011).

Senescence also plays an important role during embryonic development. Senescent cells are responsible for the morphogenesis of certain structures (Munoz-Espin et al. 2013; Storer et al. 2013). Apoptosis only partially compensates for the morphogenesis during embryonic development, thus senescence is critical during embryonic tissue development (Lecot et al. 2016).

These are some of the beneficial roles of senescence and the SASP. In the next section, I am discussing the detrimental side of senescence.

Negative effects of senescence and SASP (Figure 1.2)

The SASP consists of pro-inflammatory and pro-tumorigenic factors. Thus, the SASP creates a vulnerable microenvironment for tumorigenesis. SASP factors disrupt and remodel tissue structure to support tumor cell invasion and metastasis (Coppe et al. 2008; Rodier and Campisi 2011). Proteases secreted by senescent cells degrade the ECM, rendering the tissue structure more relaxed and thus facilitating the invasion of cancer cells (Coppe et al. 2008). SASP factors also induce an epithelial-to-mesenchymal transition in neighbouring cells, which facilitates tumor cell invasion (Laberge et al. 2012; Kuilman et al. 2008). Selective clearance of p16INK4-positive cells delays tumorigenesis and attenuates the age-related deterioration of several organs (Baker et al. 2011; Baker et al. 2016). Senescent cells promote the proliferation and assembly of endothelial cells for neo-angiogenesis by secreting a variety of angiogenic factors (Davalos et al. 2010). Senescent cells recruit macrophages and stimulate them to adopt a pro-angiogenic M2 phenotype, which indirectly promotes angiogenesis (Kelly et al. 2007). The SASP establishes a microenvironment that is immunosuppressive, which promotes tumor growth. Moreover, senescent cells inhibit CD8 T-lymphocyte-mediated killing of tumor cells by secreting cytokines that recruit myeloid-derived suppressor cells (Toso et al. 2014). Thus, the SASP has a prominent role in tumor progression.

1.5 Role of senescence in aging diseases

Chronic inflammation is one of the characteristics of aging that initiates or promotes most of the age-related diseases (Franceschi et al. 2007; Chung et al. 2009). It can destroy cells and tissues by remodeling the microenvironment. Senescent cells secrete the SASP, which affects cell growth and migration, tissue architecture, blood vessel formation, and differentiation. The inappropriate presence of the SASP factors disrupts tissue structure and function. For example, morphological and functional differentiation of breast epithelial cells is inhibited in the presence of MMP3 secreted by senescent fibroblasts (Parrinello et al. 2005) and this can promote tumor growth (Liu and Hornsby 2007). In addition inflammatory oxidative damage can suppress immune surveillance and stimulate malignant phenotypes (Allavena et al. 2008; Grivennikov, Greten, and Karin 2010; Freund et al. 2010). Cellular senescence can deplete tissues of stem or progenitor cells in Klotho-deficient mice (Liu et al. 2007). This depletion leads to

compromised tissue repair, regeneration, and normal turnover (Drummond-Barbosa 2008).

1.6 Senescence in brain cancer and neurodegeneration

The brain is composed of glioma stem cells (GSCs) and differentiated non-stem glioma cells (NSGCs). Glioblastoma (GBM) is a highly invasive and lethal brain tumor (Soroceanu et al. 2013; Marcu et al. 2010). In GBM patients, the standard therapy is surgical resection, followed by radiotherapy and/or chemotherapy (Carlsson, Brothers, and Wahlestedt 2014). Tumor recurrence in GBM patients is very high and the survival rate remains poor (Kirkpatrick et al. 2017). Therefore, it is important to understand the mechanisms of GBM recurrence for therapeutic advances.

Interestingly, recent studies are showing the presence of senescent cells in the brain and their role in promoting brain tumors (Ouchi et al. 2016; Jeon et al. 2016). NSGCs are capable of undergoing senescence and secrete SASP-like factors, which promote angiogenesis leading to the growth of GSC-derived tumors. These NSGCs become senescent due to the downregulation of telomerase and shortened telomeres, and then secrete IL-6 and IL-8. Conditioned media from senescent NSGCs are able to promote proliferation of brain endothelial cells. Further, tumorigenic potential of GSCs is enhanced when implanted with senescent NSGCs into mice. Overall, the paracrine effect of the SASP secreted by senescent NSGCs promotes malignant progression of GBM (Ouchi et al. 2016). Importantly, clinical GBM samples contained tumor cells expressing the senescence markers, which show the clinical significance of senescent NSGCs (Ouchi et al. 2016).

Another recent study by Jeon et al. shows that irradiation leads to 17–20 % of GBM cells to die, but 60–80 % of GBM cells undergo permanent growth-arrest after irradiation treatment. These growth-arrested GBM cells display an increase of various senescence markers, such as the senescence-associated beta-galactosidase, p53 and p21. These senescent GBM cells also show an increase in the expression of SASP mRNAs and NFκB transcriptional activity. Moreover, co-injection of irradiated GBM cells with non-irradiated GBM cells resulted in faster growth of tumors with the histological features of human GBM (Jeon et al. 2016).

In addition to their role as promoters of GBM growth, astrocytes have also been showed to play a major role in the brain microenvironment. They secrete a number of chemokines and cytokines associated with tumor cell invasion. In co-culture models of astrocytes and GSCs, there is an upregulation of genes that have been previously associated with tumor cell invasion in GSCs. Treatments using conditioned media from astrocytes on GSCs also promoted the invasion of GSCs (Rath et al. 2013).

Other than brain cancer, senescence has also been studied in neurodegenerative diseases, which include various disorders such as amyotrophic lateral sclerosis (ALS), Alzheimer's disease (AD), Huntington's disease (HD) and Parkinson's disease (PD) (Maragakis and Rothstein 2006). Accumulation of senescent cells leads to compromised Blood Brain Barrier (BBB) integrity (Yamazaki et al. 2016). Thus, senescence can be one of the important mechanisms providing insights into the BBB disruption related to biological aging. Decades of pathological and physiological studies have shown that astrocytes are important players in these, and other,

neurological disorders. Development of various animal models in which astrocyte-specific proteins and pathways have been manipulated, as well as mouse models of neurodegenerative diseases, have revealed astrocyte-specific pathologies that contribute to neurodegeneration (Gurney et al. 1994; Wong et al. 1995; Bruijn et al. 1997; Teismann and Schulz 2004; Behrens et al. 2002; Wisniewski and Wegiel 1991; DeWitt et al. 1998). In 2012, Bhat et al. showed presence of senescent astrocytes in AD. These astrocytes secrete various SASP factors. In Figure 1.3 and Table 1.1, I present various inflammatory factors, which are secreted by astrocytes, and their involvement in brain pathologies. Astrocytes are the most abundant cell type in the brain and have very specific star-shaped morphology. Astrocyte morphology is such that their processes are near blood vessels and synapses, providing functional support for various processes in the brain. Figure 1.4 shows the basic support functions of astrocytes. These functions allow neurons, and the brain in general, to function optimally.

Thus, it is important to perform in-depth study of senescence in brain cells, such as the astrocytes, to develop novel treatments for brain pathologies.

Figures

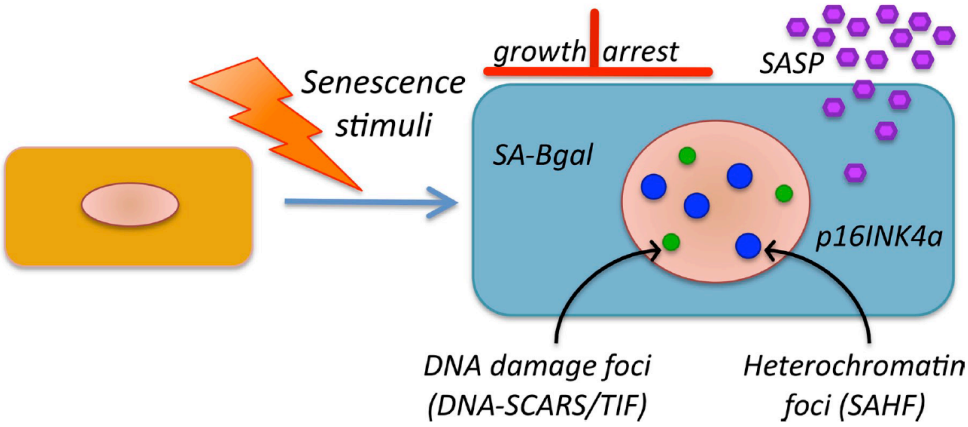

Figure 1.1 Senescence induction and characteristics. Upon senescence stimuli, proliferating cells become senescent. Senescent cells exhibit multiple characteristics including irreversible growth arrest, expression of SA-β-gal and p16INK4a, robust secretion of numerous growth factors, cytokines, proteases and other proteins (SASP), and nuclear foci containing DDR proteins (DNA-SCARS/TIF) or heterochromatin (SAHF). The pink circles in the non-senescent cell (left) and senescent cell (right) represent the nucleus (Rodier and Campisi 2011).

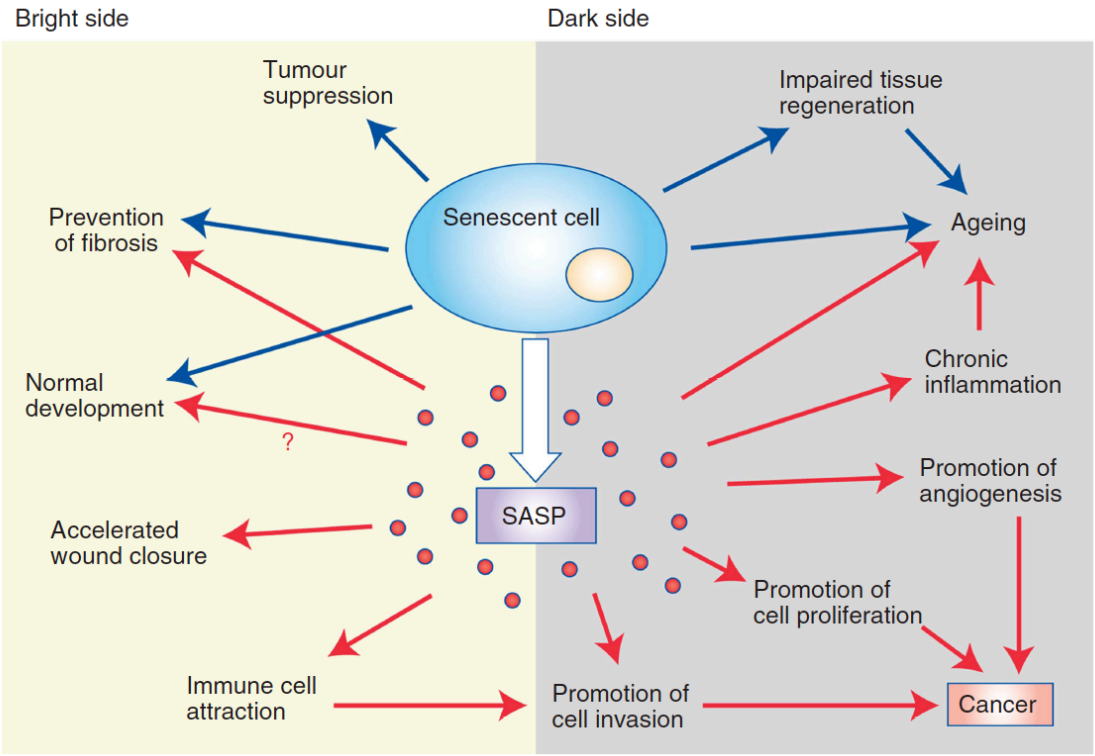

Figure 1.2 Bright and dark sides of senescence. The blue arrows represent the effects of senescence growth arrest and the red arrows represent the effects of the SASP. The left side on the diagram represents the bright side of senescence, including preventing tumorigenesis, limiting fibrosis, regulating normal embryonic development, accelerating wound closure and attracting immune cells. The dark side of senescence is represented on the right side, which includes impaired tissue regeneration, and promoting aging by increasing the chronic inflammatory state in the tissue microenvironment. The SASP also contains factors that promote angiogenesis, cell proliferation and cancer cell invasiveness. Furthermore, immune cells attracted by the SASP can disrupt the local microenvironment and promote tumor cell invasion. These final activities result in cancer progression (Lecot et al. 2016).

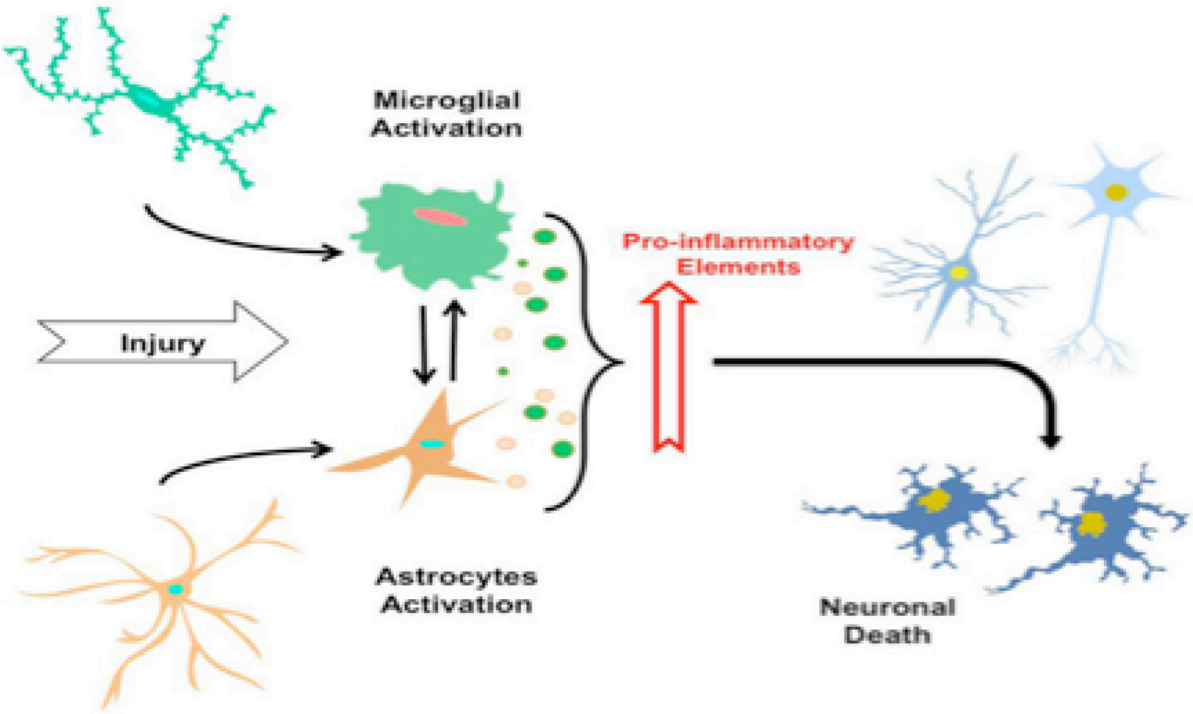

Figure 1.3 Inflammation in the brain. Various injuries or brain diseases lead to damage in normal astrocytes and glia cells. The damaged astrocytes and glia cells then secrete pro-inflammatory factors promoting neuronal cell death (Morales et al. 2014).

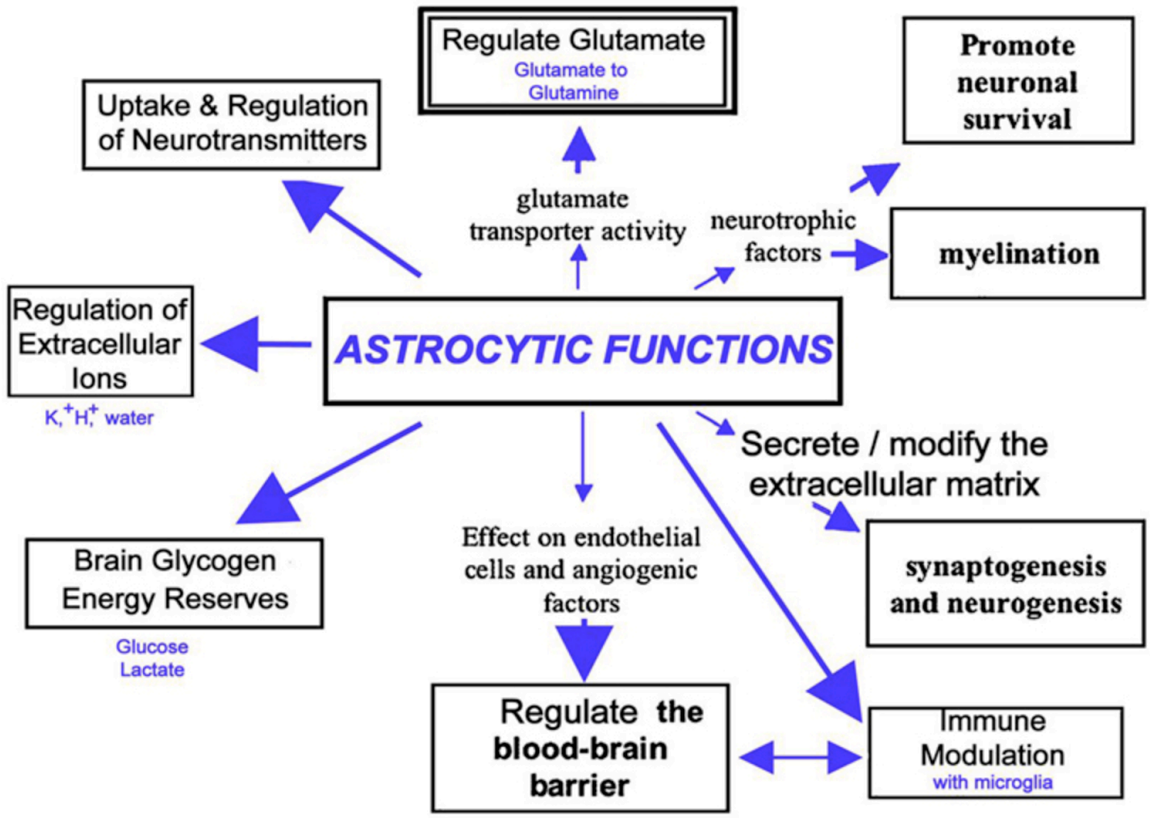

Figure 1.4 Function of astrocytes. Astrocytes have several important functions in the brain, which are necessary for healthy neurons, including regulation of various ions, neurotransmitters and water. Astrocytes also regulate the blood-brain barrier and neurogenesis (UCSF Astrocyte Functions).

Pro-inflammatory factors	**Effects**
Chemokines	Dysfunction, apoptosis and necrosis of neurons, microglia and astrocytes
IL-6, IL-1 beta, IL-12, INF-gamma, TNF-alpha	Astrocytes and microglia activation, dysfunction, apoptosis and necrosis of neuron, microglia and astrocytes

Table 1.1 Pro-inflammatory factors secreted by astrocytes and their effects during brain pathologies. Astrocytes secrete various pro-inflammatory factors similar to the SASP during brain pathologies. These factors damage healthy neurons, microglia and astrocytes.

Chapter 2: The senescent phenotype in human primary astrocytes compared to the senescent phenotype in fibroblasts

2.1 Senescence in various cell types

As presented in the previous chapter, cellular senescence is induced in response to various stresses such as telomere shortening, DNA damage, oncogene activation, and mitochondrial dysfunction (van Deursen 2014; Lecot et al. 2016). Senescent cells can be detected in culture and in vivo since they display several markers including SA-β-gal, upregulation of p16 and the SASP, secretion of HMGB1, and downregulation of LMNB1 (Rodier and Campisi 2011). So far, senescence has been studied in several cell types including fibroblasts, epithelial cells, muscle cells, hepatocytes and endothelial cells (Krtolica et al. 2001; Zhou et al. 2011; Minamino et al. 2003; Schnabl et al. 2003; Minamino et al. 2002; Wiley et al. 2016).

Figure 2.1 represents an example of senescence induced in human fibroblasts, HCA-2, and pre-adipocyte cells. Senescence was induced by X-irradiation (10 Gy) and mock radiation was used as a control. RNA was isolated from non-senescent (NS) control and senescence (SEN) cells at Day 4 and Day 10 of treatment, respectively. NS and SEN cells were also fixed for SA-β-gal and antibody staining at the same time points (Figure 2.1A). SA-β-gal staining showed progressively increased staining with time. About 82% of SEN HCA-2 and 5% of senescent pre-adipocyte cells stained positive in comparison to the NS controls at Day 4 after irradiation, where as 95% of SEN HCA-2 and 70% of pre-adipocytes were positive for SA-β-gal staining in comparison to the NS controls at Day 10 after irradiation (Figure 2.1B). The RNA expression of p16 was upregulated in SEN cells compared to NS controls (Figure 2.1C).

Importantly, previous studies have demonstrated a key role of cellular senescence during aging and various age-related pathologies, including neurodegenerative diseases (Bhat et al. 2012; Rodier and Campisi 2011; Chinta et al. 2015). However, very little is known about the potential role of senescence in the brain and about the identity of brain cells susceptible to undergo senescence. Among the essential cell types in the brain, astrocytes represent the most abundant population. Astrocytes retain proliferative capacities, and their functions are crucial for neuron survival (Jakel and Dimou 2017). Astrocytes are critical for mediating homeostasis of ions, growth factors and neurotransmitters in the brain (Devinsky et al. 2013). Previous studies have shown that astrocyte dysfunction is associated with multiple brain pathologies including ALS, AD, HD and PD (Bitto et al. 2010; Maragakis and Rothstein 2006). Bhat et al. identified senescent astrocytes in aged and Alzheimer's disease brain tissues (Bhat et al. 2012), and other studies have identified several factors that are responsible for inducing senescence in astrocytes (Bhat et al. 2012; Bitto et al. 2010; Mombach, Vendrusculo, and Bugs 2015). These studies reported a link between an inflammatory environment and neurodegenerative diseases, but there was no in-depth analysis to identify the effects of senescence on the function of the brain in general, and on the role of astrocytes in particular.

2.2 Comparing the senescence markers in fibroblasts and astrocytes

Here, I have characterized the senescent phenotype of human primary astrocytes in

comparison to the well-characterized senescent phenotype of human fibroblasts IMR90s. In all the experiments, I used X-irradiation to induce senescence. Then, using real-time PCR, ELISA and cell based assays, I characterized the senescent phenotype of astrocytes and compared it to the phenotype of human primary fibroblasts. I determined that astrocytes undergo senescence after X-irradiation and exhibit various markers similar to senescent fibroblasts, including upregulation of p16 and the SASP.

Irradiation induces senescence and a SASP in human primary astrocytes

To investigate the senescent phenotype of astrocytes, I used human primary astrocytes obtained from three different donors. Astrocyte purity was confirmed as we detected 95% of GFAP-positive cells before the initiation of the experiment, whereas IMR90 cells did not stain positive for GFAP (Figure 2.2). Senescence was induced by X-irradiation (10 Gy) and mock radiation was used as a control. RNA and conditioned media (CM) from non-senescent (NS) control and senescence (SEN) cells were collected at Day 4, 7, 10, 14, and 21 of treatment as shown in the experiment time line (Figure 2.3). NS and SEN cells were also fixed for SA-β-gal and antibody staining at the same time points. SA-β-gal staining progressively increased with time after irradiation in the two cell types, astrocytes and IMR90s (Figure 2.4A,B). SA-β-gal quantification showed 97-98% of IMR90 cells were positively staining at Day 7 and continued to be positive until Day 21. Astrocytes displayed a more progressive staining, 60% at Day 7, 90% at Day 10 and 97-98% at Days 14 and 21 (Figure 2.4C).

As SA-β-gal is not the only marker of senescence, I tested several other markers in SEN cells. RNA analysis for senescent markers showed that p16 was gradually upregulated (Figure 2.5A). In order to determine the expression of senescence markers at the protein level in astrocytes, I performed immunofluorescence (IF) and ELISA for HMGB1 for NS and SEN (Day 14 after irradiation) samples. HMGB1 (high mobility group box 1) is a non-histone nuclear protein, which bends DNA to provide transcription factor access to promoter region (Davalos et al. 2013). HMGB1 is secreted out of the nucleus upon cellular senescence (Davalos et al. 2013). The IF results showed loss of HMGB1 from the nucleus of SEN astrocytes, but not from the NS cells (Figure 2.5B, left panel). The HMGB1 ELISA test on CM samples from NS and SEN samples confirmed that HMGB1 was secreted and upregulated in SEN cells compared to NS cells (Figure 2.5B, right panel). I also investigated the SASP, including IL-6, IL-8, CXCL-1 and TGF-a, in both cell types. All of the SASP factors were upregulated in SEN cells compared to NS cells in fibroblasts and astrocytes (Figure 2.6A-D). Interestingly, astrocytes showed stronger upregulation of SASP factors at earlier time points, i.e., at Day 7, and the SASP progressively decreased with time. Even though the SASP was lower at later time points than Day 7, it was still higher compared to NS samples. IMR90 cells showed gradual upregulation of all the factors with time, and no plateau was detected.

Irradiation induces senescence and a SASP in mouse primary astrocytes

In order to determine whether mouse astrocytes undergo senescence, and therefore express senescence markers, I also used mouse astrocytes for further experiments. I checked the purity of the astrocytes using GFAP staining, and

determined that 94% of the cells stained positive (Figure 2.7). The irradiation protocol was the same as for the human astrocytes except that only one time point, Day 14, was analyzed for mouse cells. RNA analysis showed SEN cells upregulated p16 and some SASP markers, including IL-6, CXCL-1, CXCL-10, and MMP-3 (Figures 2.8 and 2.9), whereas LMNB1 expression was downregulated in SEN cells compared to NS cells (Figure 2.8).

2.3 Future directions and conclusion

These results show that astrocytes do also undergo senescence, i.e., they express some of the typical senescence markers and SASP. However, it was interesting to note that the expression of SASP factors in astrocytes was upregulated at Day 7, but progressively decreased at later time points. We still have to determine the mechanisms responsible for the progressive SASP decline at later time points. Importantly, even though the SASP decreased progressively at later time points in SEN astrocytes, at the latest time point (Day 21 after irradiation) the cells still expressed a higher SASP than NS control cells.

Together, these data indicate that X-irradiation treatment induces all the major characteristics of senescence and the SASP in astrocytes, which was similar to the phenotype induced in human fibroblasts. SASP includes various pro-inflammatory factors, which may contribute to aging pathologies related to the brain, including cancer and neurodegenerative diseases. Recently, Jeon et al. showed that irradiation led GBM, the most aggressive type of brain cancer, to undergo senescence (Riemenschneider and Reifenberger 2009; Jeon et al. 2016). These senescent GBM cells secreted a SASP and promoted tumor cell growth. Therefore, as a next step, it was important to investigate how non-cancerous senescent astrocytes may play a key role in promoting brain-related aging diseases by affecting the surrounding cells and leading to a perturbed microenvironment.

Figures

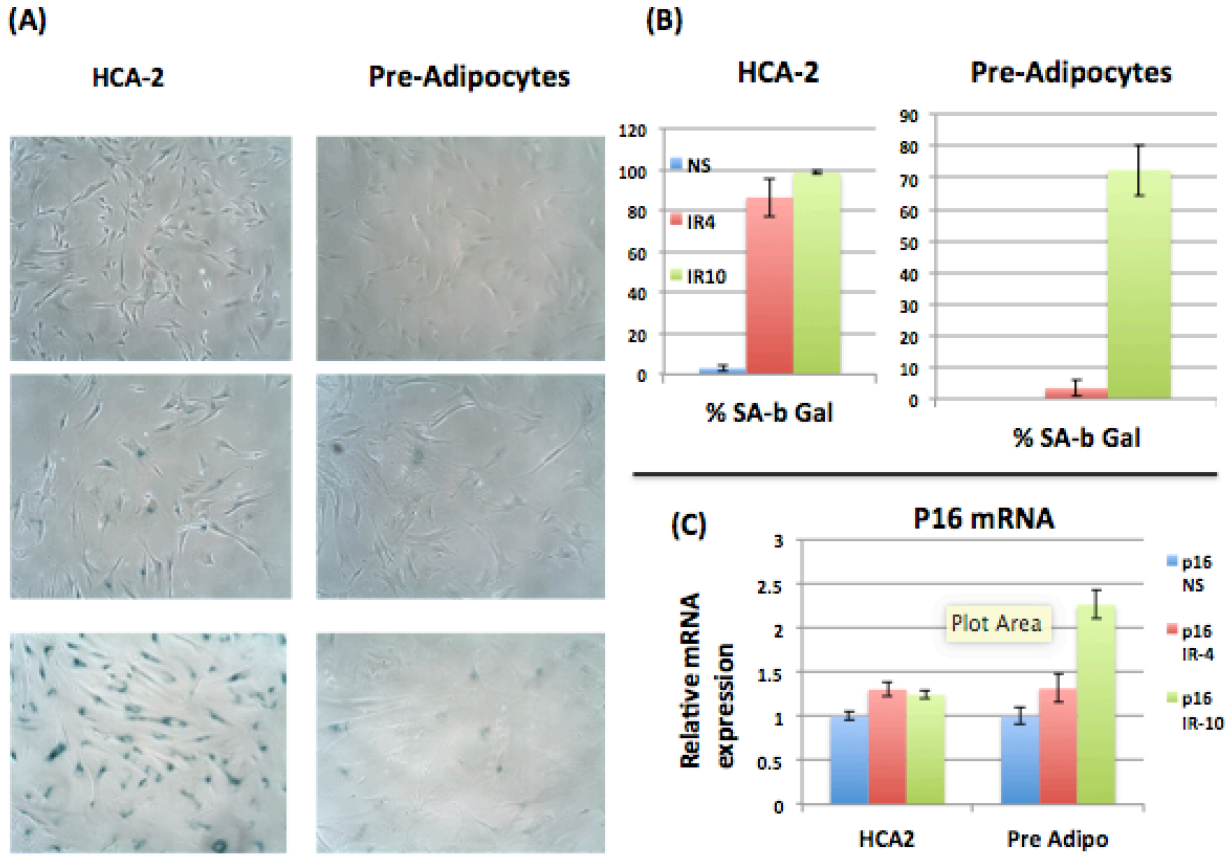

Figure 2.1 Senescence markers in senescent fibroblasts and pre-adipocytes. (A) SA-β-gal was performed on NS and SEN HCA-2 fibroblasts and pre-adipocytes. (B) The SA-β-gal staining for HCA-2 and pre-adipocytes was quantified. (C) Real-time PCR of p16 mRNA expression was performed in NS and SEN HCA-2 and pre-adipocytes.

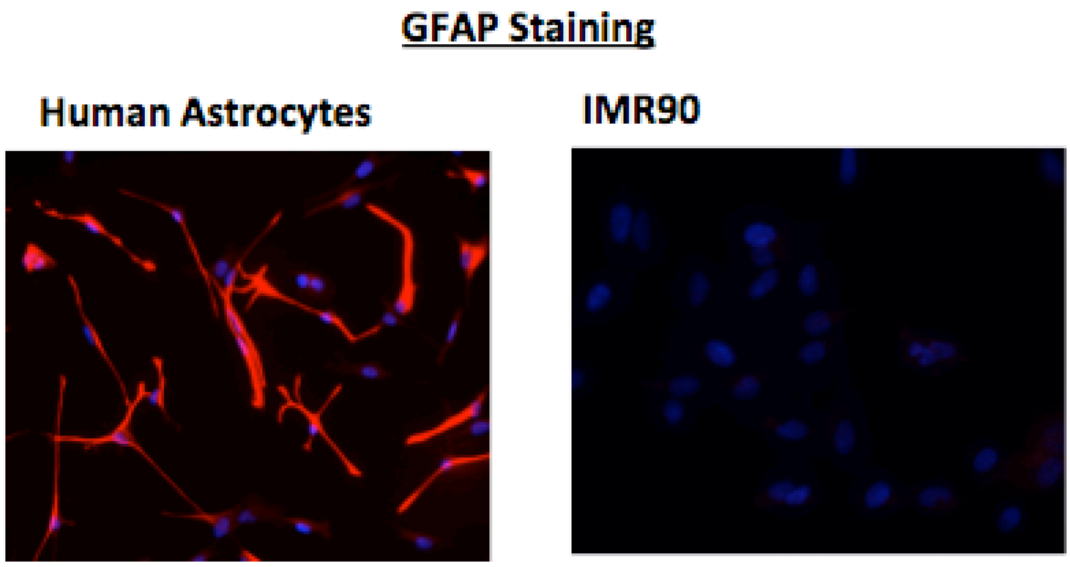

Figure 2.2 Immunofluorescence staining for the astrocyte marker GFAP was performed on primary human astrocytes and IMR90 fibroblasts.

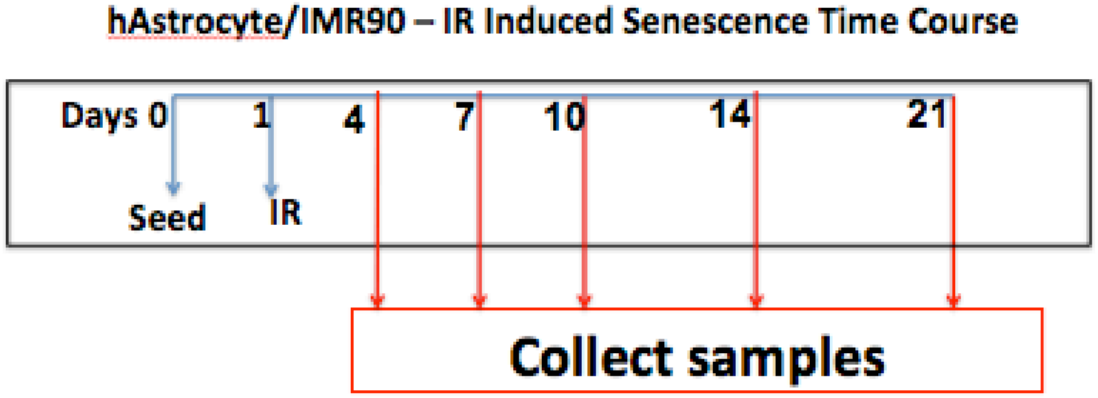

Figure 2.3 Timeline for irradiation (IR) experiments. Time course experiments were performed on cells after X-irradiation. Samples were collected at Day 7, 10, 14, 21 after treatment.

(A)

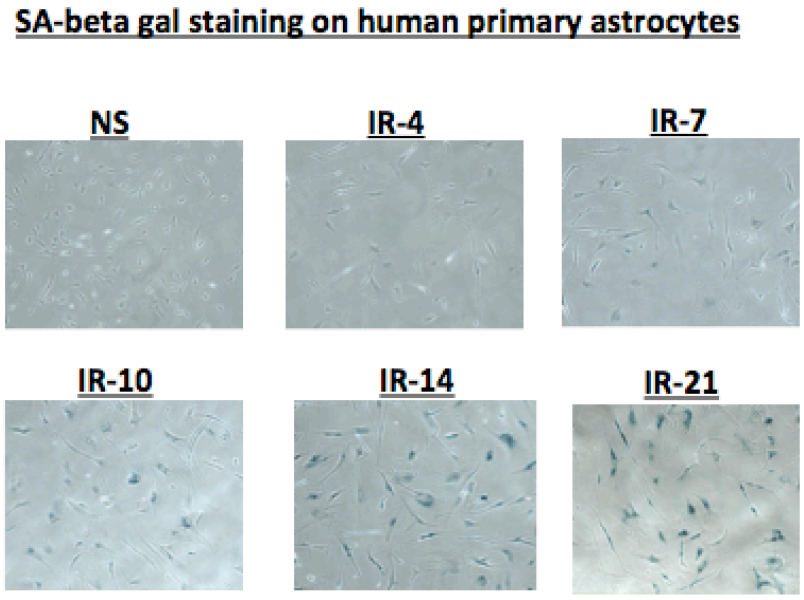
SA-beta gal staining on human primary astrocytes
NS
IR-4
IR-7
IR-10
IR-14
IR-21

(B)

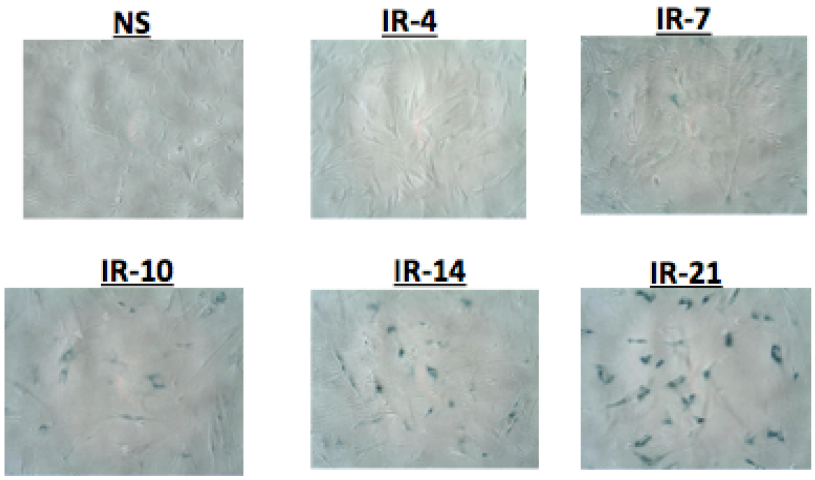
SA-beta gal staining on IMR90s
NS
IR-4
IR-7
IR-10
IR-14
IR-21

(C)

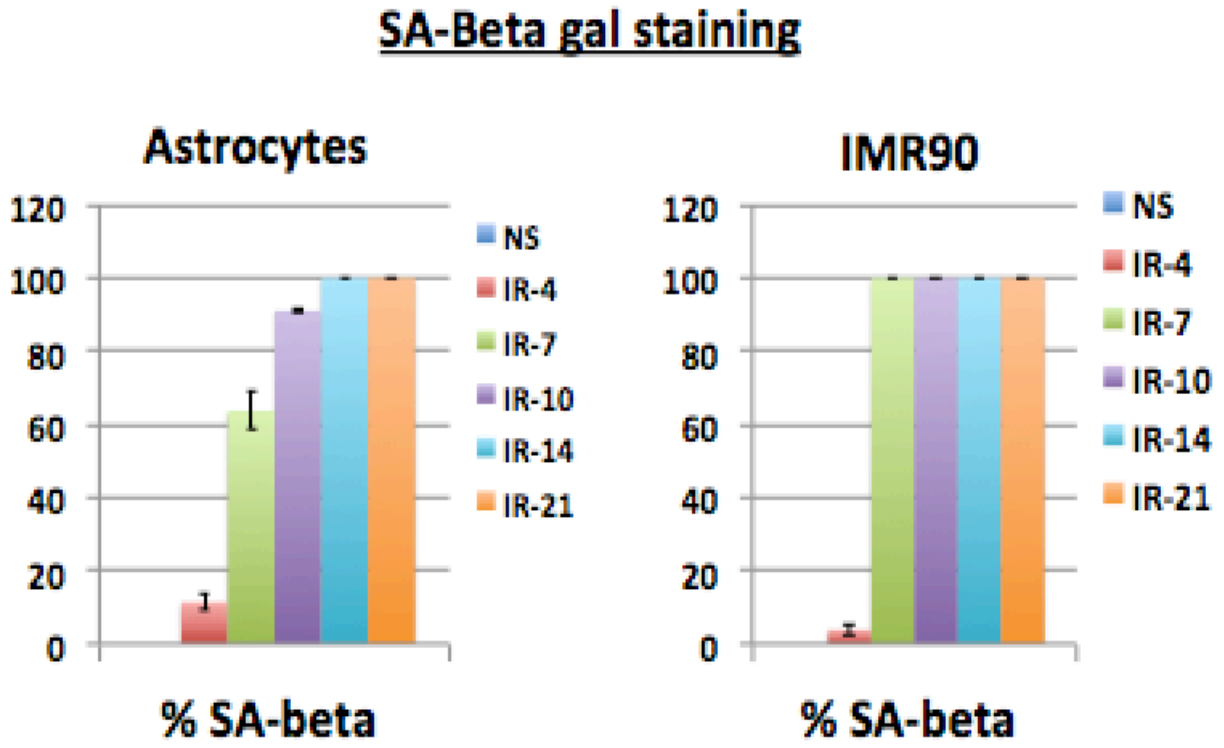

Figure 2.4 Human primary astrocytes undergo senescence upon X-irradiation and express SA-β-gal similar to senescent fibroblasts. (A, B) Cellular senescence (SEN) was induced in astrocytes using X-irradiation. On Day 4, 7, 10, 14 and 21 after IR (IR-4, IR-7, IR-10, IR-14, IR-21), SA-β-gal staining was performed on NS control cells and irradiated senescent human primary astrocytes (A) and IMR90 fibroblasts (B). (C) The quantification of SA-β-gal staining for human primary astrocytes and IMR90 fibroblasts is shown.

(A)

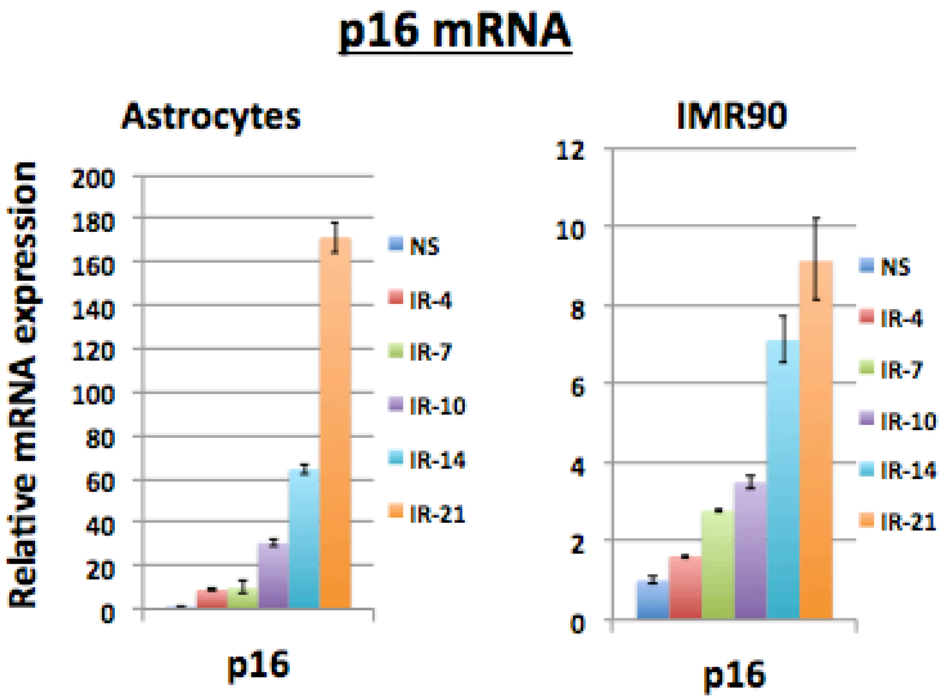
p16 mRNA
Astrocytes
Relative mRNA expression
200
180
160
140
120
100
80
60
40
20
0
p16
NS
IR-4
IR-7
IR-10
IR-14
IR-21
IMR90
12
10
8
6
4
2
0
p16
NS
IR-4
IR-7
IR-10
IR-14
IR-21

(B)

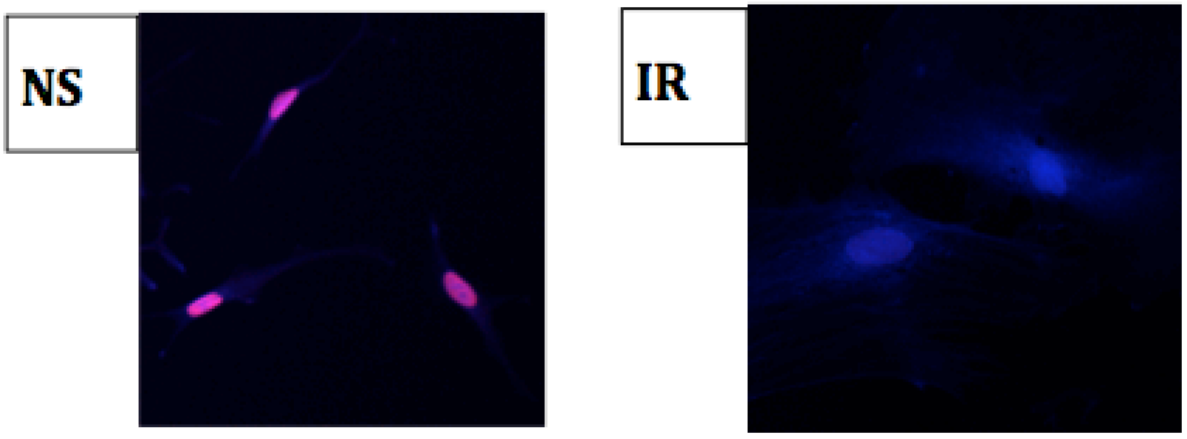
NS
IR

(C)

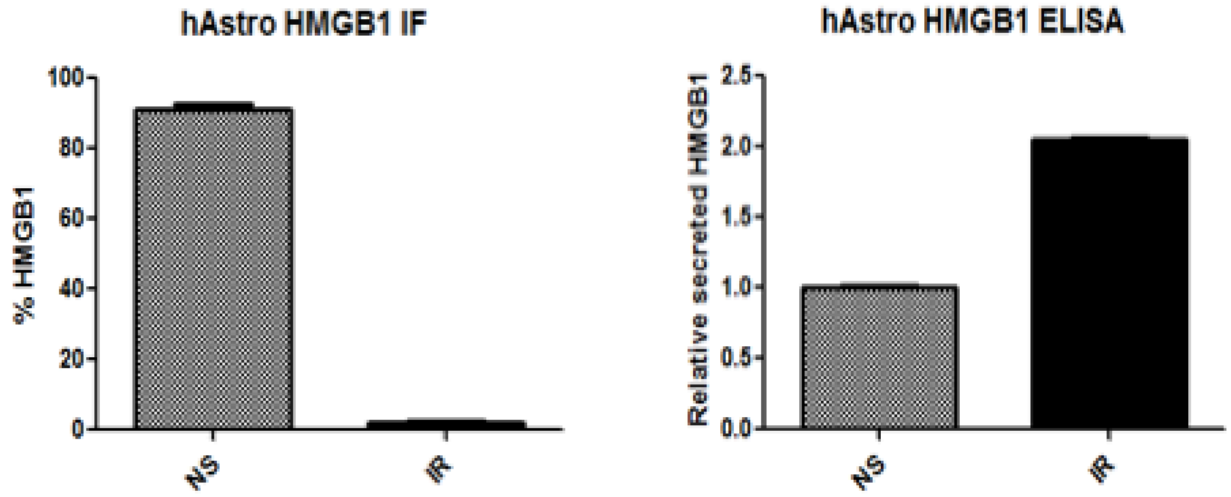

Figure 2.5 Human primary astrocytes undergo senescence upon X-irradiation and express classical senescence markers similar to senescent fibroblasts. (A) Cellular senescence (SEN) was induced in cells using X-irradiation. On Day 4, 7, 10, 14 and 21 after IR (IR-4, IR-7, IR-10, IR-14, IR-21), p-16 mRNA analysis was performed using real-time PCR on NS control cells, and irradiated senescent human primary astrocytes and IMR90 fibroblasts. (B) High mobility group box 1 (HMGB1) immunofluorescence staining was performed on NS and SEN cells, and (C) HMGB1 immunofluorescence was quantified (left panel). HMGB1 ELISA was performed using conditioned media (CM) collected from NS and SEN cells (right panel).

(A)

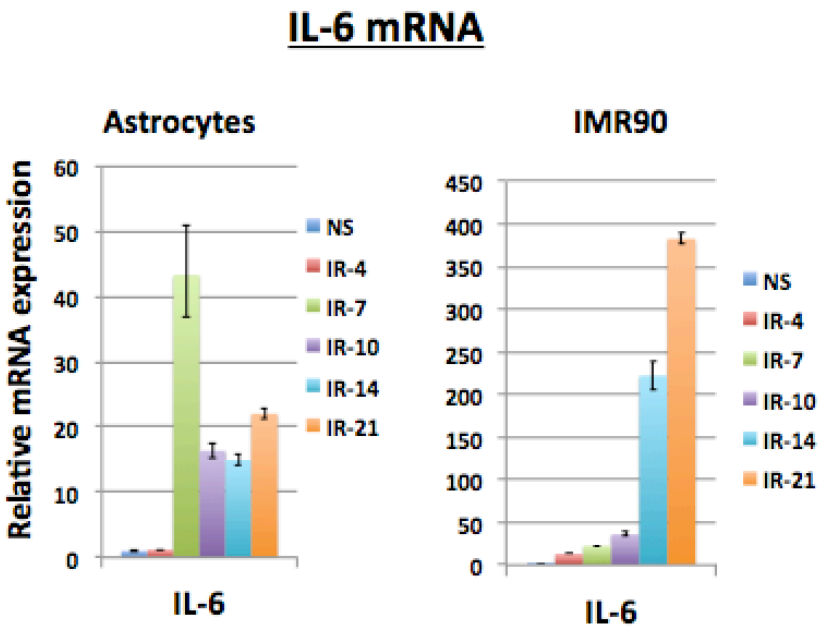
IL-6 mRNA
Astrocytes
IMR90
Relative mRNA expression
60
50
40
30
20
10
0
450
400
350
300
250
200
150
100
50
0
NS
IR-4
IR-7
IR-10
IR-14
IR-21
IL-6
IL-6

(B)

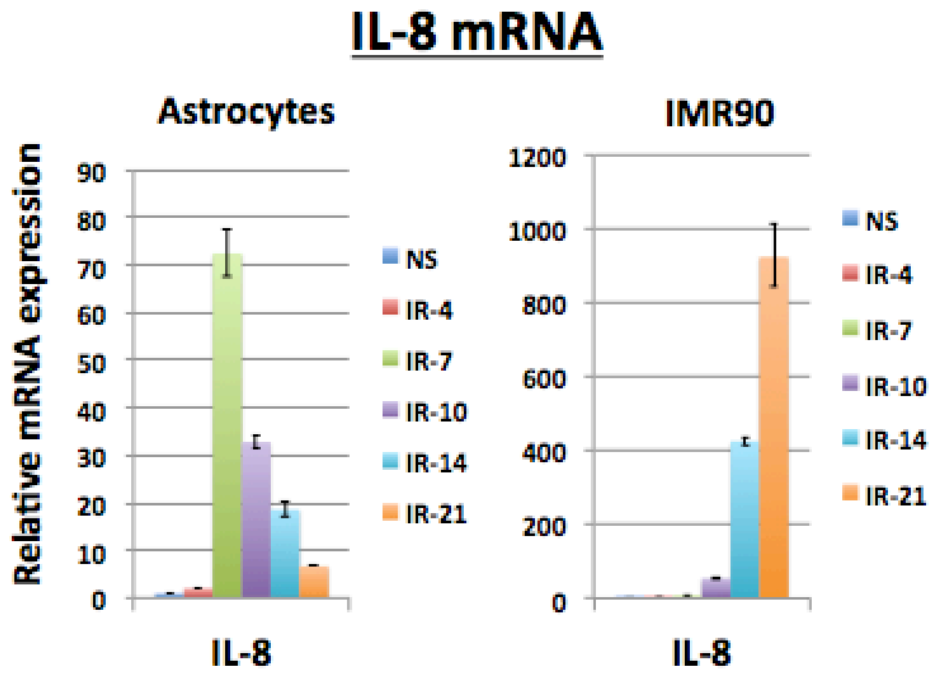
IL-8 mRNA
Astrocytes
IMR90
Relative mRNA expression
90
80
70
60
50
40
30
20
10
0
1200
1000
800
600
400
200
0
NS
IR-4
IR-7
IR-10
IR-14
IR-21
IL-8
IL-8

(C)

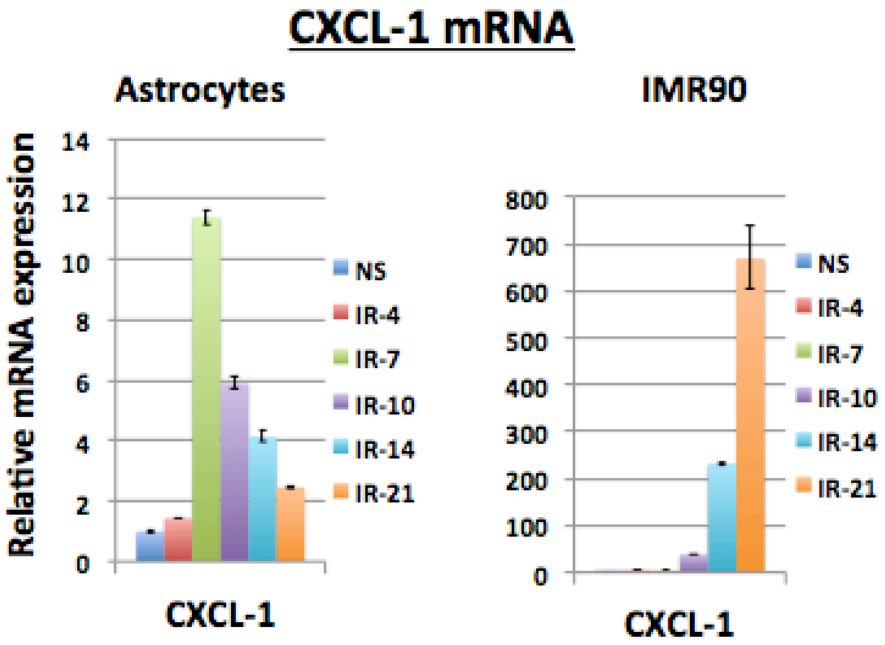

(D)

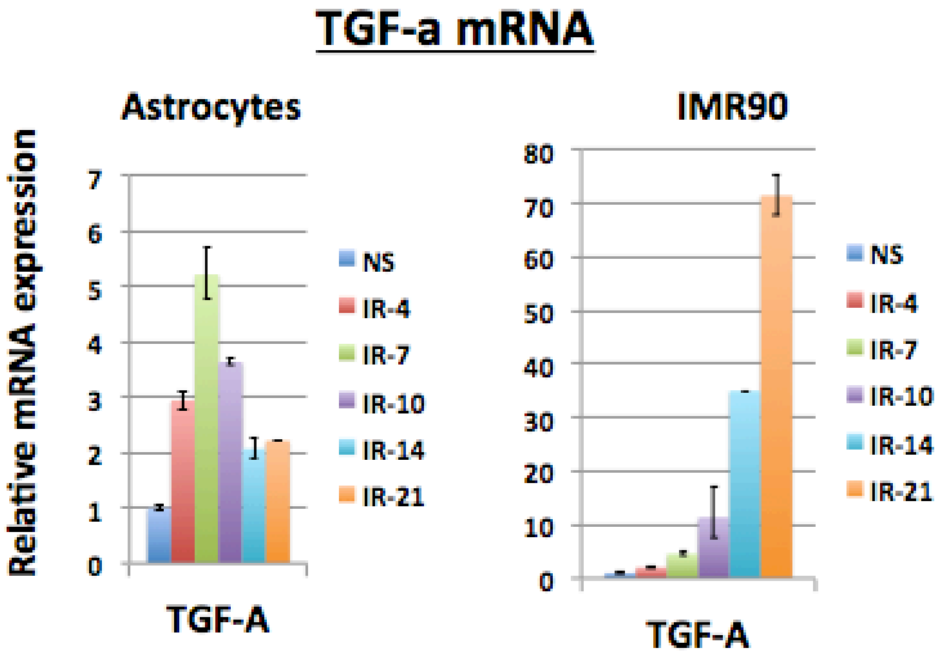

Figure 2.6 Human primary astrocytes undergo senescence upon X-irradiation and express classical SASP factors similar to senescent fibroblasts. (A-D) Cellular senescence (SEN) was induced in cells using X-irradiation. On Day 4, 7, 10, 14 and 21

after IR (IR-4, IR-7, IR-10, IR-14, IR-21), SASP factors (A: IL-6; B: IL-8; C: CXCL1; D: TGF-a) mRNA analysis was performed using real-time PCR on non-senescent (NS) control cells and irradiated senescent human primary astrocytes and IMR90 fibroblasts.

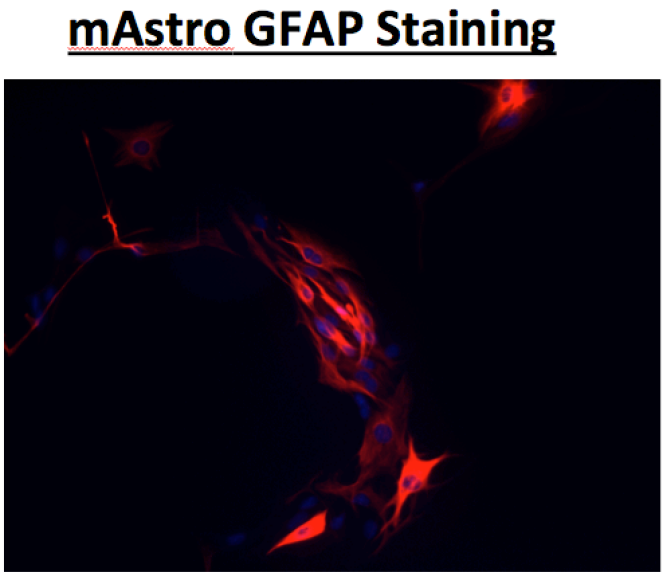

Figure 2.7 Immunofluorescence staining for the astrocyte marker GFAP was performed on primary mouse astrocytes.

(A)

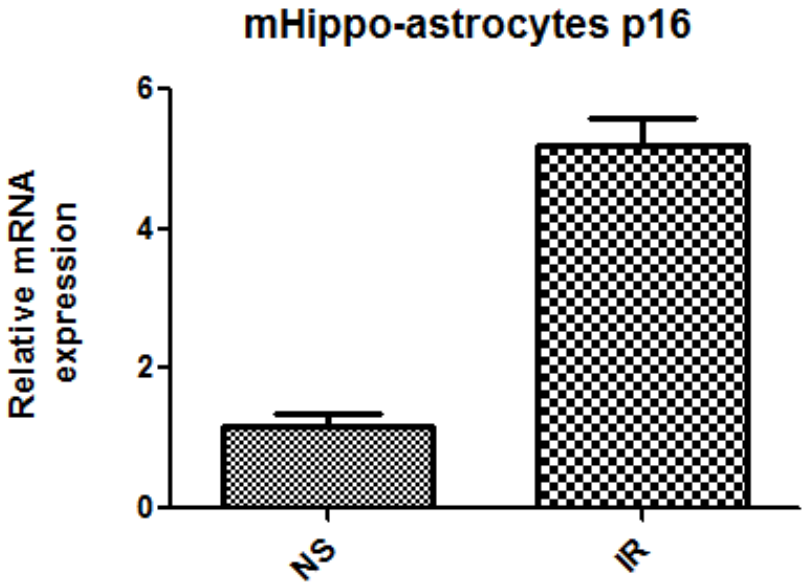

(B)

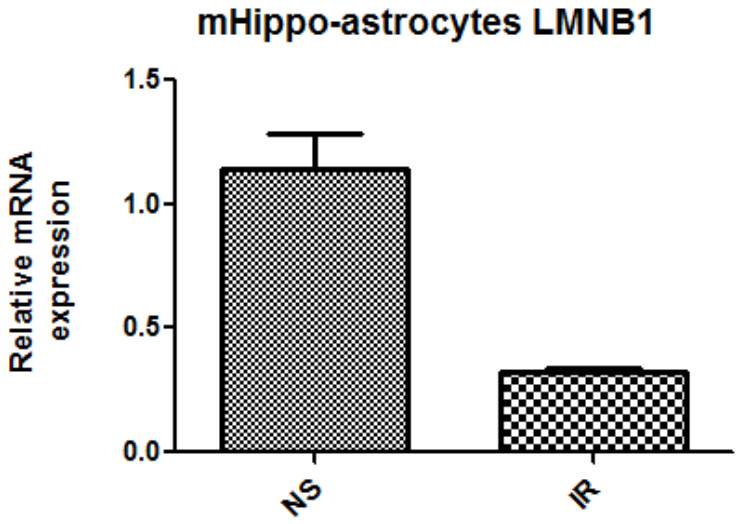

Figure 2.8 Mouse primary astrocytes undergo senescence upon X-irradiation and express classical senescence markers. (A-B) Cellular senescence (SEN) was induced in astrocytes using X-irradiation. On Day 14 after IR, (A) p-16 and (B) LMNB1 mRNA analysis was performed using real-time PCR on non-senescent (NS) control cells and irradiated senescent (IR) mouse primary astrocytes.

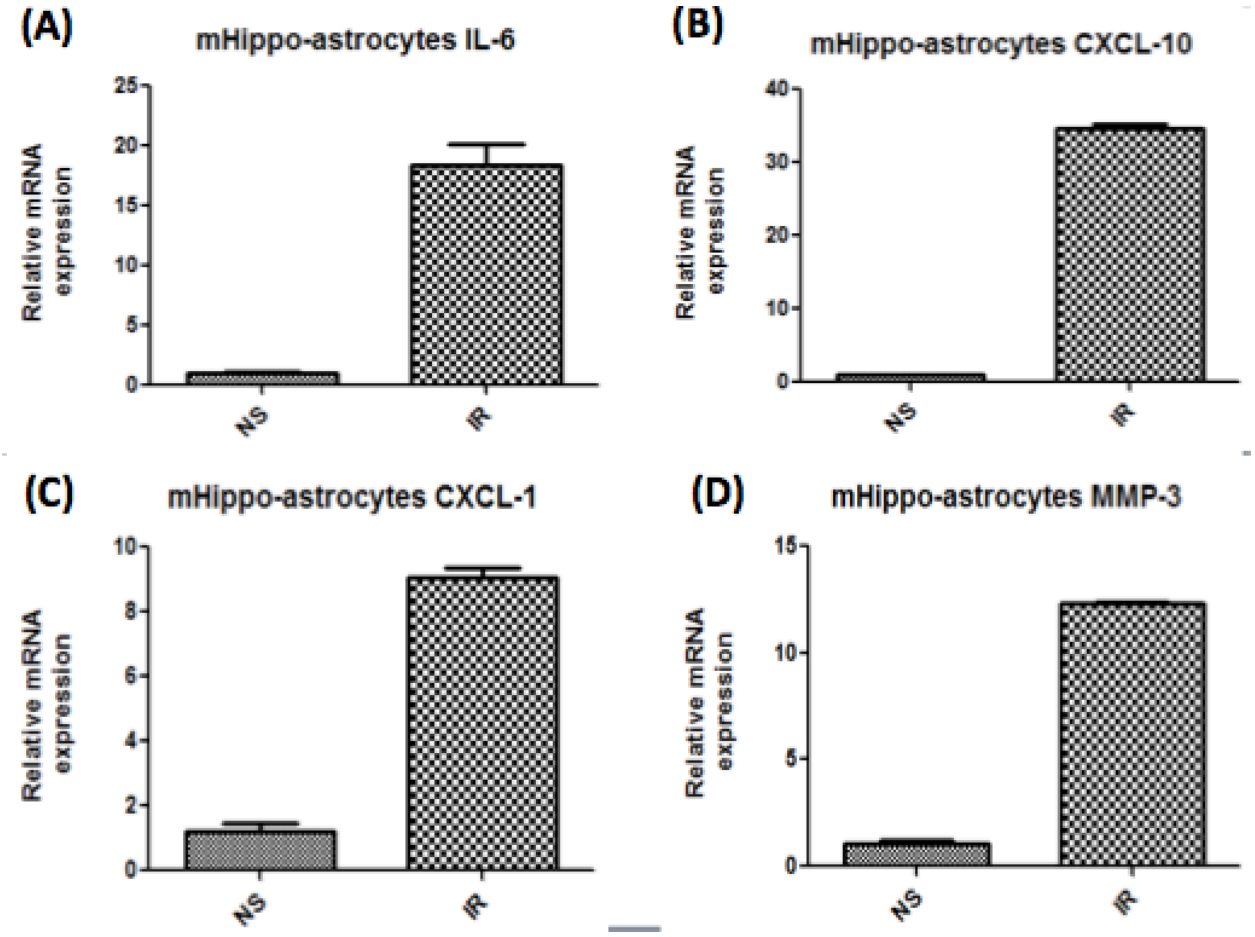

Figure 2.9 Mouse primary astrocytes undergo senescence upon X-irradiation and express classical SASP factors. (A-D) Cellular senescence (SEN) was induced in astrocytes using X-irradiation. On day 14 after IR, (A) IL-6, (B) CXCL-1, (C) CXCL-10, (D) MMP-3 mRNA analysis was performed using real-time PCR on non-senescent (NS) control cells and irradiated senescent (IR) mouse primary astrocytes.

Chapter 3: Modulation of specific pathways upon induction of senescence in astrocytes

3.1 Glutamate – Glutamine cycle and role of potassium and aquaporin transporters in astrocytes

Glutamate-glutamine cycles occur between neurons and astrocytes for their homeostasis. Pre-synaptic neurons secrete glutamate (Glu), which stimulates post-synaptic neurons, and the remaining Glu from the synaptic cleft is then taken up by astrocytes. Astrocytes have Na+-dependent excitatory amino acid transporters (EAATs) on their cell surface. Human astrocytes express EAAT1 and EAAT2 as glutamate transporters. GLAST and GLT-1 are the mouse homologues of Glu transporters. These transporters have high affinity for Glu and are responsible for Glu uptake in astrocytes. Glu is converted to glutamine (Gln) via glutamine synthase (GS). Gln is released from the astrocytes and taken up by neurons for glutamate production. The resulting Glu is repackaged in vesicles for further synaptic release (Stobart and Anderson 2013) (Figure 3.1).

Glutamate and excitotoxicity

For maintaining low ambient levels of Glu, Glu uptake by high-affinity membrane transporters is essential. As soon as pre-synaptic neuron releases Glu into the synaptic space, most of it is removed from the extracellular space by astrocytic transporters. Glu uptake prevents spill-out of transmitter from the synaptic cleft, thus regulating crosstalk between neighboring synapses and the activation of perisynaptic or extrasynaptic Glu receptors. Astrocytes are optimized for Glu uptake due to their high (negative) resting potential, which enhances the sodium electrochemical gradient that drives transport, and low cytoplasmic Glu concentration.

If Glu is not taken up by astrocytes it leads to toxicity, also known as excitotoxicity (Devinsky et al. 2013). Excitotoxicity is defined as an excessive activation of neuronal amino acid receptors. Excitotoxic cascade is triggered by the excessive accumulation of Glu in the synaptic space. This can be due to various factors, such as alteration in the normal cycling of intracranial Glu to increase the release of Glu into the extracellular space, decreased Glu uptake or transport from the synaptic space, or by spillage of Glu from injured neurons (Mark et al. 2001). In many disorders, excitotoxicity triggered by Glu leads to neuronal death. Understanding the mechanisms related to excitotoxicity and Glu uptake by astrocytes can answer many fundamental questions as why neurons die in some diseases (Mark et al. 2001) (Figure 3.2).

Potassium and aquaporin transporters

In addition to Glu amounts, astrocytes regulate water and K+ flow between brain cells and the extracellular space (Figure 3.2). AQP4 mediates the bidirectional flow of water between the extracellular space and the blood, thus regulating interstitial fluid osmolarity and extracellular space volume. AQP4 dysfunction impairs water delivery to the extracellular space leading to swelling astrocytes, contracting the extracellular space, and increasing excitably (Gunnarson et al. 2008; Yao et al. 2008). The inward rectifying K+ channels (Kir) carry K+ ions into cells, accompanied by water entry through AQP4 to maintain osmotic balance. Kir4.1 dysfunction can compromise K+ spatial buffering.

Conditional knockout of Kir4.1 depolarizes glial membranes, inhibits potassium and glutamate uptake (Djukic et al. 2007).

3.2 Senescent astrocytes downregulate specific functional pathways such as the glutamate and potassium transporters, glutamine synthetase and aquaporin

Astrocytes are responsible for maintaining homeostasis of Glu, Gln, potassium and water in the brain. EAAT1 and EAAT2 transporters on astrocyte cell surface are responsible for Glu transport. The efficient Glu uptake by astrocytes also requires the potassium transporter Kir4.1. Furthermore, astrocytes maintain water balance through the AQP4 transporters on their cell surface (Figure 3.2). I therefore compared the expression of all these genes in NS and SEN astrocyte samples at the mRNA level and determined that all these genes were downregulated in SEN cells compared to NS cells (Figure 3.3A,B). Figure 3.3B shows downregulation of 3 different transcripts of glutamine synthetase (GS/GLUL). Next, I investigated whether these downregulations were transient for the genes important for protecting neurons from excitotoxicity, i.e., EAAT1, EAAT2, Kir4.1, and AQP4. To address this question, I performed a time course in SEN astrocytes following X-irradiation. I collected mRNA from SEN cells on Day 7, 10, 14 and 21 after X-irradiation. The RT-PCR results show that the levels of EAAT1, EAAT2, Kir4.1 and AQP4 mRNA expression gradually declined with time, reaching a maximum downregulation after 14 days (Figure 3.4A-C).

Since, Glu uptake happens at the protein level, we tested whether the transporters were downregulated in SEN cells, not only at the mRNA level, but also at the protein level. I extracted proteins from NS and SEN cells 14 days after X-irradiation. Western blot analysis shows that EAAT1, Kir4.1, AQP4, and glutamine synthetase were downregulated in SEN cells compared to NS cells (Fig. 3.5). Western blot quantification also shows that all these transporters were downregulated 5- to 10-fold, which is consistent with the mRNA data (Figure 3.5).

3.3 Senescent astrocytes trigger Glu-toxicity and neuronal death in cell culture assays

Glutamate concentration optimization

In order to determine Glu toxicity on neuronal cells in the presence or absence of senescent astrocytes, I performed the following experiments. First, I determined the non-toxic concentrations of Glu for both NS and SEN astrocytes. At 10 mM, Glu did not trigger any significant morphological changes compared to 0 mM, nor it triggered any cell death. However, at 20 mM, there was a substantial increase in cell death observed in both NS and SEN astrocytes. Thus, for the astrocyte/neuron co-culture experiments, I used a Glu concentration of 10 mM (Figure 3.6).

Astrocyte/neuron co-culture experiments in the presence and absence of Glu

To determine Glu toxicity on neuronal cells in the presence or absence of senescent astrocytes, I performed co-culture assays. The cells were seeded as described in the Material and Methods section. After 24 hours of the co-culture, neurons still survived whether cultured with NS or SEN cells in the absence of Glu. However, in the presence of 10 mM of Glu, neurons started to die when co-cultured with SEN astrocytes. On the contrary, neurons did not show any sign of cell death in the presence of Glu when cultured with NS astrocytes. Using phase contrast, surviving neurons are shown in Figure 3.7. In order to quantify neuronal cell survival in co-culture assays, I pre-labeled the astrocytes with CMPTX red, and I then performed the co-cultures with neurons in the presence or absence of 10 mM Glu. After 24 hours of co-culture, the cells were fixed and stained with DAPI. For quantification purposes, red+DAPI specifically stained astrocytes whereas neurons were only stained with DAPI (Figure 3.8A,B). Quantification showed that almost 50% of the neurons died in the presence of 10 mM Glu when co-cultured with SEN astrocytes. These data indicate that SEN astrocytes are not taking up Glu efficiently, which leads to neuronal cell death in co-culture assays (Figure 3.8C,D).

3.4 RNA-seq study to determine senescent astrocyte-specific pathways

In order to obtain a comprehensive understanding about the pathways up- or down-regulated in astrocytes upon senescence induction, we performed RNA sequencing (RNA-seq) comparing senescent and non-senescent astrocytes. Transcriptome studies give a complete set of transcripts for a cell at a given time. It is important to characterize the transcriptome for interpreting the functional elements of the genome and revealing the molecular constituents (Wang, Gerstein, and Snyder 2009). RNA-seq allows the de novo detection of both protein coding and non-coding RNAs unlike microarrays and real-time PCR (Nikitina et al. 2017). RNA-seq samples were prepared and processed as described in the Material and Methods section. Briefly, senescence was induced using X-irradiation and, 14 days after irradiation, RNA extracted from SEN and NS cells were sent for RNA-seq. The samples were prepared from six different populations of human astrocytes.

Before sending out the samples for RNA-seq, I confirmed that some major senescence markers, including p16 and two SASP factors (IL-6 and IL-8), were upregulated in SEN samples compared to NS samples. All six sets of NS and SEN samples showed upregulation of p16, IL-6 and IL-8 at various levels as shown in Figure 3.9A,B. I also determined the levels of glutamate and potassium transporters in all six sets. All three transporters, including EAAT1, EAAT2 and Kir4.1, were downregulated at various levels in SEN samples compared to NS samples for all six sets as shown in the Figure 3.10A,B.

After RNA-seq was performed on all six sets of NS and SEN samples, bioinformatics analysis was performed to analyze the data and to determine the differential expression of genes between NS and SEN samples. NS_1 to NS_6

correspond to non-senescent samples and IR_1 to IR_6 correspond to senescent samples. The raw data was filtered and trimmed, and the reads were compared to raw data. The data showed very good alignment as presented in Table 3.1. The hierarchical clustering and Jensen-Shannon metric (or JS metric) was used to resolve the ambiguity of uncertain segments. To determine the similarity of the expression patterns between samples, and to analyze differential alternative splicing events, JS metric measurements were also used (Tasnim et al. 2015). The hierarchical clustering and JS metric analysis showed very close clustering and very high similarity of expression patterns for all the NS (NS_1 to NS_6) and SEN (IR_1 to IR_6) samples (Figure 3.11,12). Differential expression analysis showed there were 5,809 significantly differentially expressed genes in the analysis. It also showed that there were 2,915 genes significantly upregulated and 2,894 genes significantly downregulated, as presented in Figure 3.13.

Table 3.2 shows that we could detect a significant upregulation of p16 in the SEN samples compared to NS samples, and that all SEN samples significantly downregulated EAAT1, EAAT2 and Kir4.1 genes compared to NS samples.

3.5 Conclusion

Among various functions specific of astrocytes (and not detectable in fibroblasts), an efficient uptake of extra Glu from synaptic cleft is critical. Therefore, I attempted to determine whether senescence induced by X-irradiation in astrocytes could affect the glutamate transport system and homeostasis of other molecules. Interestingly, and specific to astrocytes, I detected a downregulation of a glutamate, potassium and water transporters, both at the RNA and protein levels. I also confirmed these results using unbiased RNA-seq study. Downregulation of various transporters in senescent cells leads to Glu toxicity and neuronal cell death in co-culture assays. Overall, these findings show the critical role of senescence in disrupting homeostasis of neurotransmitters in the brain, potentially leading to brain pathologies.

Figures

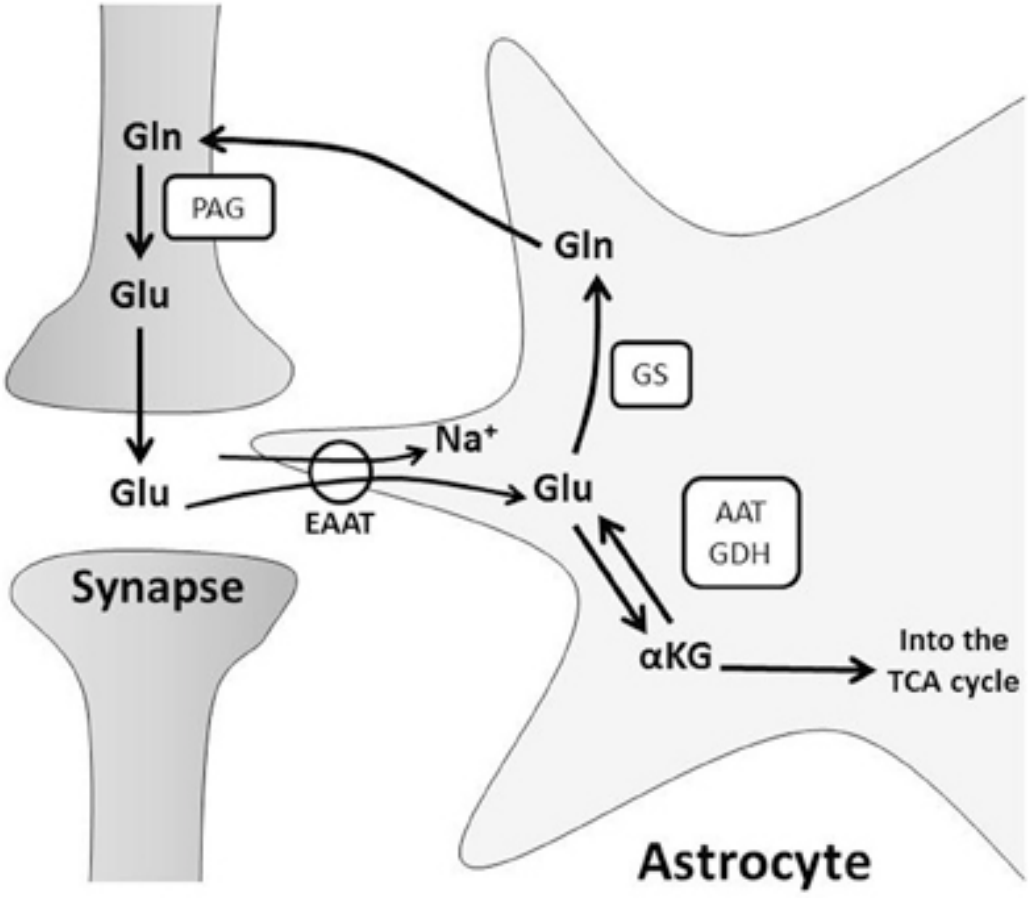

Figure 3.1 Representation of glutamate-glutamine cycles in astrocytes. Neurotransmitter Glu is released from pre-synaptic neurons to stimulate post-synaptic neurons, and the signal is terminated by uptake of Glu from the synaptic cleft into astrocytes. Glu is primarily transported into astrocytes through EAATs transporters. Glu is converted to glutamine (Gln) via glutamine synthase (GS). Gln is shuttled to neurons for glutamate production (Storer et al. 2013).

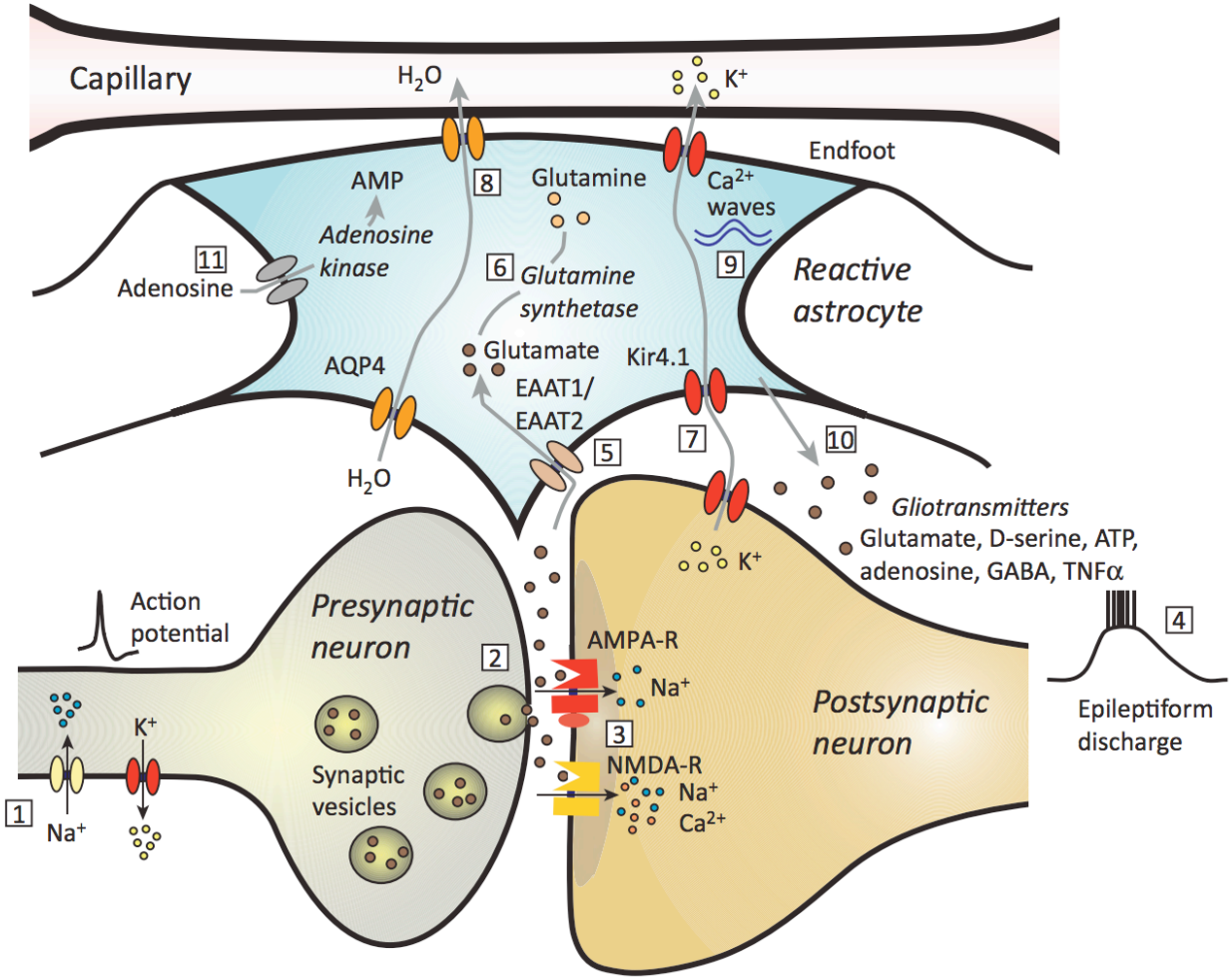

Figure 3.2 Representation of various transporters on astrocytes and interaction between astrocytes and neurons near synapses. Voltage-gated Na+ and K+ channels (1) generate action potentials in the presynaptic neuron, leading to the exocytotic synaptic release of neurotransmitter glutamate (2). Glutamate activates AMPA and NMDA receptors (3) in the postsynaptic membrane, causing excitatory synaptic potentials generated by influx of Na+ and Ca2+ (4). Glutamate is taken up into reactive astrocytes by the EAAT1 (GLAST) and EAAT2 (GLT-1) transporters (5) and is converted to glutamine by glutamine synthetase (6). Glutamine is a substrate for the production of GABA in inhibitory GABAergic neurons (not shown). Loss of glutamine synthetase in reactive astrocytes leads to a decrease in GABA production. K+ released from neurons by voltage-gated (outwardly rectifying) K+ channels enters astrocytes via inwardly rectifying K+ channels (Kir4.1) (7) and is distributed into capillaries. Aquaporin-4 (AQP4) concentrated at astrocytic endfoot processes regulates water balance (8). Ca2+ waves (9) stimulate the release of gliotransmitters (10) that can influence neuronal excitability (Devinsky et al. 2013).

(A)

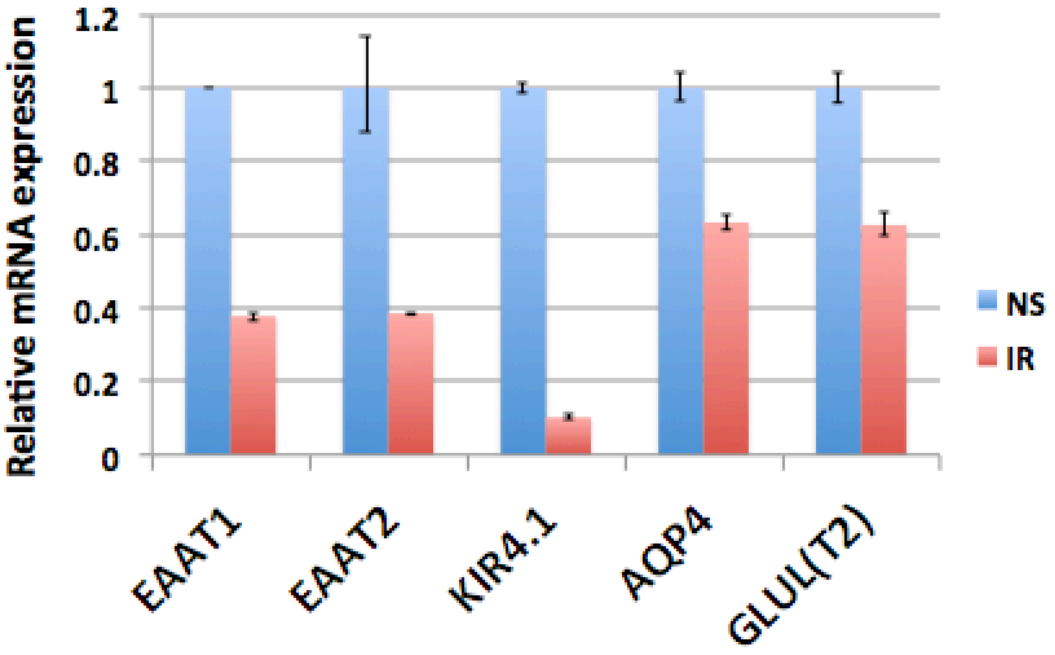

(B)

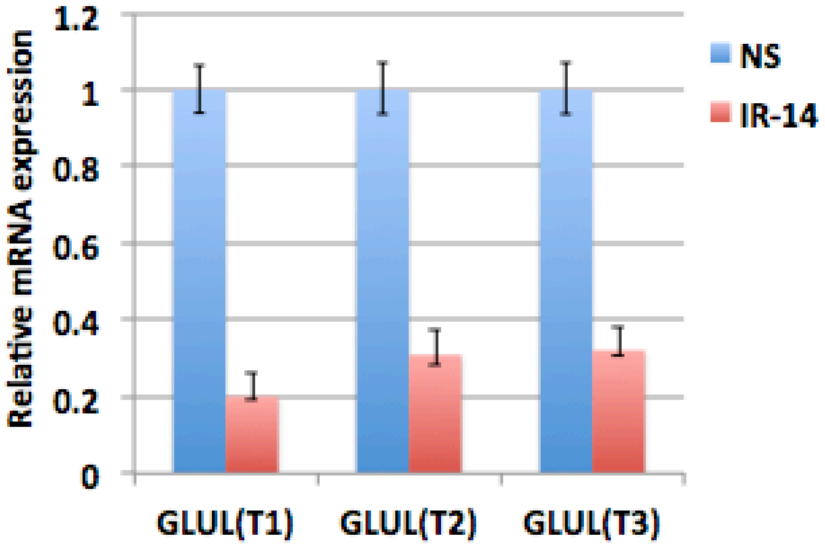

Figure 3.3 X-irradiation-induced senescence causes downregulation of various functional genes at the mRNA level in astrocytes. (A) Real-time PCR was performed for EAAT1, EAAT2, Kir4.1, AQP4, and GLUL using mRNA samples from NS and SEN cells. (B) Real-time PCR was performed on NS and SEN samples to test three different transcripts of glutamine synthetase GLUL(T1), GLUL(T2), GLUL(T3).

(A)

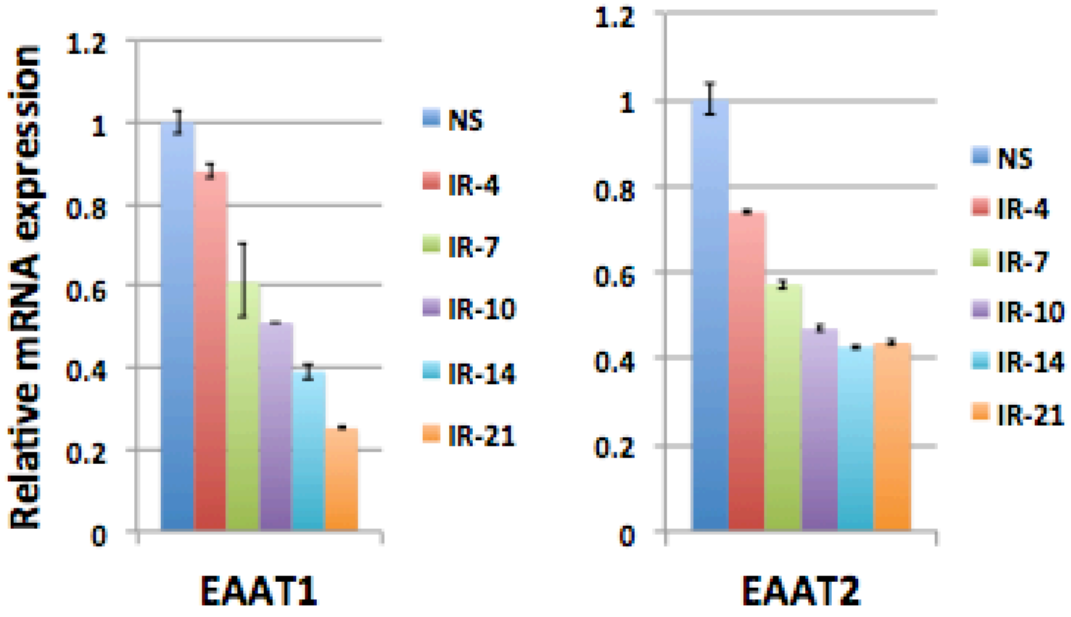
Relative mRNA expression
1.2
1
0.8
0.6
0.4
0.2
0
NS
IR-4
IR-7
IR-10
IR-14
IR-21
EAAT1
EAAT2

(B)

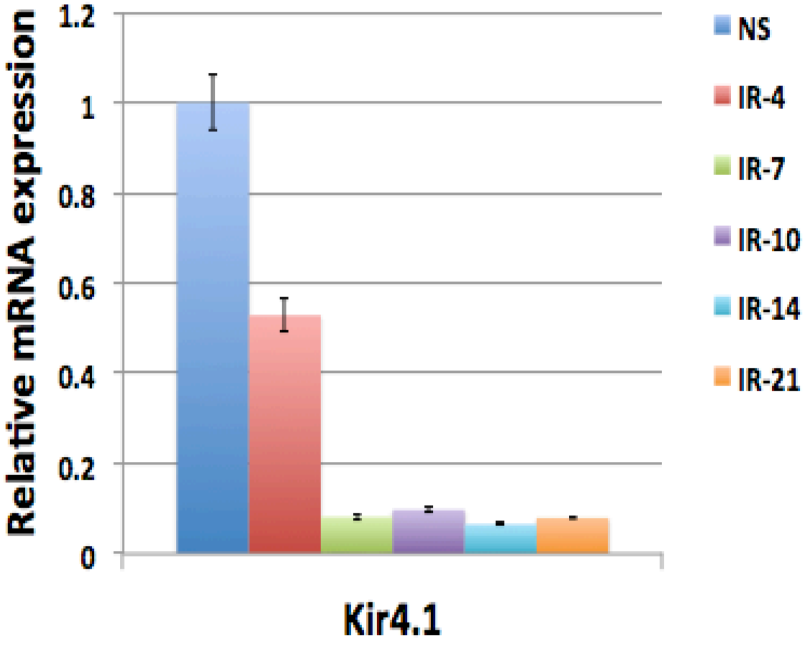
Relative mRNA expression
1.2
1
0.8
0.6
0.4
0.2
0
NS
IR-4
IR-7
IR-10
IR-14
IR-21
Kir4.1

(C)

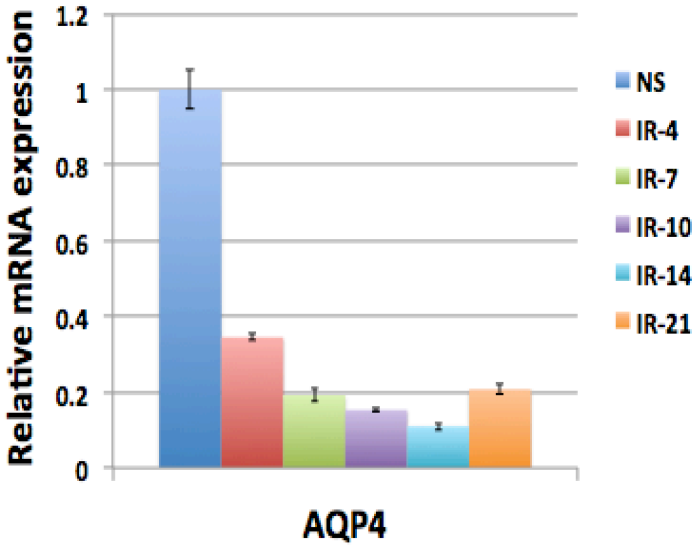

Figure 3.4 Kinetics of downregulation of various transporters in senescent astrocytes. (A-C) Time course experiments were performed on astrocytes after X-irradiation. Samples were collected at Day 7, 10, 14, and 21 after treatment. Real-time PCR was performed on NS samples and SEN samples at the different times. (A) corresponds to EAAT1 and EAAT2 gene expression, (B) corresponds to Kir4.1 gene expression, and (C) corresponds to AQP4 expression.

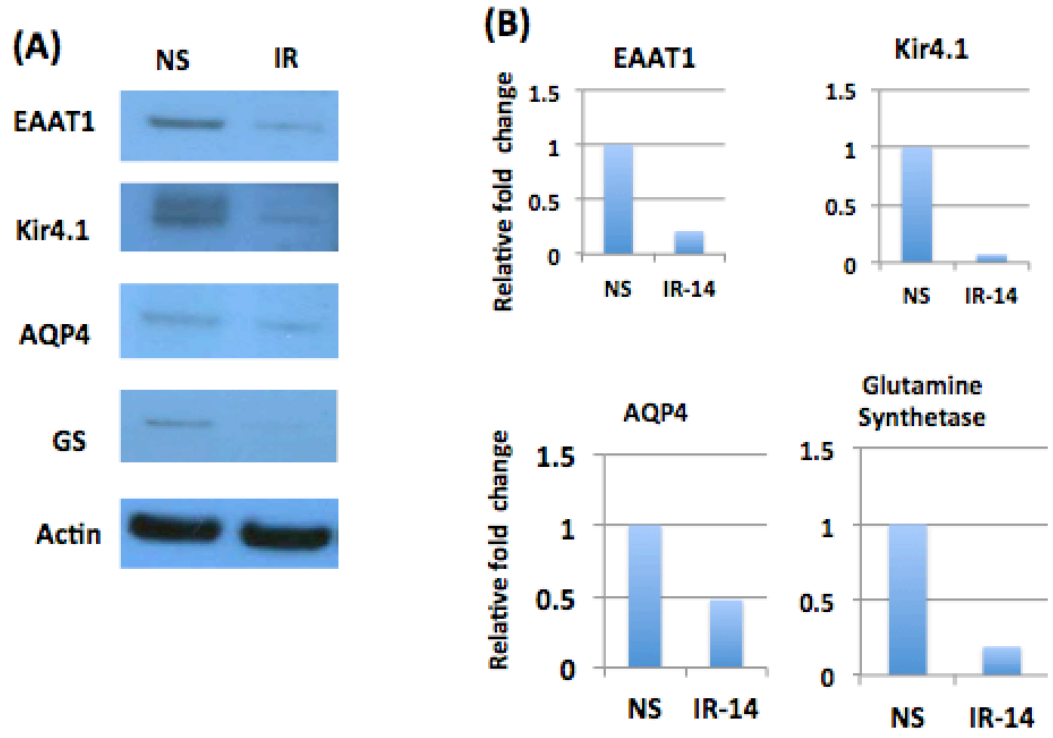

Figure 3.5 X-irradiation-induced senescence causes downregulation of various functional genes at the protein level in astrocytes. (A) Western blotting was performed using extracts from NS and SEN after 14 days X-irradiation. EAAT1, Kir4.1, AQP4, and glutamine synthetase antibodies were used. (B) Western blots shown in (A) were quantified using ImageJ.

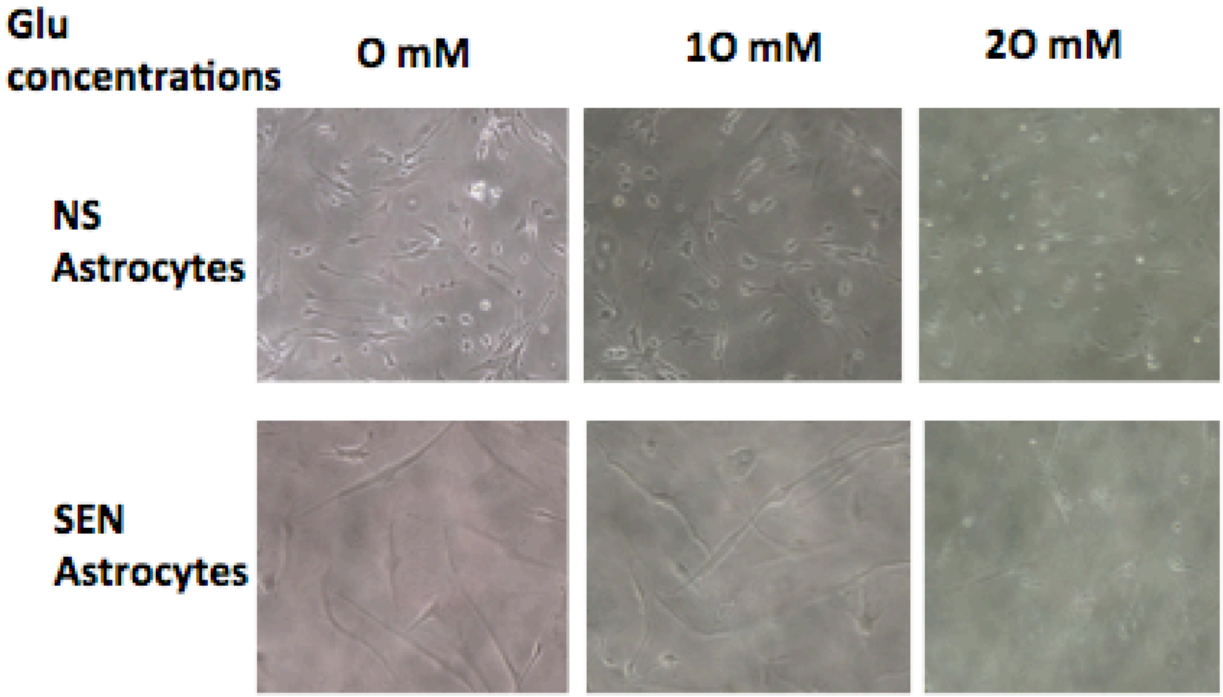

Figure 3.6 10 mM glutamate is the optimal concentration to use on astrocytes. NS and SEN astrocytes were used to determine the optimal concentration of Glu to be used for co-culture assays. Cells were seeded at 5,000/cm2 and treated with 0, 10 or 20 mM of Glu.

(A)

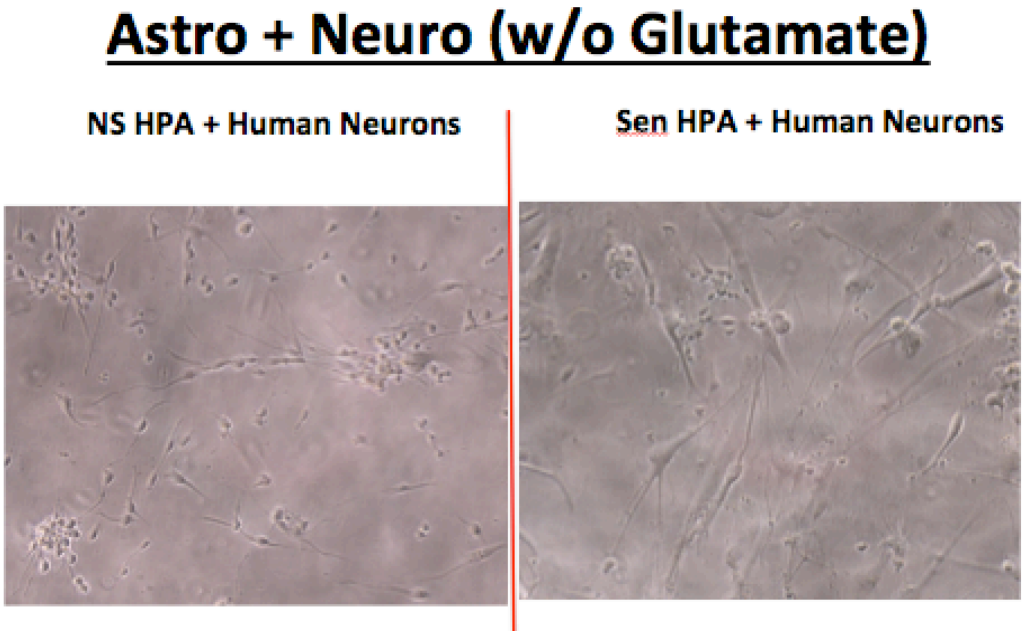

(B)

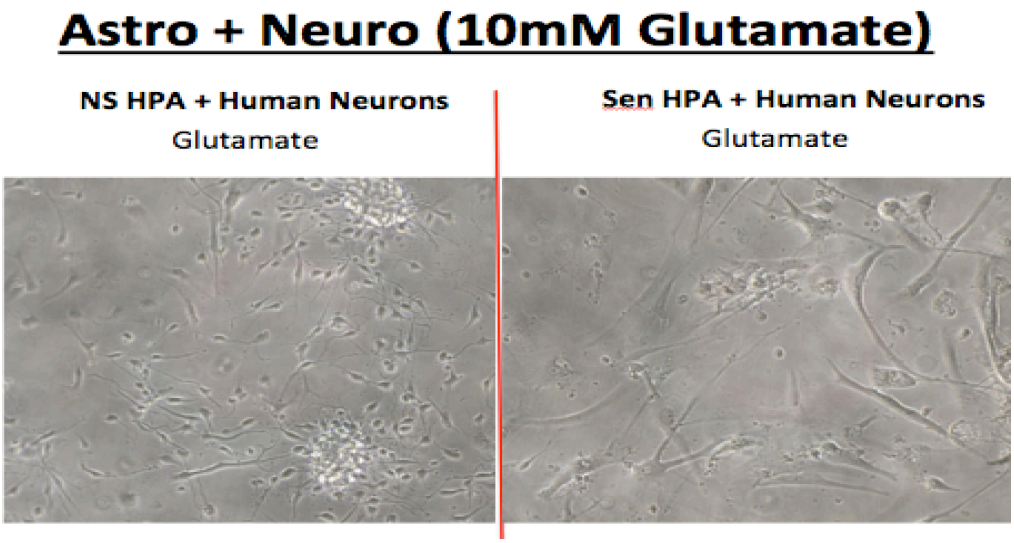

Figure 3.7 Phase contrast images of co-culture assays show neuronal cell death when co-cultured with SEN astrocytes in the presence of 10 mM Glu. (A-B) Neurons (clustered cells) were co-cultured with NS or SEN astrocytes in neuronal media, and the co-cultures were then treated with either (A) control or (B) 10 mM Glu for 24 hours.

(A)

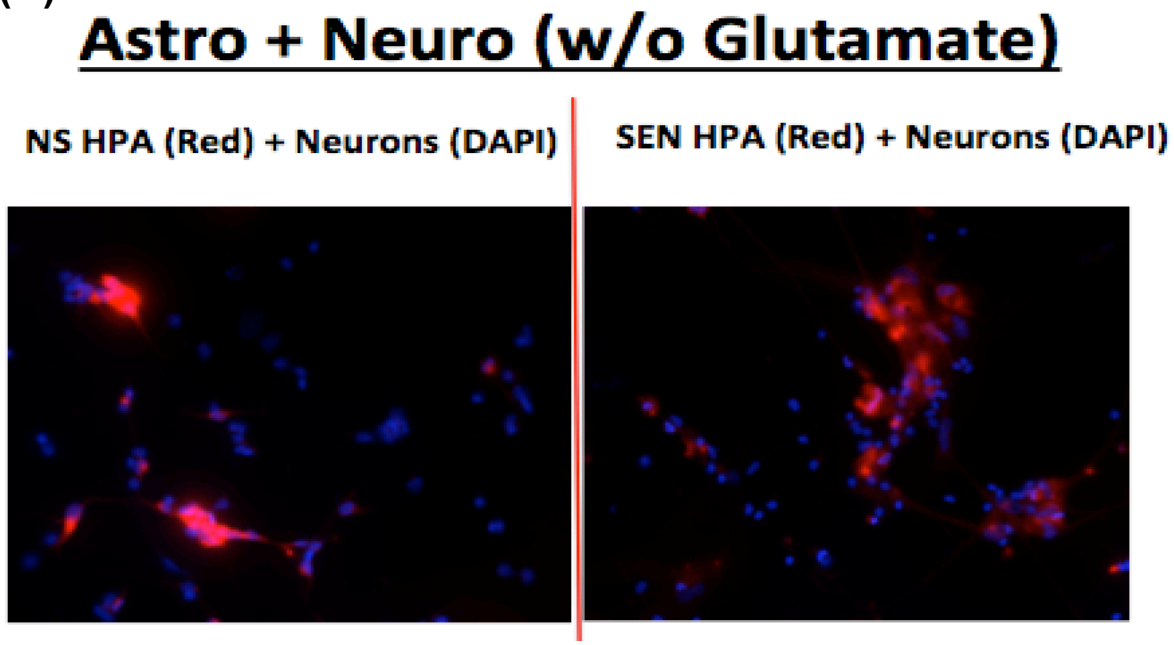

(B)

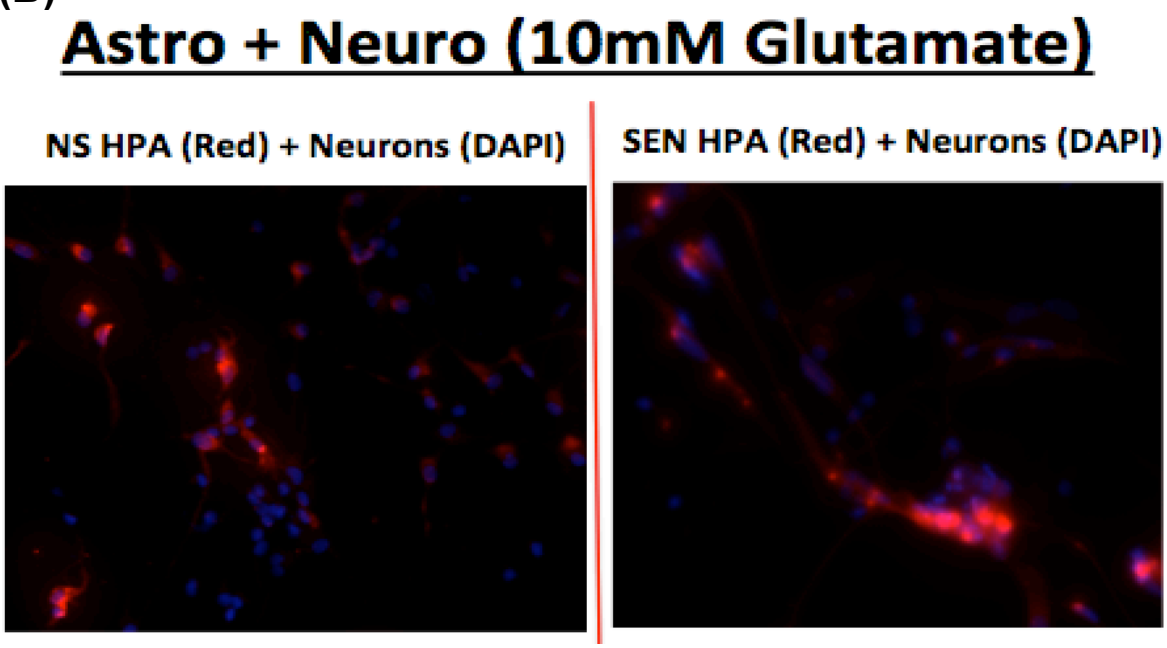
Astro + Neuro (10mM Glutamate)
NS HPA (Red) + Neurons (DAPI)
SEN HPA (Red) + Neurons (DAPI)

(C)

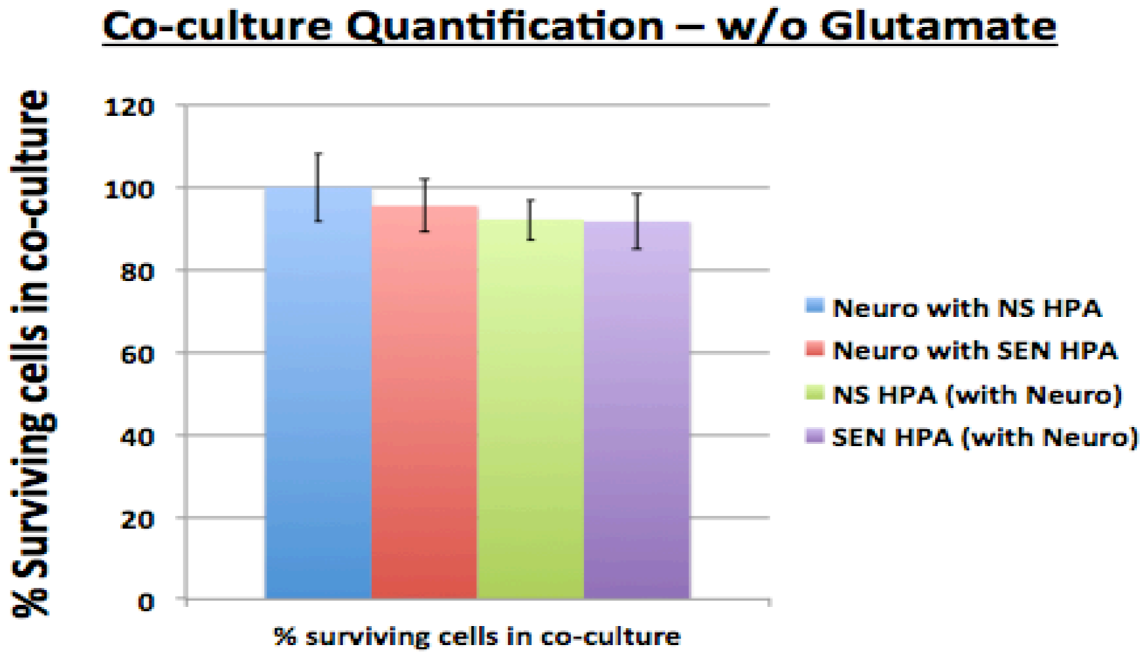
Co-culture Quantification – w/o Glutamate
% Surviving cells in co-culture
120
100
80
60
40
20
0
% surviving cells in co-culture
Neuro with NS HPA
Neuro with SEN HPA
NS HPA (with Neuro)
SEN HPA (with Neuro)

(D)

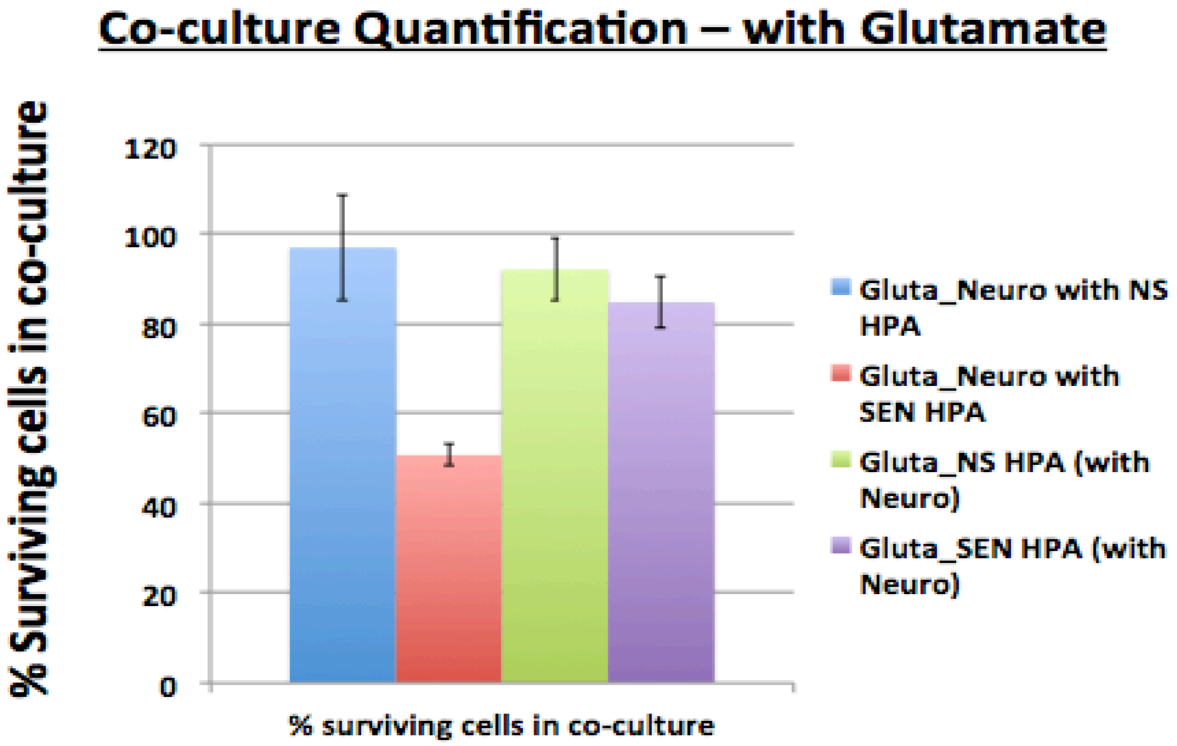

Figure 3.8 Fluorescent images and quantification of neuronal cell survival show that 50% of the neurons co-cultured with SEN astrocytes die in the presence of 10 mM Glu. (A-B) Neurons (only DAPI-stained cells) were co-cultured with NS or SEN astrocytes (CMPTX red + DAPI-stained cells) in neuronal media. The co-cultures were then treated with either (A) control media or (B) media containing 10 mM Glu for 24 hours. (C-D) The quantification of neurons and NS or SEN astrocytes after a 24-hour treatment with either (C) control media or (D) media containing 10 mM Glu is shown.

(A)

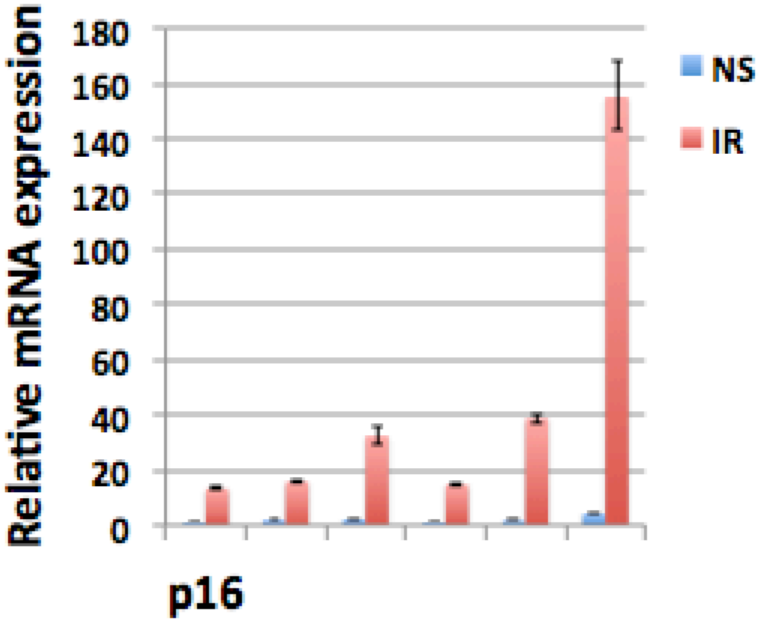

(B)

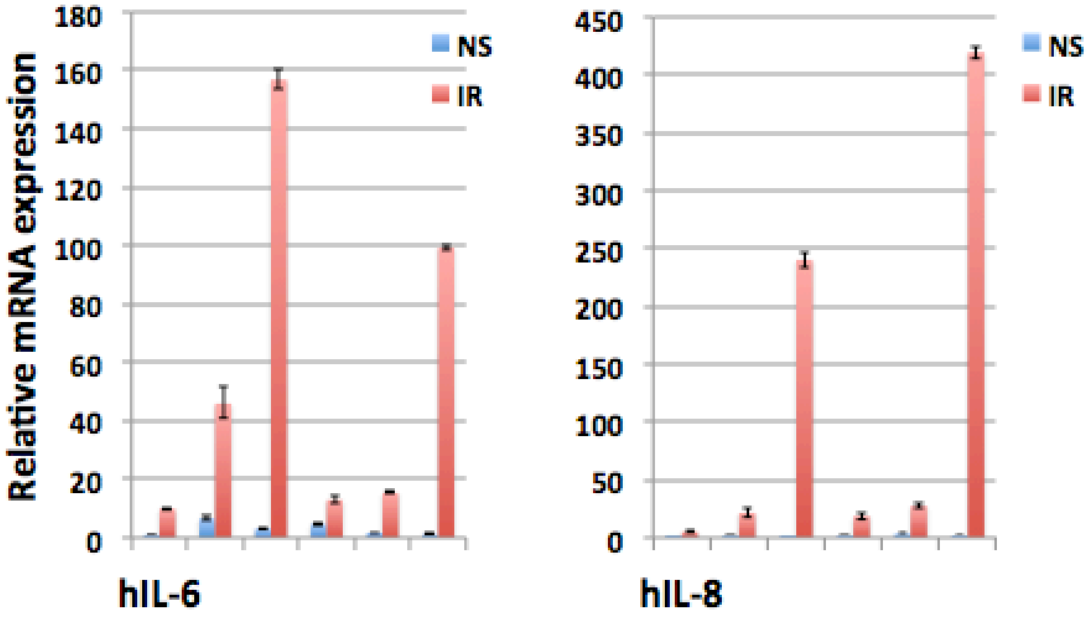

Figure 3.9 RNA extracted from SEN astrocytes corresponding to six different human samples was compared to RNA extracted from NS samples. (A-B) (A) p16 and (B) SASP factors, including IL-6 and IL-8, were analyzed by real-time PCR using RNA extracted from NS and SEN astrocytes obtained from six different individuals.

(A)

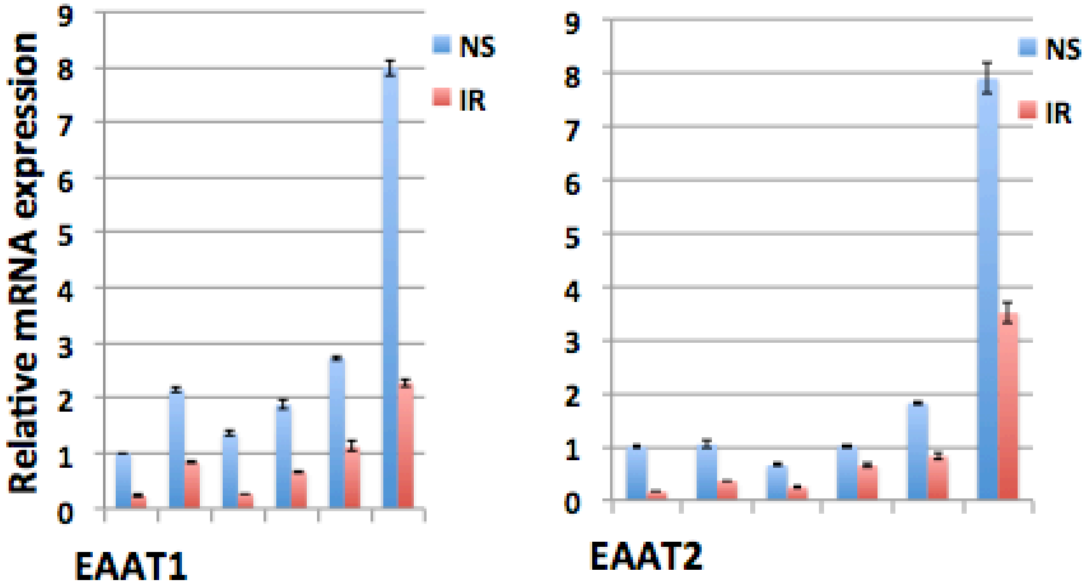

(B)

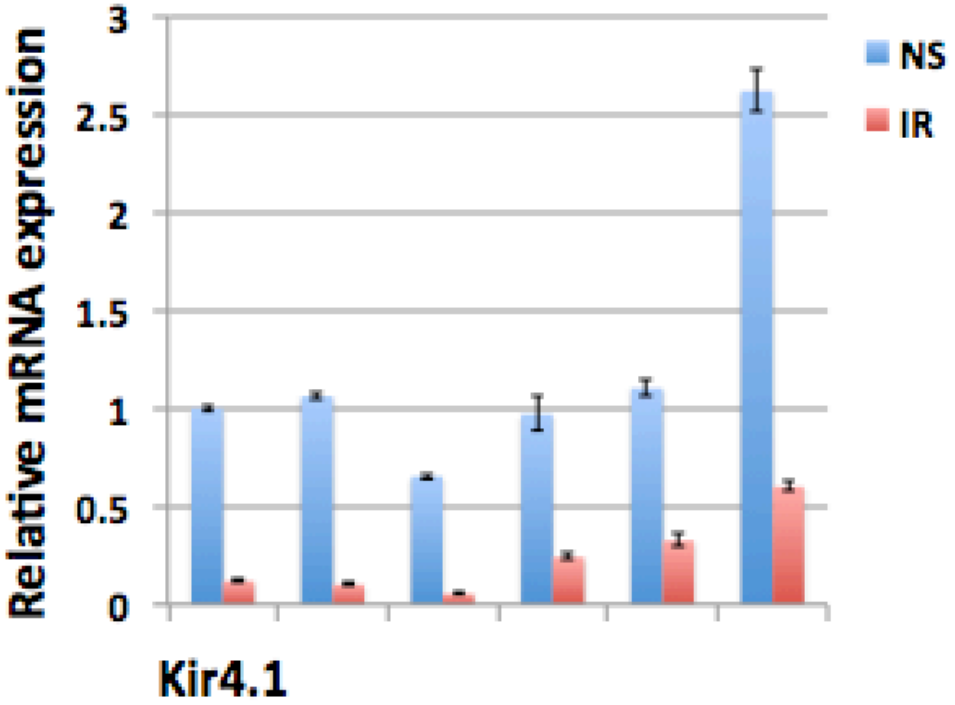

Figure 3.10 SEN astrocytes from six different human samples show a downregulation of glutamate and potassium transporters on Day 14 after irradiation. (A-B) (A) EAAT1 and EAAT2 mRNAs, and (B) Kir4.1 mRNA, were analyzed using real-time PCR in NS and SEN samples from astrocytes obtained from six different individuals.

Sample	Raw Data	After filtering and trimming	Pair Mapped	Multiple Align.	Discordant align.
NS_1	23,809,882	23,403,727	21,062,807 (89.7%)	272,898 (1.3%)	70,179 (0.3%)
NS_2	23,258,856	22,891,123	20,713,954 (90.1%)	262,005 (1.3%)	78,048 (0.4%)
NS_3	20,585,129	20,228,224	18,234,258 (89.8%)	244,790 (1.3%)	69,056 (0.4%)
NS_4	23,682,267	23,395,688	20,988,408 (89.3%)	292,662 (1.4%)	104,818 (0.5%)
NS_5	24,312,598	23,918,805	21,615,591 (90.1%)	278,877 (1.2%)	67,248 (0.3%)
NS_6	21,107,010	20,778,234	18,845,265 (90.4%)	254,497 (1.4%)	69013 (0.4%)
IR_1	25,526,314	25,094,062	22,553,948 (89.5%)	267,033 (1.2%)	86,884 (0.4%)
IR_2	25,858,196	25,429,881	22,858,881(89.6%)	284,919 (1.2%)	7964,026 (0.3%)
IR_3	23,236,065	22,894,407	20,594,937 (89.5%)	253,335 (1.2%)	97,101 (0.5%)
IR_4	23,682,267	23,331,471	21,023,811 (89.8%)	249,858 (1.2%)	83,460 (0.4%)
IR_5	25,643,811	25,238,390	22,749,668 (89.9%)	274,290 (1.2%)	70,478 (0.3%)
IR_6	23,633,802	23,248,316	20,898,565 (89.6%)	272,593 (1.3%)	72,010 (0.3%)

Table 3.1 Results of reads preprocessing and mapping. Summary of Trimmomatics1 results is shown in the 3rd column. The percentage of filtered reads was 1.7 or less across all samples. Summary of TopHat22 results is shown in the 4th-8th columns. The percentage of concordance mapping is between 98% and 90% across all samples.

(A)

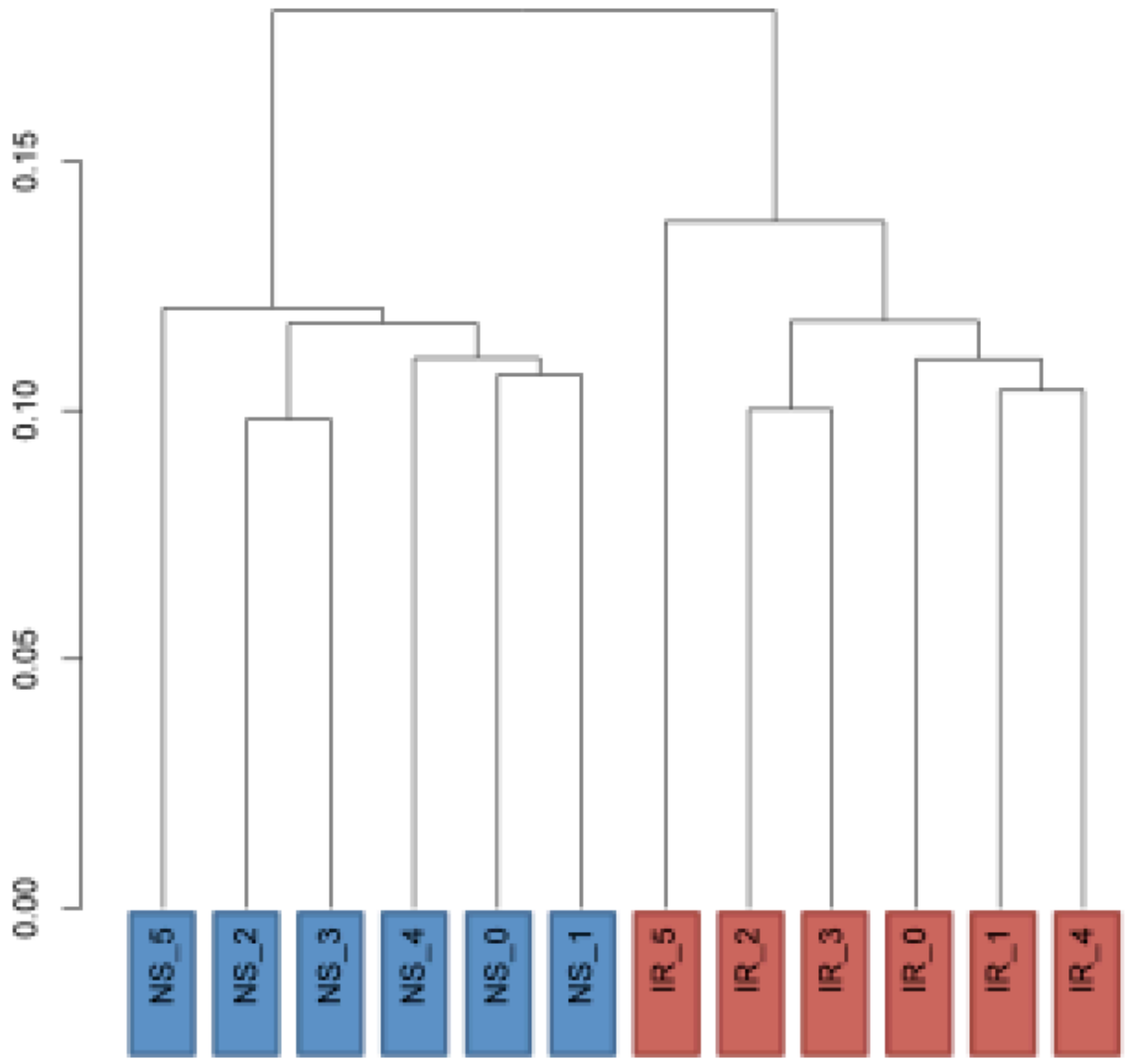

(B)

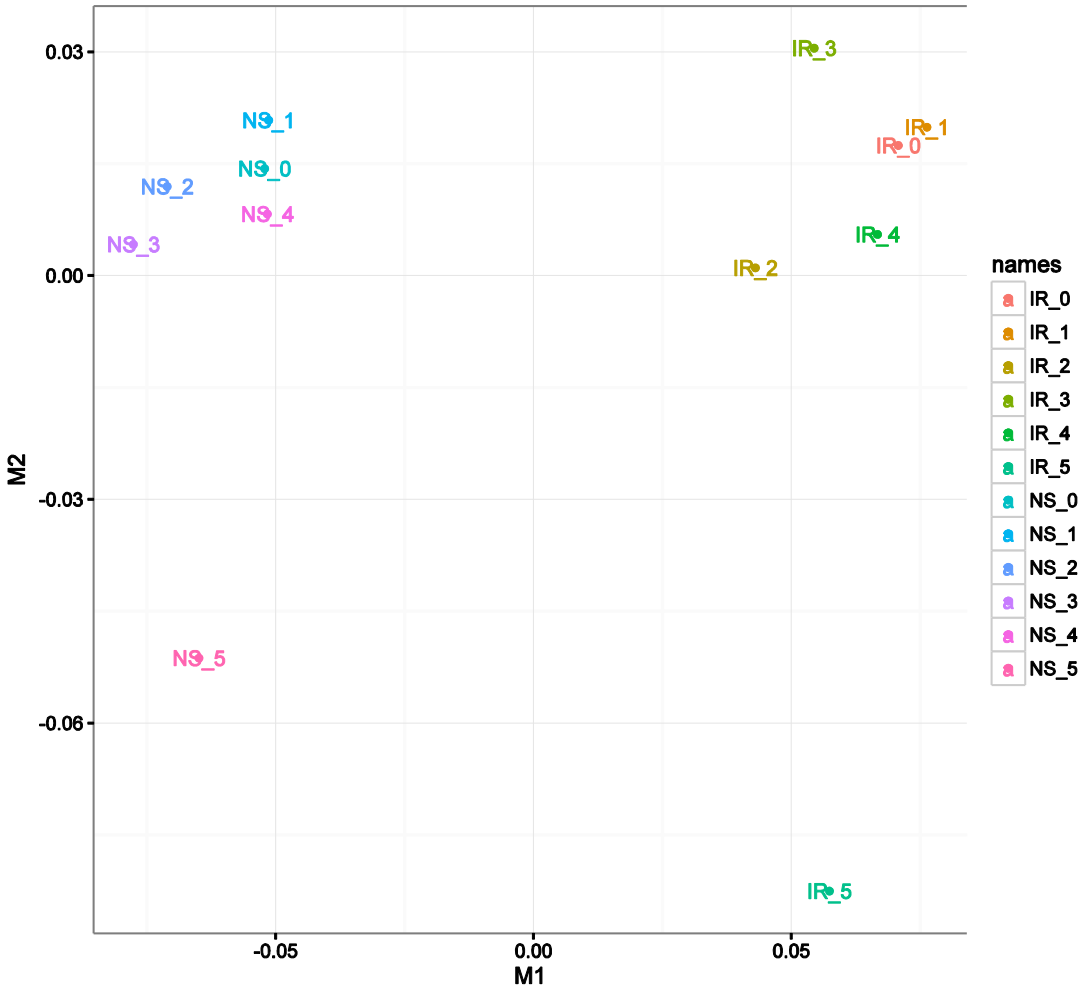

Figure 3.11 Hierarchical Clustering Dendrogram of Jensen-Shannon distances between conditions based on gene expression levels and Multidimensional scaling. (A) Expression levels were normalized (FPKM values) produced by the CsDendro function of the CummeRbund R package. (B) The graph shows the projection of expression levels in normalized FPKM values across all samples on the first two dimensions. Distance on the plot approximates the expression differences between the samples (produced by the MDSplot function of the CummeRbund R package). The plot shows good separation between senescence samples (IR) and control (NS). It also shows separation of one sample in each condition (IR_5 and NS_5) from the rest of the samples in the same condition.

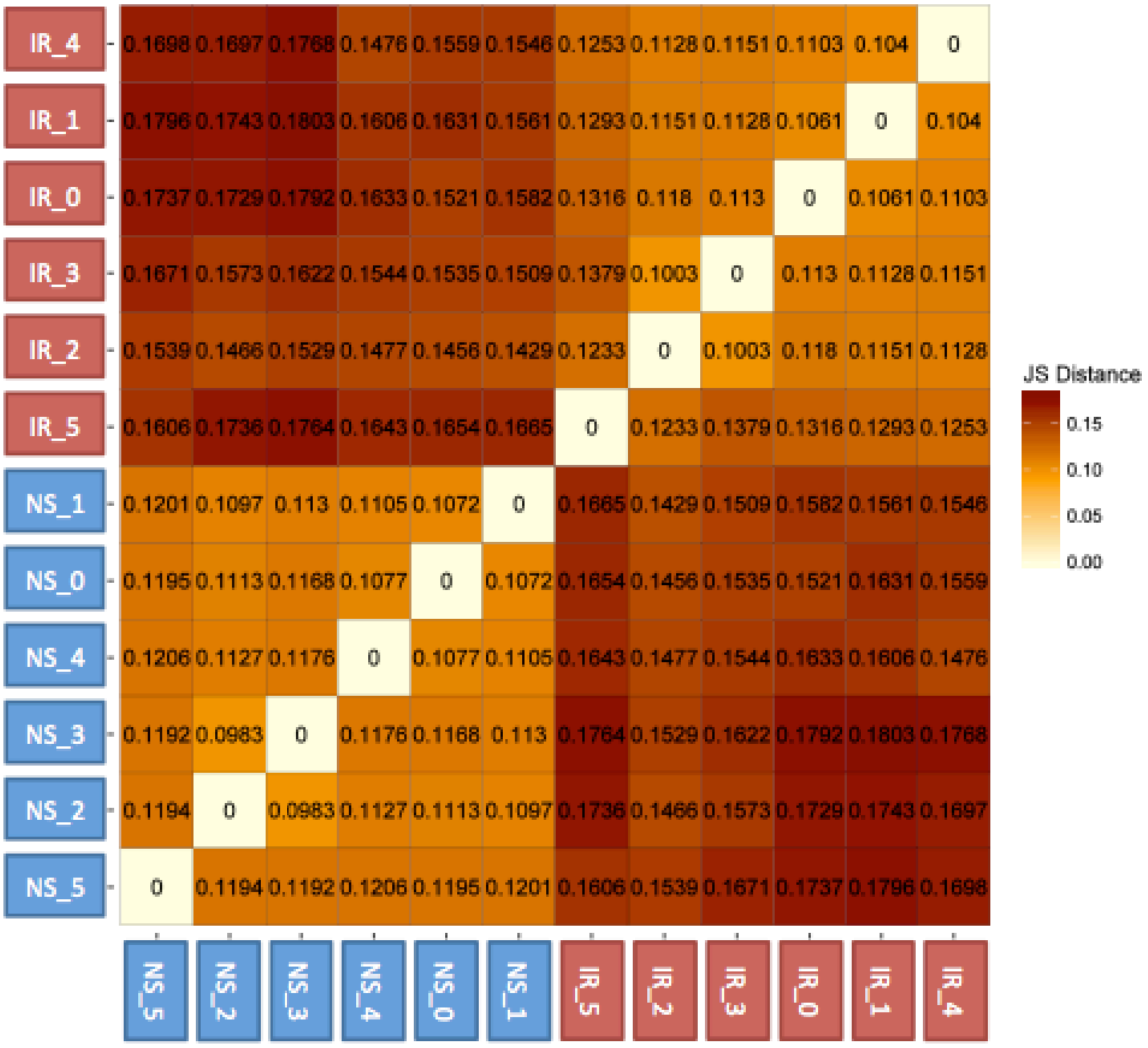

Figure 3.12 Pairwise similarities between replicates and conditions. The heatmap of Jensen-Shannon distances between conditions based on expression levels in normalized FPKM values is shown (produced by the csDistHeat function of the CummeRbund R package).

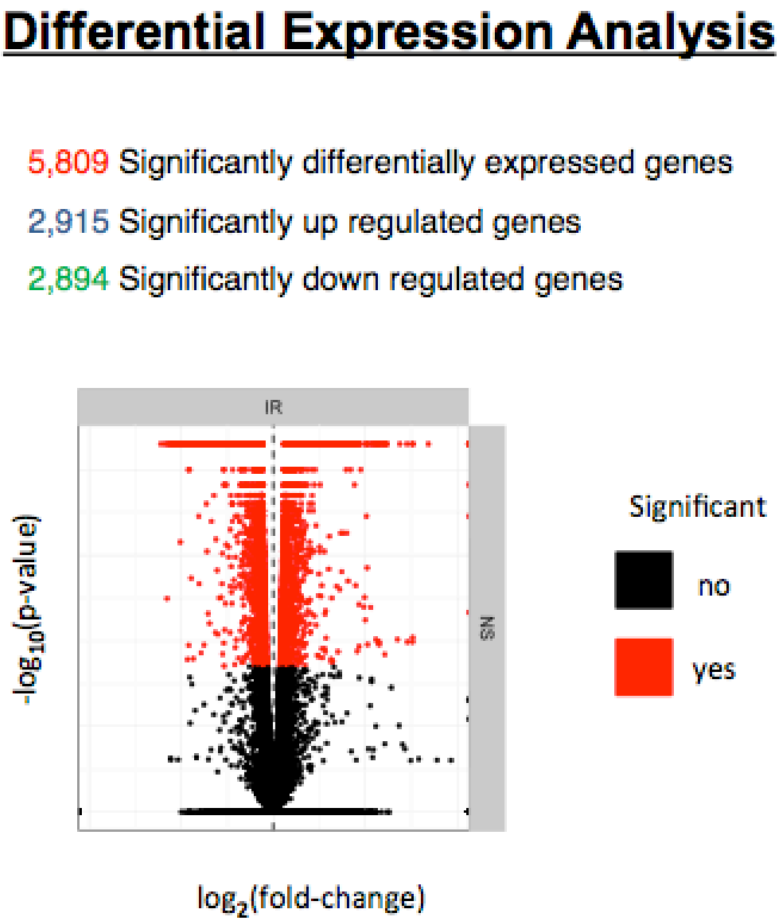

Figure 3.13 Volcano plot of differentially expressed genes. The X axis shows the log fold change in expression values between senescence (IR) and control (NS). The Y axis shows the statistical significance of the differences as log(p-val).

Gene Id	Gene Name	locus	NS	IR	log2(fold_change)	p_value	q_value	significant
SLC1A3	EAAT-1	Chr5 36606354-36688334	162.23	44.19	-3.84	5.00E-05	0.00025	yes
SLC1A2	EAAT-2	Chr11 35251204-35420063	5.20	1.89	-1.46	5.00E-05	0.00025	yes
KCNJ10	Kir4.1	Chr1 160037466-160070261	11.95	1.99	-5.16	5.00E-05	0.00025	yes
CDKN2A	P16	Chr9 21967138-21994491	24.96	120.88	5.0	5.00E-05	0.00025	yes

Table 3.2 RNA-seq data confirming downregulation of glutamate and potassium transporters and upregulation of p16 in IR (SEN) astrocytes compared to NS astrocytes.

Chapter 4: Investigation of senescence in the brain using mouse models

4.1 Induction of brain senescence/SASP during natural aging of C57BL/6 mice

To study the senescent phenotype in the brain, I used young and old C57BL/6 mice. I harvested the brains from three different age groups of mice (3, 20 and 26 months). Since the cortex region contains a high number of astrocytes, I first extracted RNA from the cortex. RNA was isolated as described in the Material and Methods section. RNA analysis for senescent markers showed that p16 was significantly unregulated in the cortex of 20- and 26-months old mice compared to 3-months young controls (Figure 4.1A). I also investigated the expression of some SASP factors, including IL-6, CXCL-1, CXCL-10 and IL-1b, all of which were upregulated in the samples from 20- and 26-months old mice compared to the 3-months young controls (Figure 4.1B-E).

Then, in order to determine how the senescence profile varies in different parts of the brain at different ages, I isolated brain samples from various age groups of mice starting from 2 months to 22 months (Table 4.1). Ten different brain parts were harvested (Table 4.2), and Figure 4.2 shows the location of each part of the brain that I analyzed.

I performed RNA analysis for the expression of senescent markers and SASP factors. The results showed that p16 and SASP factors were upregulated in various brain regions of aged mice compared to the 2-months control group (Figure 4.3 A-D). All the brain parts showed gradual upregulation of p16 with age, except in the amygdala (amygdala showed the pick of p16 expression in the samples from 12-months old mice). The SASP factors were gradually upregulated with age in all parts of the brain whereas LMNB1 was downregulated in most of the brain regions at 19 months of age, except in the mid brain and cerebellum. At 22 months of age, frontal cortex, striatum, thalamus and olfactory bulb showed downregulation of LMNB1, a decline that was not detected in the other brain regions. Overall the strongest downregulation of LMNB1 was found in striatum in aged mice compared to samples obtained from 2-months mice.

These experiments using wild type mice indicate that senescence and the SASP are induced in the brain of naturally aging mice.

4.2 Irradiation induces senescence and a SASP in C57BL/6 mice brain

To determine whether radiotherapy employed for brain cancer treatment could induce senescence in the brain, I treated mice with non-lethal dose of 7 Gy of X-irradiation (IR) (and mock irradiation was used as a control). I used the p16-3MR transgenic mouse model on a C57BL/6 background that I previously mentioned in Chapter 1 (Demaria et al. 2014). Briefly, senescent cells in this model become luminescent and fluorescent, due to the presence of luciferase and red fluorescence protein under the p16 promoter that is specifically expressed during senescence (Figure 4.4). This feature allows us to monitor the accumulation of senescent cells in vivo. This

mouse model also allows us to specifically eliminate senescent cells by administering a drug called ganciclovir (GCV).

The mice were irradiated at the age of 3 months, and four months after irradiation the mice were euthanized and brain samples were collected. Figure 4.5 shows the experimental timeline. I found that luminescence was significantly upregulated in IR-treated mice compared to mock-treated mice (Figure 4.6A). RNA analysis showed that p16 and two major SASP factors were upregulated in IR samples compared to mock samples (Figure 4.6B-D). This set of data demonstrates that irradiation causes induction of senescence in the brain and triggers the upregulation of inflammatory factors.

4.3 Induction of senescence/SASP in a mouse model of Alzheimer's disease

To investigate the potential role of senescence in neurodegenerative diseases, I used an Alzheimer's disease (AD) mouse model called J20. This J20 model overexpresses the human amyloid precursor protein (APP) that harbors two mutations linked to familial AD (the Swedish and Indiana mutations). Mutant APP expression is driven by the human platelet-derived growth factor (PDGFb chain) promoter, thus enabling high levels of expression of human APP in neurons (Figure 4.7) (Mucke et al. 2000). To test for the presence of senescence in J20 mouse brains, I isolated both cortex and hippocampus tissues from 12-months old J20 and age-matched wild type (WT) mice as controls.

RNA analysis showed that p16 and two major SASP factors (CXCL10 and MMP3) were upregulated in the hippocampus of J20 mice compared to WT controls (Figure 4.8A-C). The cortex samples did not show any significant difference between J20 and WT mice regarding the expression of p16 and the two SASP markers (Figure 4.9). Further, I tested whether the expression of the glutamate (GLAST, GLT-1) and potassium (Kir4.1) transporters was affected in J20 mice compared to WT mice. The results showed that GLAST, GLT-1 and Kir4.1 were significantly downregulated at the RNA level in J20 mouse hippocampus compared to the WT hippocampus samples (Figure 4.10), whereas cortex samples did not show any difference (data not shown).

These results indicate that senescence is induced in a mouse model of AD and creates an inflammatory environment in the brain. I also found that there is a correlation between the induction of senescence and the downregulation of glutamate and potassium transporters in the hippocampus, suggesting that senescence may be the cause of the downregulation of various transporters in AD, and may be responsible for glutamate toxicity and neuronal death.

Figures

(A)

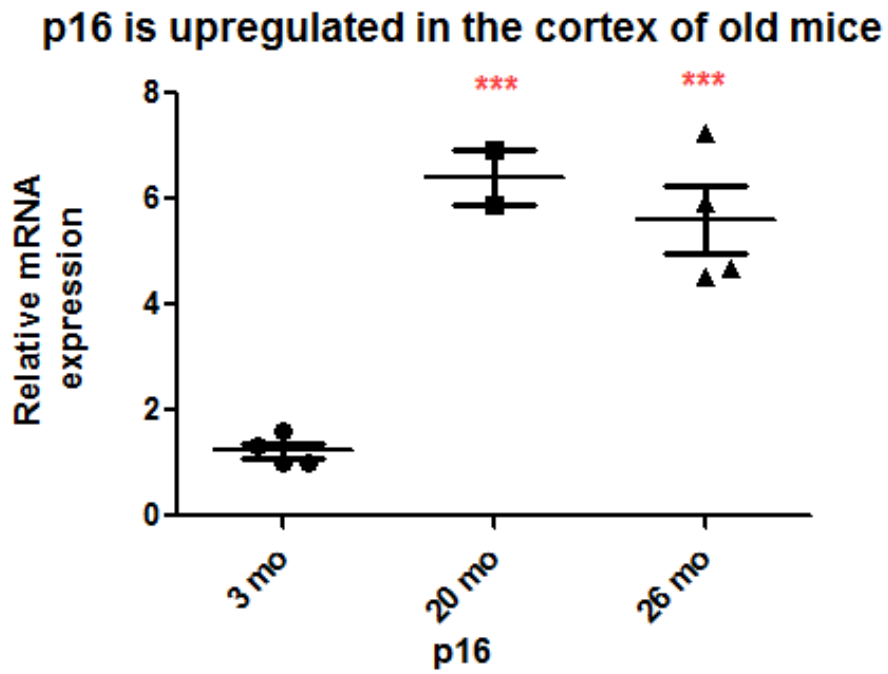
p16 is upregulated in the cortex of old mice
Relative mRNA expression
0
2
4
6
8
***
***
3 mo
20 mo
26 mo
p16

(B)

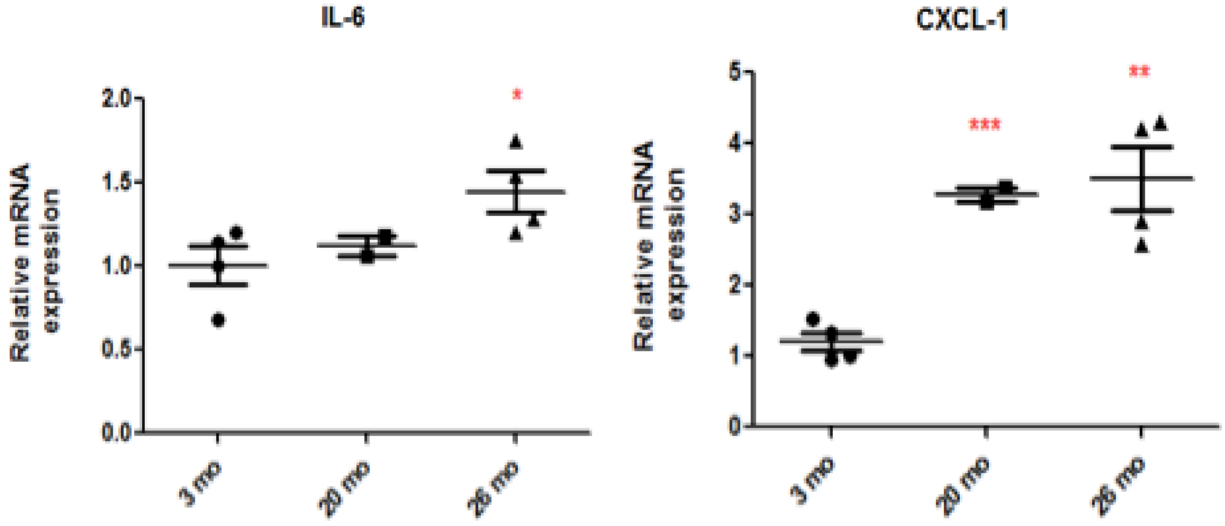
IL-6
Relative mRNA expression
0.0
0.5
1.0
1.5
2.0
*
3 mo
20 mo
26 mo
CXCL-1
Relative mRNA expression
0
1
2
3
4
5
***
**
3 mo
20 mo
26 mo

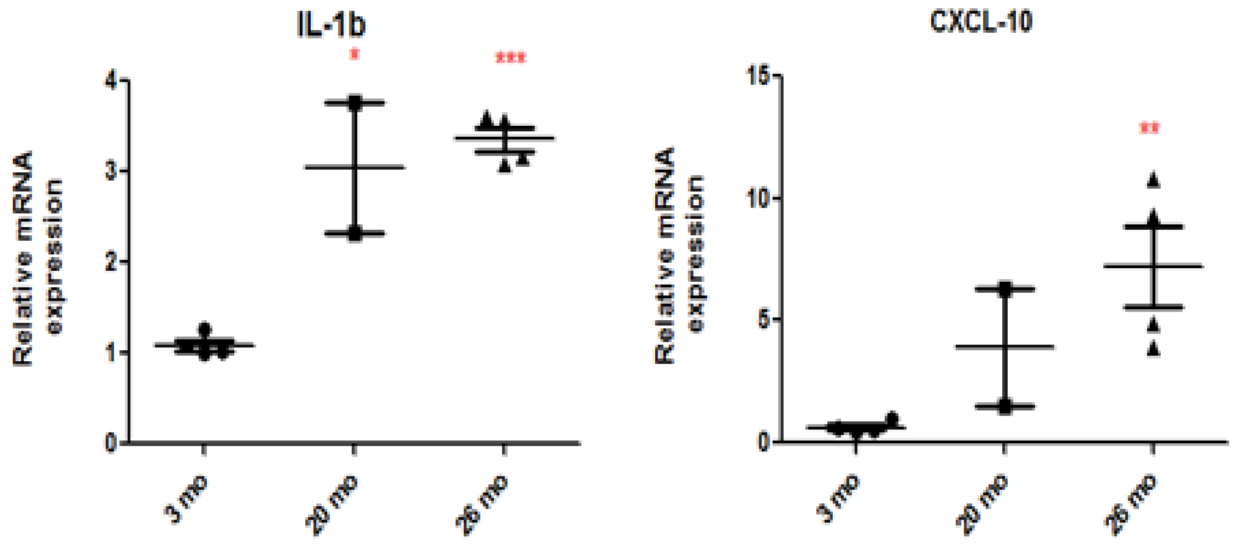

Figure 4.1 Senescence markers are upregulated in the mouse brain during natural aging. (A) Brain cortex samples from 3-month, 20-month, and 26-month old mice were tested for the expression of p16 using real-time PCR. (B) Brain cortex samples from 3-month, 20-month, and 26-month old mice were tested for the expression of SASP factors, including IL-6, IL-1b, CXCL-1, CXCL-10, using real-time PCR.

Gender	Age Groups	Quantity
Males	2 mo	5
	6 mo	5
	12 mo	5
	19 mo	5
	22 mo	5

Table 2.1 List of gender, age and number of mice used for analyzing various parts of the brain at the mRNA level.

	Brain Parts	Functions
1	Olfactory Bulb	Sense of smell
2	Frontal Cortex	Decision Making
3	Striatum	Facilitating voluntary movement
4	Thalamus	Homeostasis and Hormones
5	Hypothalamus	Homeostasis and Hormones
6	Mid Brain	Vision, Hearing and Movement
7	Hippocampus	Memory
8	Cerebellum	Motor functions
9	Amygdala	Emotions
10	Cortex	Thinking, Planning

Table 4.2 List of brain regions that were analyzed in various age groups of mice using real-time PCR.

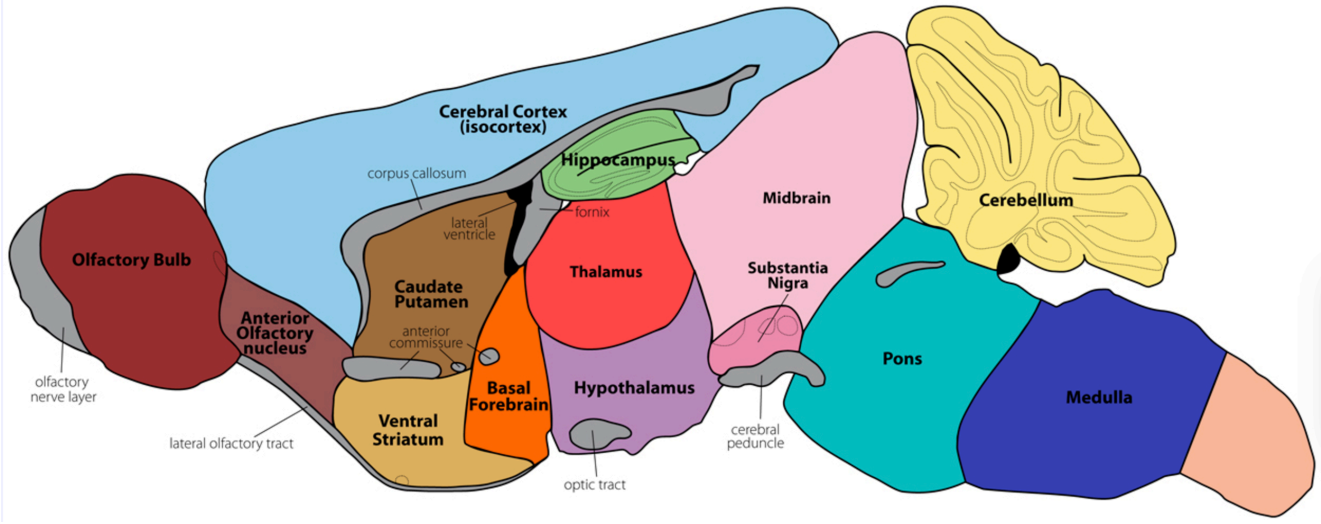

Figure 4.2 Visual location of the different parts of the brain that were analyzed in various age groups of mice using real-time PCR. (Ref: http://www.gensat.org/imagenavigator.jsp?imageID=19977).

(A)

p16

	2 mo	6 mo	12 mo	19 mo	22 mo
Hippo	1	2.879613127	6.588157293	8.720283268	16.95189909
F. Cortex	1	5.344296314	9.072499046	20.35766231	18.71988932
Striatum	1	4.015974197	6.605876509	12.36979769	14.61370414
Hypothalamus	1	1.816716538	7.340271028	12.23831755	8.918699362
Mid Brain	1	1.297546026	5.097485316	7.951823386	17.97332864
Amygdala	1	12.24821833	31.85614969	20.11221399	23.18307447
Cerebellum	1	2.235348855	4.307945505	8.473746677	20.75662533
Thalamus	1	3.120981921	11.49950615	11.07703607	17.39981425
Olfactory	1	7.285358669	19.85595712	33.80114001	37.28439431

(B)

LMNB1

	2 mo	6 mo	12 mo	19 mo	22 mo
Hippo	1	0.986232704	1.016070143	0.96761162	1.029896957
F. Cortex	1	0.904379378	0.989999705	0.946385582	0.92562517
Striatum	1	0.832775771	0.811127156	0.818469182	0.825019429
Hypothalamus	1	0.965267025	1.017127122	0.879039561	1.067695309
Mid Brain	1	1.000346634	0.966271155	1.058484395	1.047899238
Amygdala	1	0.897199051	0.929482753	0.791137301	1.110338834
Cerebellum	1	1.078854269	1.084477409	1.00556058	1.174055004
Thalamus	1	0.906576079	0.903752727	0.921464186	0.937246215
Olfactory	1	0.902500727	0.894094978	0.85027416	0.934651216

(C)

CXCL10

	2 mo	6 mo	12 mo	19 mo	22 mo
Hippo	1	0.973329374	2.363623094	1.63977742	2.953652292
F. Cortex	1	2.200757219	3.894667052	3.399918114	5.022828443
Striatum	1	1.526259209	4.334903867	5.747760706	6.832909411
Hypothalamus	1	3.335724175	3.279554841	4.092549879	5.466055089
Mid Brain	1	1.066955495	2.190864106	4.444434915	4.768382607
Amygdala	1	0.977047089	2.612624884	4.152557082	3.73471978
Cerebellum	1	1.612724494	4.639598618	5.031539887	9.583150328
Thalamus	1	2.372651155	2.208397694	6.448662652	11.49950615
Olfactory	1	1.494849249	1.820708548	1.514666316	2.318995467

(D)

IL-1b

	2 mo	6 mo	12 mo	19 mo	22 mo
Hippo	1	1.556170353	3.30351066	2.427548299	6.795124574
F. Cortex	1	1.29145735	2.299786603	1.74896328	2.288654996
Striatum	1	1.439931319	3.246758324	3.338037125	5.301865236
Hypothalamus	1	1.258757174	3.094057483	3.090842199	5.658815106
Mid Brain	1	1.645470315	4.026426505	3.901421846	7.11813848
Amygdala	1	1.764794256	3.927197082	4.016670173	7.310651602
Cerebellum	1	0.923702386	3.03774338	2.286276671	5.903211371
Thalamus	1	1.855103911	3.008407503	3.305801273	7.607909053
Olfactory	1	1.151887642	1.653473587	1.353786279	3.223214052

Figure 4.3 Senescence markers are upregulated at the RNA level in various regions of the mouse brain during natural aging. Several brain regions from various

age groups of mice were isolated as described in Tables 4.1 and 4.2. RNA was extracted and all the samples were tested for senescence markers, including (A) p16 (B) LMNB1, and some SASP factors, including (C) CXCL-10 and (D) IL-1 beta.

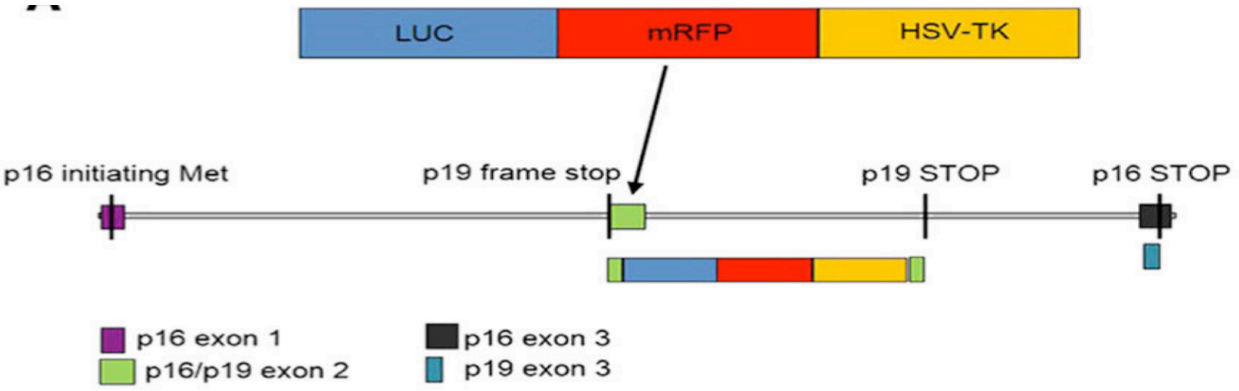

Figure 4.4 Schematic representation of the p16-3MR (tri-modality reporter) transgene (Demaria et al. 2014).

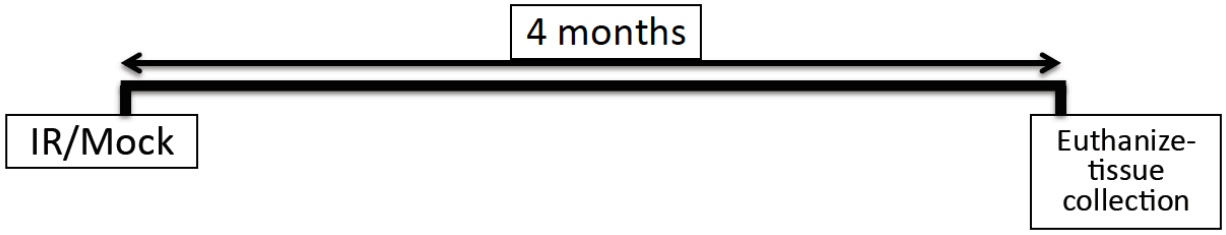

Figure 4.5 Schematic representation of timeline and approach for the irradiation experiments in vivo.

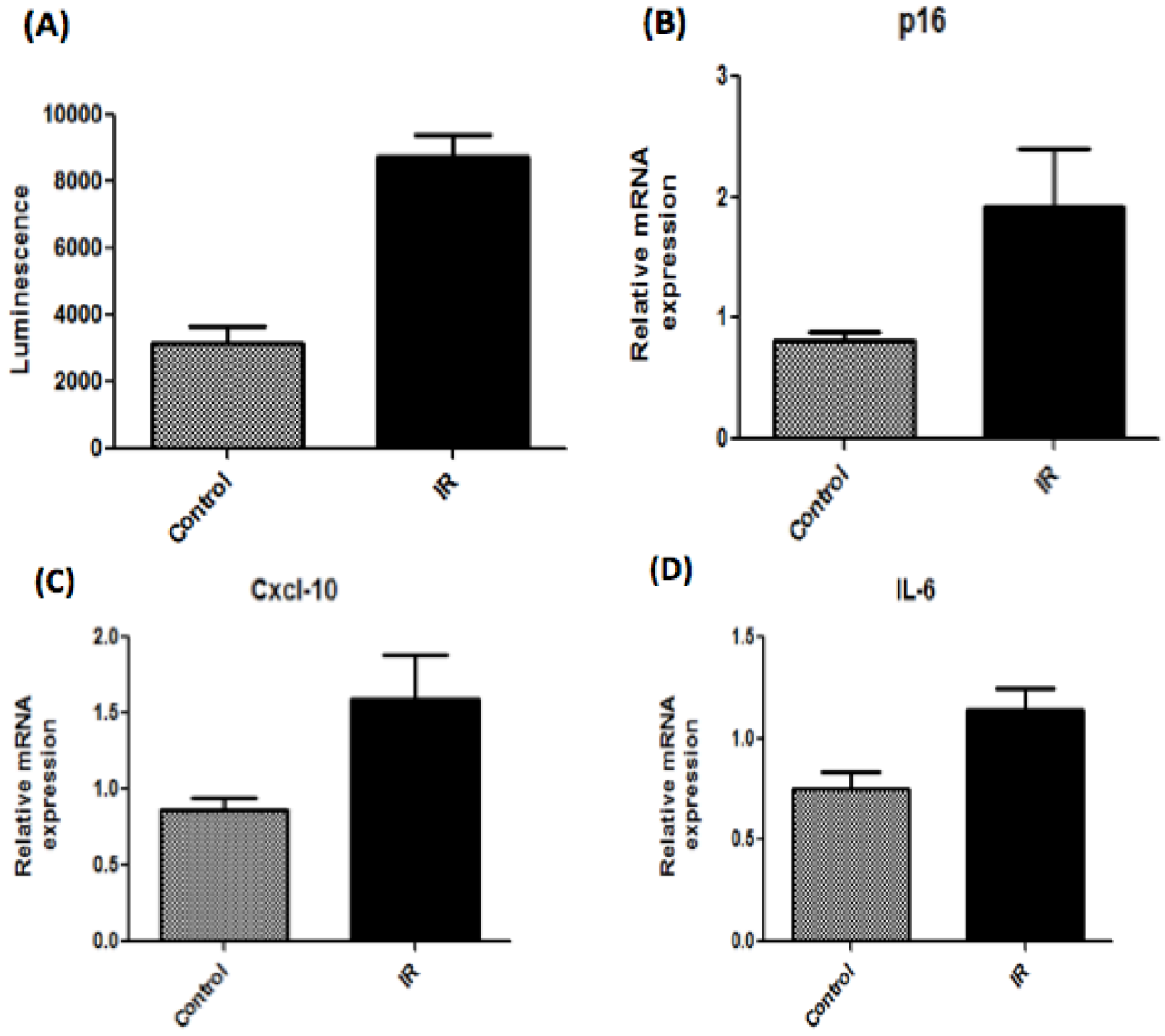

Figure 4.6 Senescence occurs in the brain of irradiated mice. (A) Luminescence was measured in 3MR mice upon irradiation compared to non-irradiated mock controls. (B) Real-time PCR was performed for p16 in IR and control brain samples. (C-D) SASP factors, including CXCL-10 and IL-6, were analyzed at the mRNA level in IR and control brain samples.

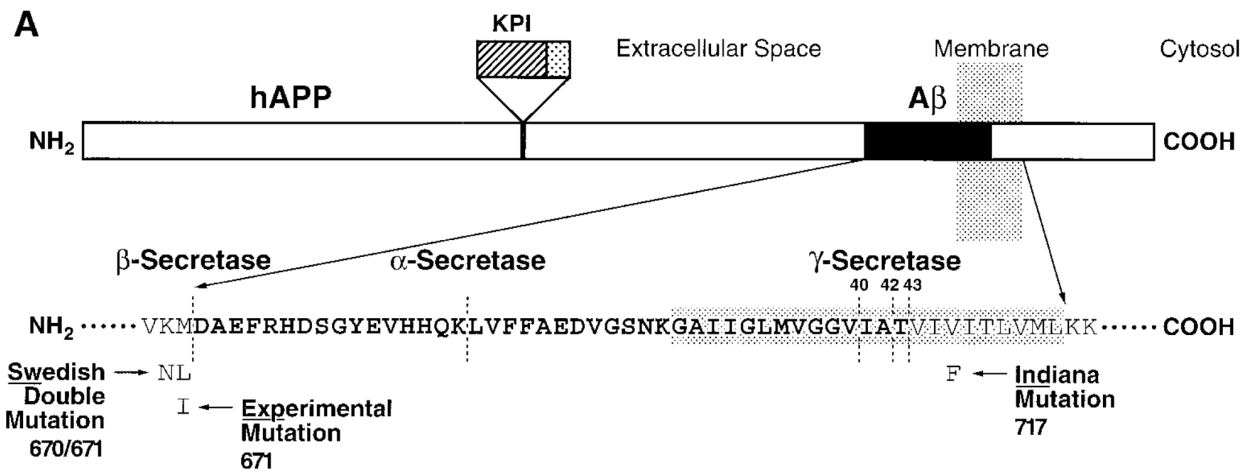

Figure 4.7 Schematic representation of the J20 transgene (Mucke et al. 2000).

(A)

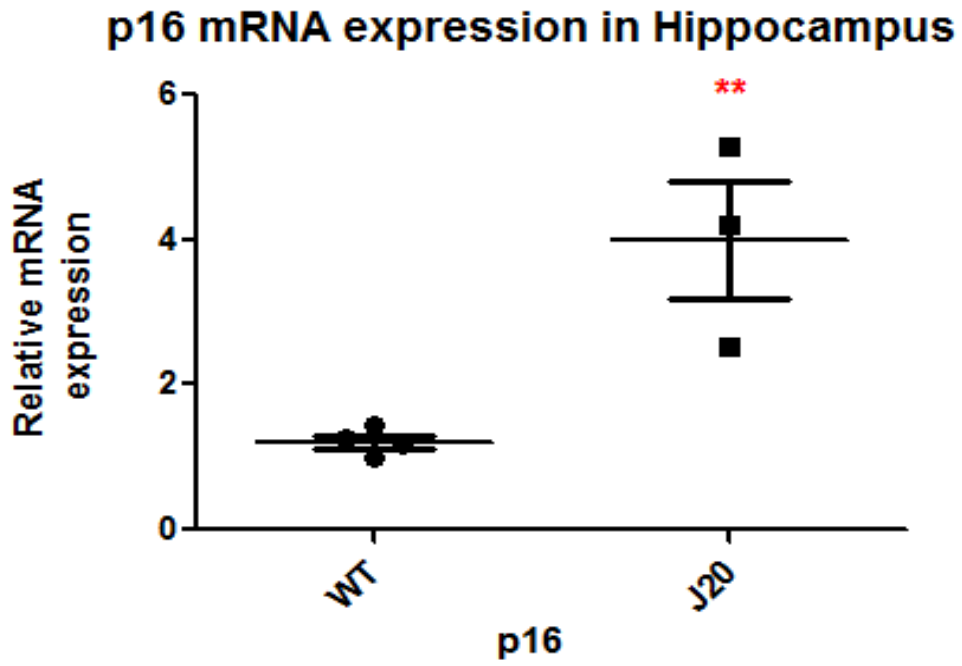

(B)

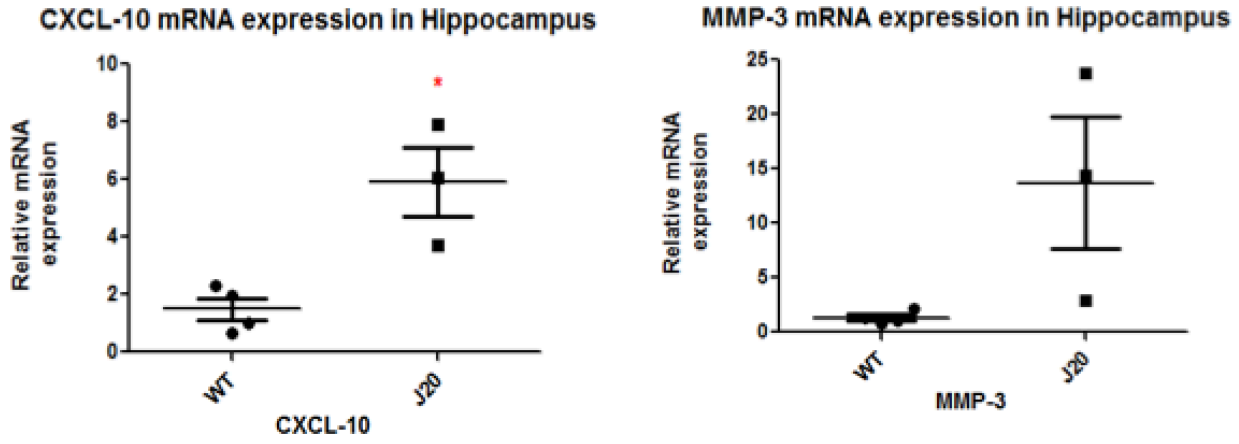

Figure 4.8 Senescence markers are upregulated at the mRNA level in J20 hippocampi compared to WT controls. Hippocampi from 12-month old WT controls and J20 mice were isolated. RNA was extracted and analyzed for (A) p16INK4a, and (B) the SASP factors CXCL-10 and MMP-3.

(A)

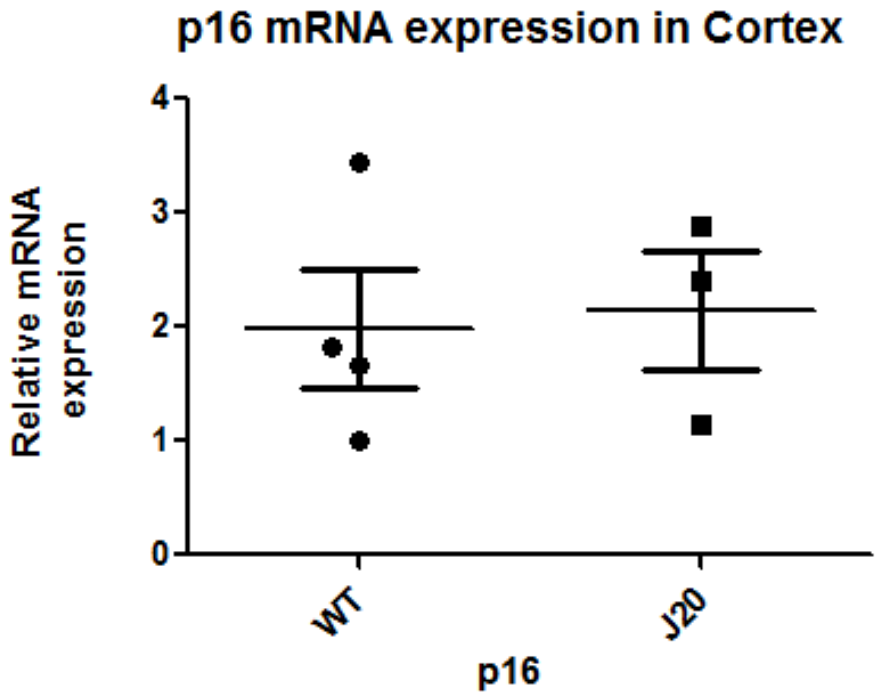

(B)

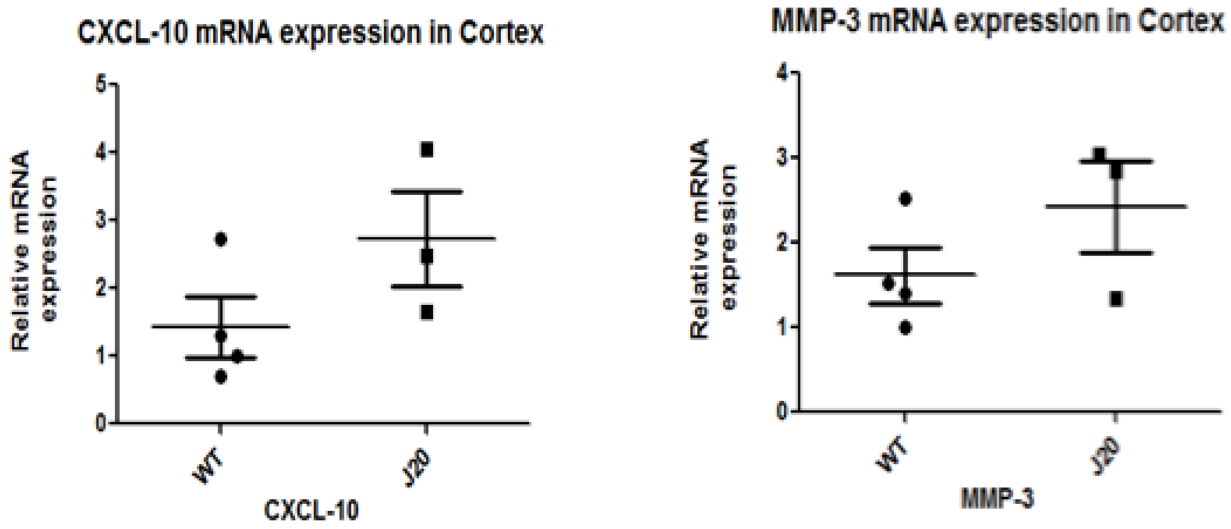

Figure 4.9 Cortex from J20 mice does not show any change in senescence marker expression relative to WT controls. Cortex from 12-month old WT controls and J20 mice was isolated. RNA was extracted and analyzed for (A) p16INK4a, and (B) the SASP factors CXCL-10 and MMP-3.

(A)

(B)

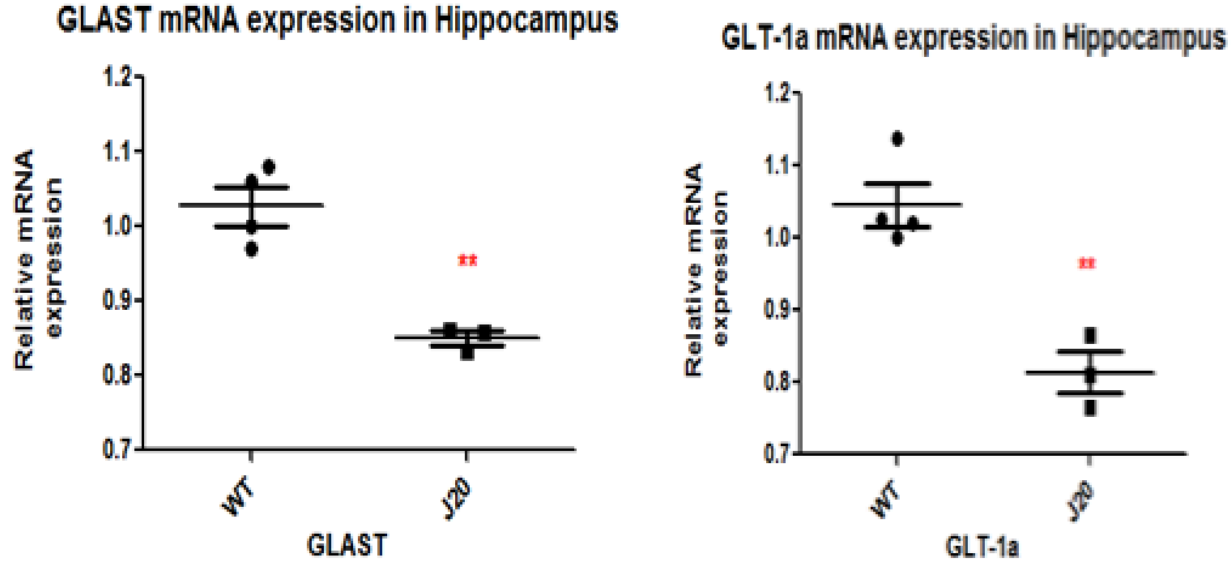

(C)

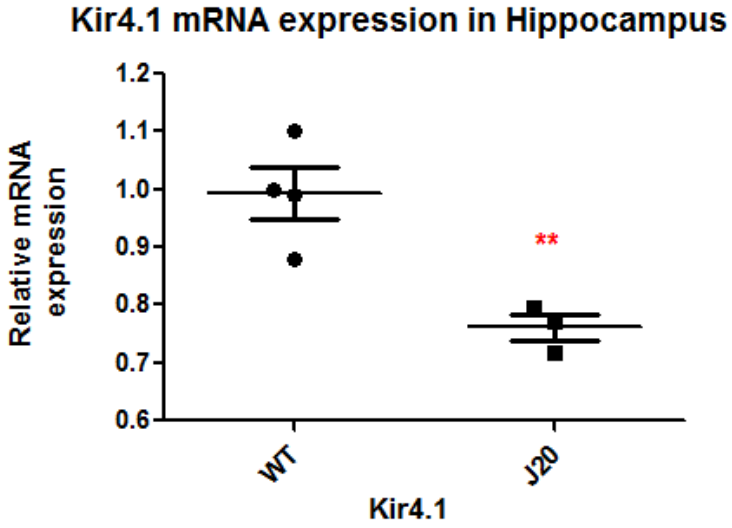

Figure 4.10 Murine glutamate (GLAST and GLT-1A) and potassium (Kir4.1) transporters are downregulated in the hippocampi of J20 mice relative to WT mice. Hippocampi from 12-month old WT controls and J20 mice were isolated. RNA was extracted and analyzed for (A) Glu transporter GLAST, (B) Glu transporter GLT-1a, and (C) potassium transporter Kir4.1.

Chapter 5: Preliminary results for potential therapeutic applications

5.1 Using an IL-1beta neutralizing antibody inhibits the SASP in senescent astrocytes

In order to determine how the SASP can affect brain function, it was important to characterize the key pro-inflammatory factor. Thornton et al. showed in 2006 that IL-1beta secreted by glia cells could lead to neurotoxicity (Thornton et al. 2006). Therefore, to determine if SEN astrocyte secreted IL-1beta, I performed RNA-seq analysis on the six different sets of NS and SEN astrocyte samples. Figure 5.1 shows that in all six sets of SEN cells, IL-1beta was upregulated at various degrees compared to NS samples.

Further, I determined whether blocking IL-1beta would affect the profile of other SASP factors in SEN astrocytes. I therefore used an IL-1beta neutralizing antibody on NS and SEN astrocytes. As shown in Figure 5.2, the IL-1beta neutralizing treatment suppressed various SASP factors secreted by SEN cells. These included IL-6, IL-8, IL-1beta, CXCL-1 and TGF-a. However, the senescence markers p16 was not downregulated upon IL-1beta neutralizing antibody treatment (Figure 5.2). These results indicate that IL-1beta plays a key role in regulating some of the major SASP factors in SEN astrocytes. Further experiments are needed to determine how this modulation of IL-1beta action could affect neuronal survival. Astrocyte/neuron co-culture assays in presence or absence of IL-1beta neutralizing antibody would allow us to determine whether IL-1beta secreted by SEN astrocytes is indeed causal of the neuronal toxicity.

5.2 TMZ induces senescence in MEF and human IMR90 cells

Most of the brain tumors are astrocytic tumors. The most frequently used chemotherapeutic drug for brain cancer is temozolomide (TMZ). In order to determine if TMZ has the capacity to induce cell senescence, I used mouse embryonic fibroblasts (MEFs) and human primary fibroblasts, IMR90.

MEFs were treated with 125 mM, 250 mM, 500 mM and 1mM of TMZ (or DMSO control) for either 24 hours or 48 hours. Then, the cells were fixed and stained using crystal violet. The results show that only 1 mM of TMZ treatment for 48 hours is able to growth arrest the MEFs (Figure 5.3). I therefore treated MEFs with 1 mM TMZ for 48 hours to determine the potential induction of senescence markers. The cells were fixed and stained for SA-β-gal. The results show positive expression of SA-β-gal in TMZ-treated cells. I also performed RNA analysis comparing TMZ- and DMSO-treated samples. As a positive control for senescence induction, I used doxorubicin, a known chemotherapeutic drug that induces senescence (Demaria et al. 2017). I found that TMZ-treated cells upregulated p16 compared to DMSO-treated cells (Figure 5.4).

Regarding the human primary fibroblasts, IMR90, I also performed TMZ concentration optimization using crystal violet. The results show that 1 mM TMZ after a 48-hour treatment induced a senescence growth arrest in IMR90 cells (Figure 5.5). To determine whether the senescence markers were expressed in IMR90 cells after 1 mM TMZ treatment for 48 hours, the cells were fixed and stained for SA-beta gal. The results show that TMZ-treated cells stain positive for SA-β-gal and RNA analysis shows

that TMZ-treated cells upregulated p16 compared to DMSO-treated controls (Figure 5.6).

These results indicate that TMZ, the most widely used chemotherapeutic agent to treat brain tumors, has a capacity to induce senescence in human and mouse primary cells. Further experiments are required to determine if TMZ can induce senescence in brain cells such as astrocytes. If this drug has the capability to induce senescence in glia cells such as astrocytes, it may promote proliferation and/or invasion of neighboring cancer cells upon the secretion of some SASP factors. Further investigation will be required to confirm this hypothesis.

5.3 Future applications

For neurodenerative diseases such as AD, there are limited treatments available (Table 5.1). Among which Memantine drug is a NMDA receptor inhibitor (Figure 5.8), which reduces glutamate toxicity to neurons. At the moment, there is only one FDA approved glutamate toxicity preventive drug in the market. It is important to understand how glutamate toxicity occurs in the brain in order to develop novel treatments for various diseases, which gets affected by glutamate toxicity. My results show that senescence in the astrocytes can be one of the mechanisms, which can trigger glutamate toxicity. Thus, by targeting senescent cells, novel treatments can be developed.

In addition, our RNA-seq data showed that there were almost 50% of the genes downregulated and 50% of the genes upregulated in SEN astrocytes compared to NS astrocytes. These finding are very interesting since they suggest that senescence may have a wide effect on various astrocytic functional pathways. It will be important to continue further analysis of the RNA-seq data to narrow down the results and utilize the data towards therapeutic purpose.

My in vivo results showed that natural aging, irradiation and pathogenic condition like AD in J20 mice, all induce senescence in the mice brain. Even though these various mouse models have given some indication about the presence of senescent cells in the brain, further studies are required in order to understand the physiological effects of senescence induction in each of these mouse models. These studies will be important as mouse models generally gives better perspective for treatment development compared to cell culture studies.

In conclusion, this thesis characterized many aspects of senescence in brain cells, specifically in astrocytes. Both, mouse and human astrocytes undergo senescence and express various senescence markers. Senescence affects some astrocyte-specific pathways. I determined that senescence could lead to neuronal death because of the dysregulation of glutamate uptake by astrocytes. This finding opens up many avenues to develop new treatments for various brain diseases. Further, the SASP factors secreted by senescent astrocytes include factors that are well known to promote brain cancer. Therefore, the discovery of novel approaches to eliminate senescent cells may open up a whole new field for brain cancer treatment.

Figures

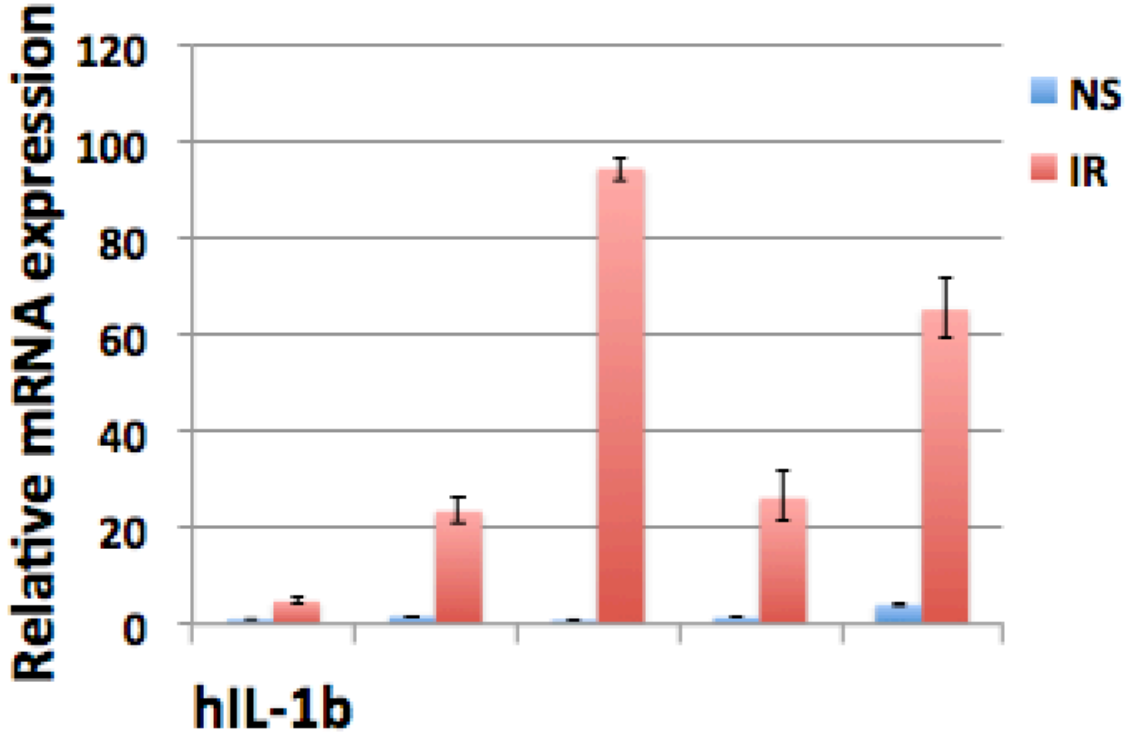

Figure 5.1 SEN astrocytes from six different human samples show an upregulation of IL-1beta on Day 14 after irradiation compared to NS samples. NS and SEN samples from astrocytes obtained from six different individuals were analyzed for IL-1beta mRNA expression using real-time PCR.

(A)

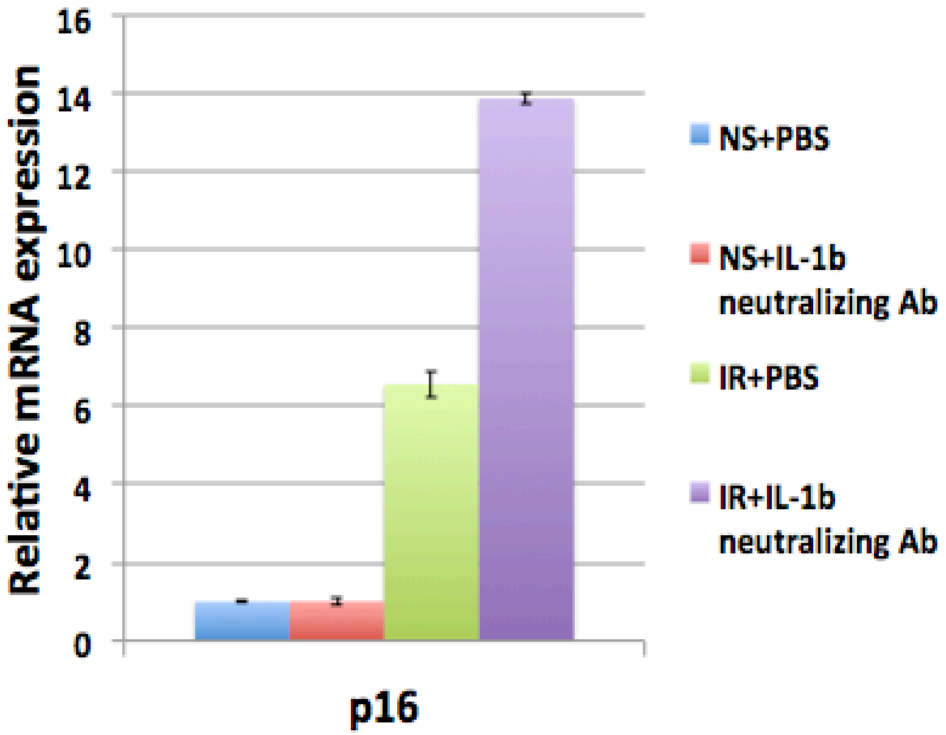
Relative mRNA expression
16
14
12
10
8
6
4
2
0
NS+PBS
NS+IL-1b neutralizing Ab
IR+PBS
IR+IL-1b neutralizing Ab
p16

(B)

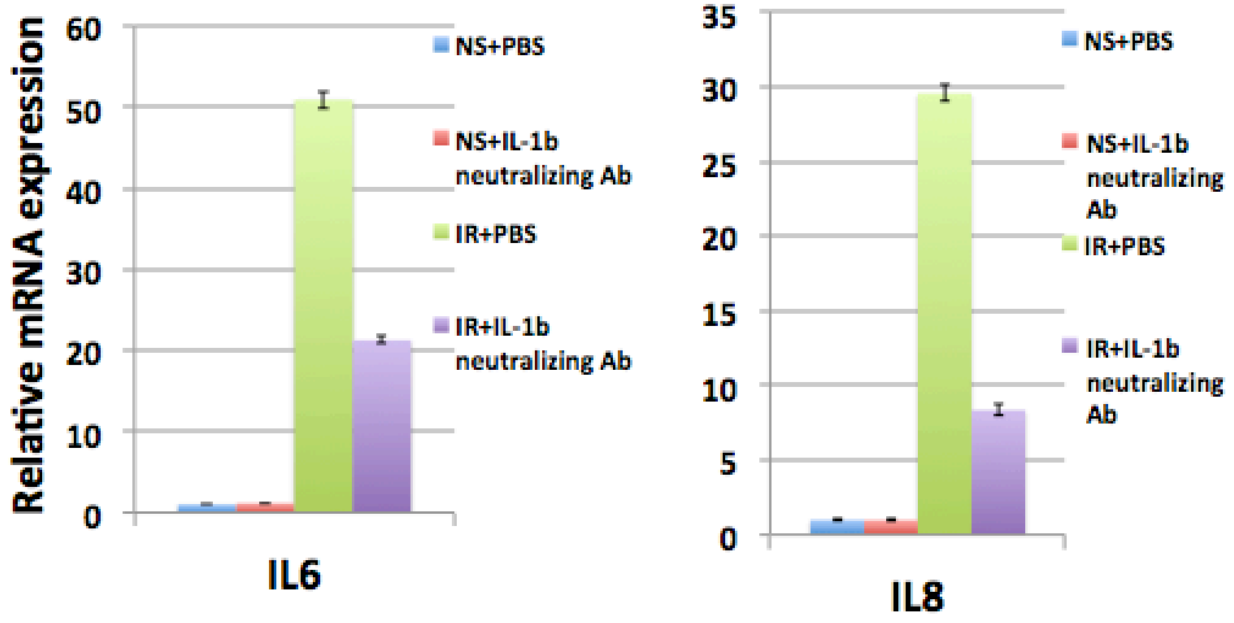
Relative mRNA expression
60
50
40
30
20
10
0
NS+PBS
NS+IL-1b neutralizing Ab
IR+PBS
IR+IL-1b neutralizing Ab
IL6
35
30
25
20
15
10
5
0
NS+PBS
NS+IL-1b neutralizing Ab
IR+PBS
IR+IL-1b neutralizing Ab
IL8

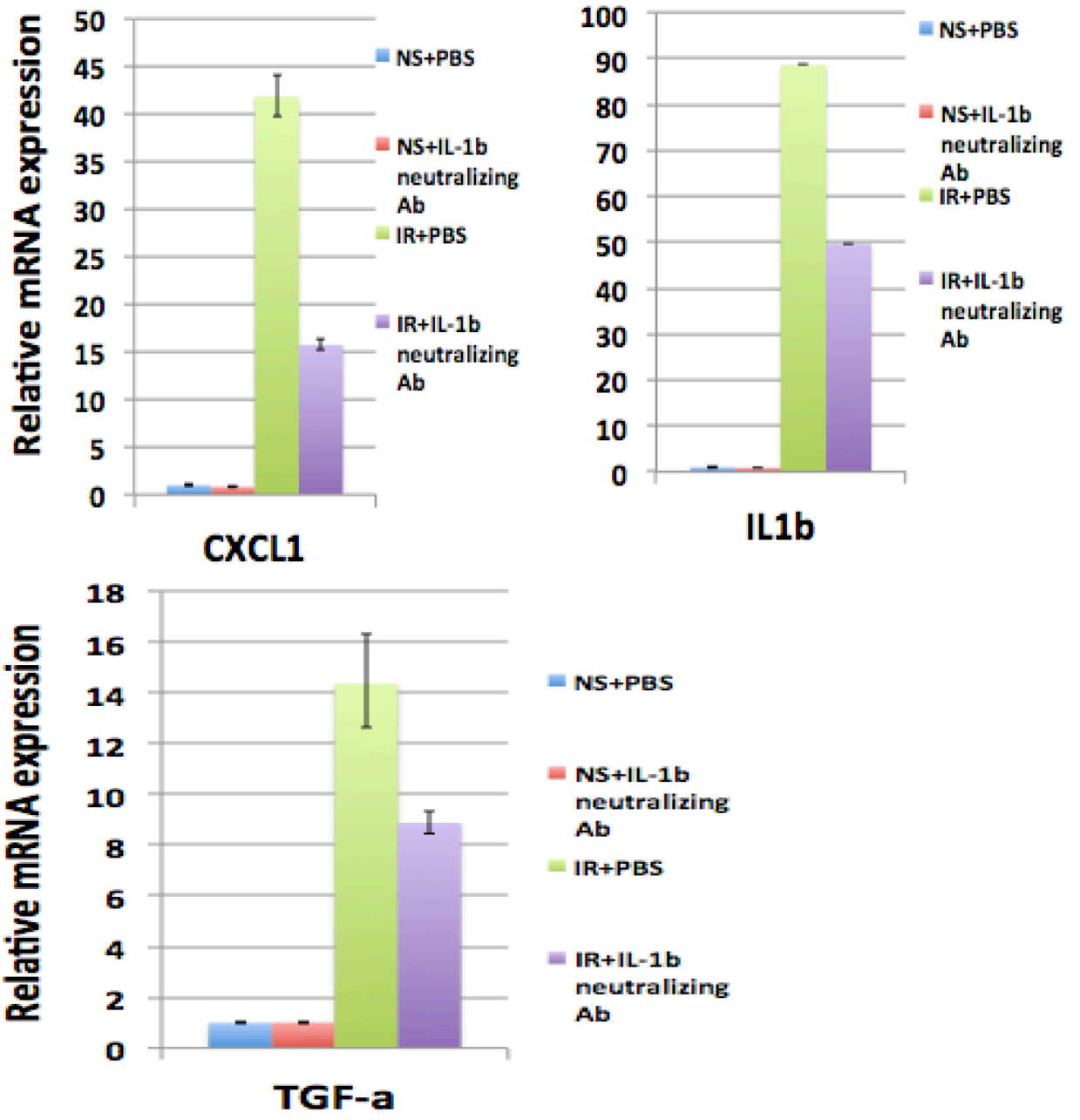

Figure 5.2 Expression of several markers in senescent astrocytes is downregulated by IL-1beta neutralizing antibody. IL-1 beta neutralizing antibody was used to block IL-1beta in NS and SEN astrocytes. Using real-time PCR, RNA was isolated and analyzed for various senescent markers including (A) p16, and (B) IL-6, IL-8, CXCL-1, IL-1beta, and TGF-a.

(A)

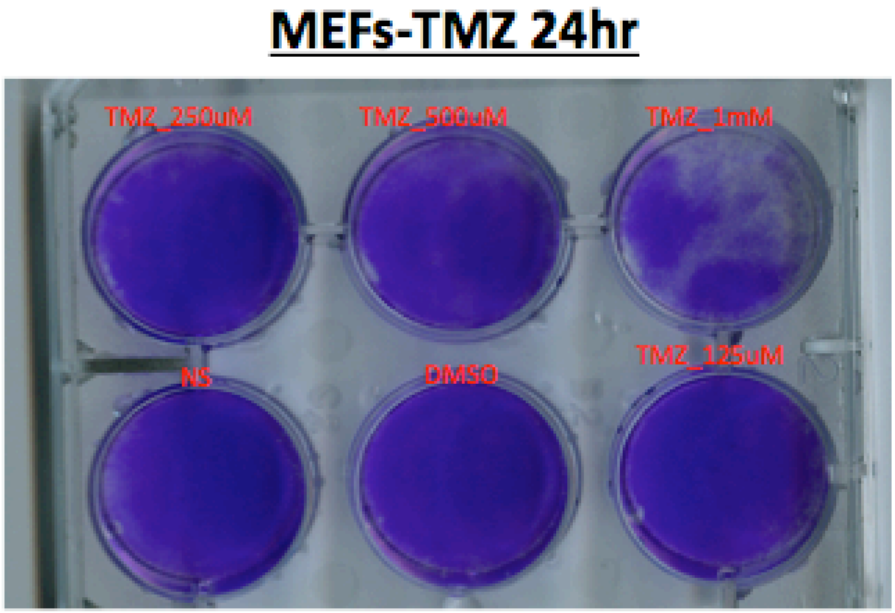

(B)

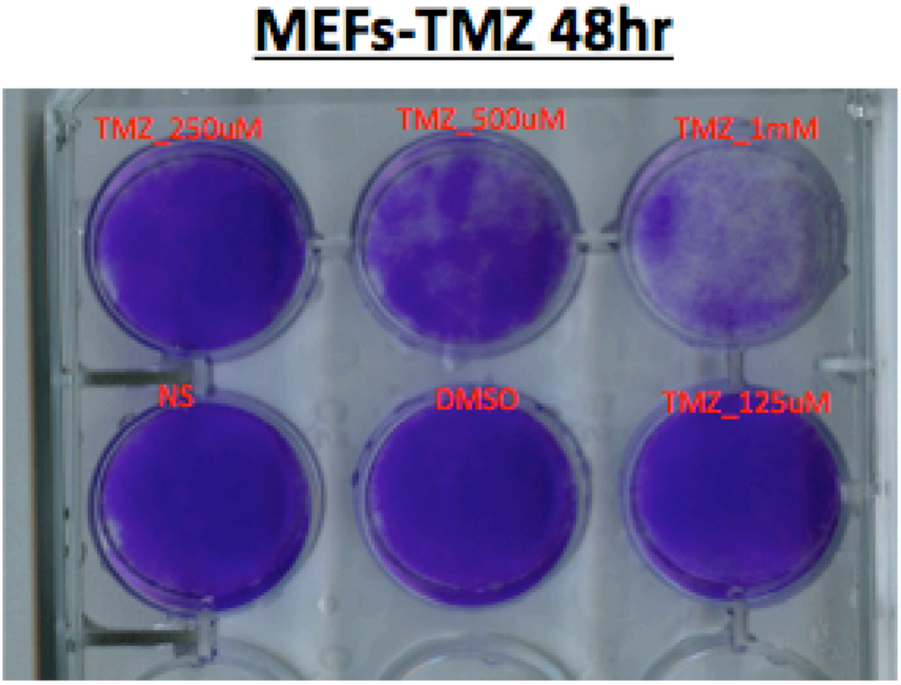

Figure 5.3 1 mM TMZ induces growth arrest in MEFs after a 48-hour treatment. MEFs were treated with various doses of TMZ as described in the text for either 24 or 48 hours. At the end of the treatment, cells were fixed with methanol and stained with crystal violet. Here are shown the results of (A) a 24-hour treatment with TMZ, and (B) a 48-hour treatment with TMZ.

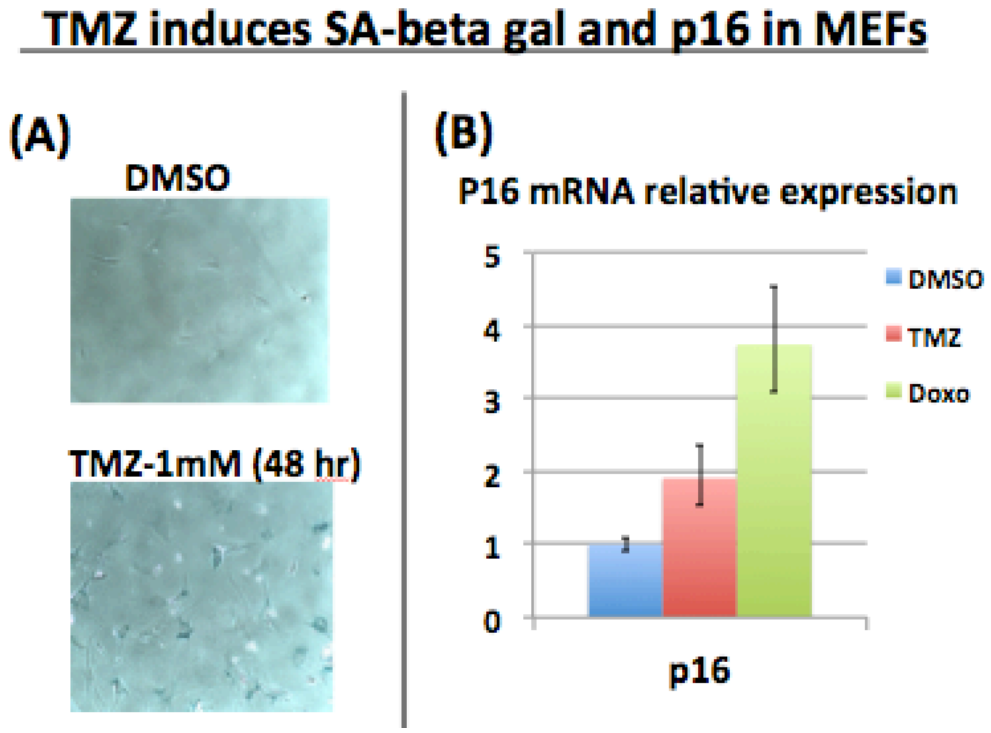

Figure 5.4 1 mM TMZ induces the expression of senescence markers in MEFs after a 48-hour treatment. MEFs were treated with 1 mM TMZ for 48 hours, then (A) cells were stained for SA-β-gal, and (B) RNA was isolated, and p16 expression was tested using real-time PCR.

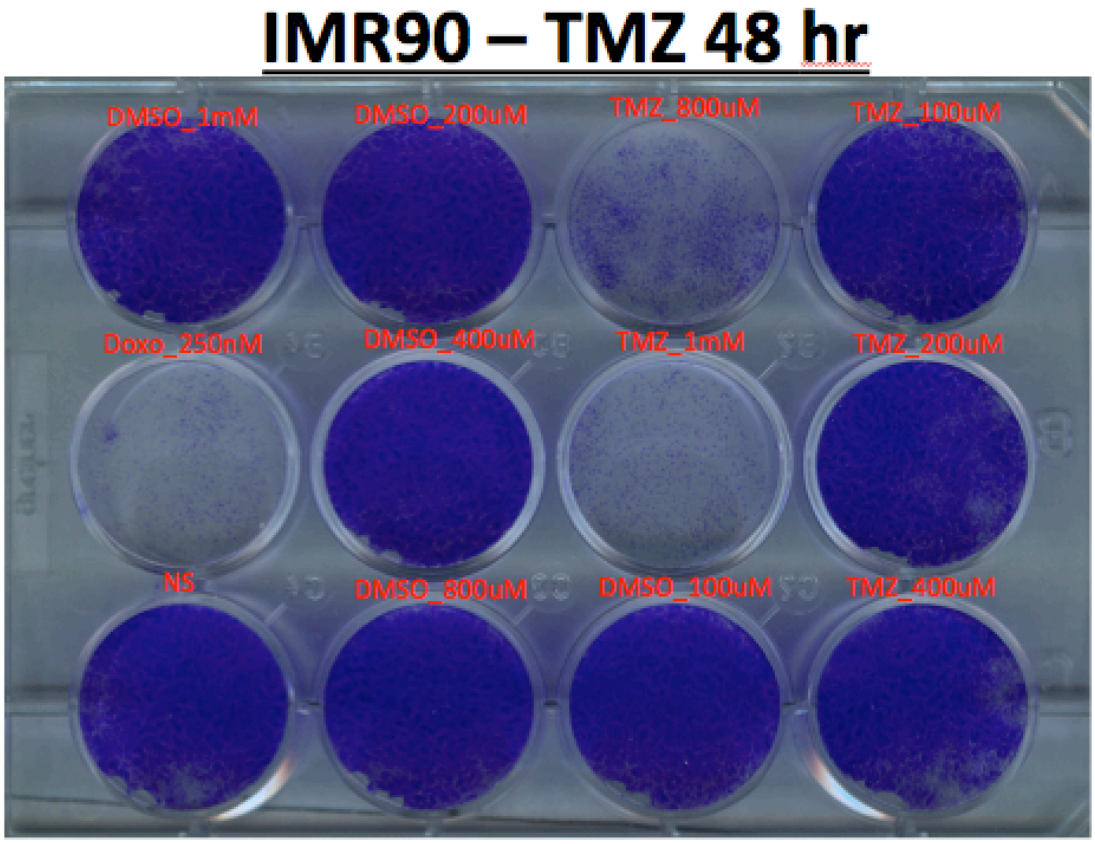

Figure 5.5 | 1 mM TMZ induces growth arrest in IMR90 fibroblasts after a 48-hour treatment. IMR90 cells were treated for 48 hours with various doses of TMZ as described in the text. At the end of the treatment, cells were fixed with methanol and stained with crystal violet.

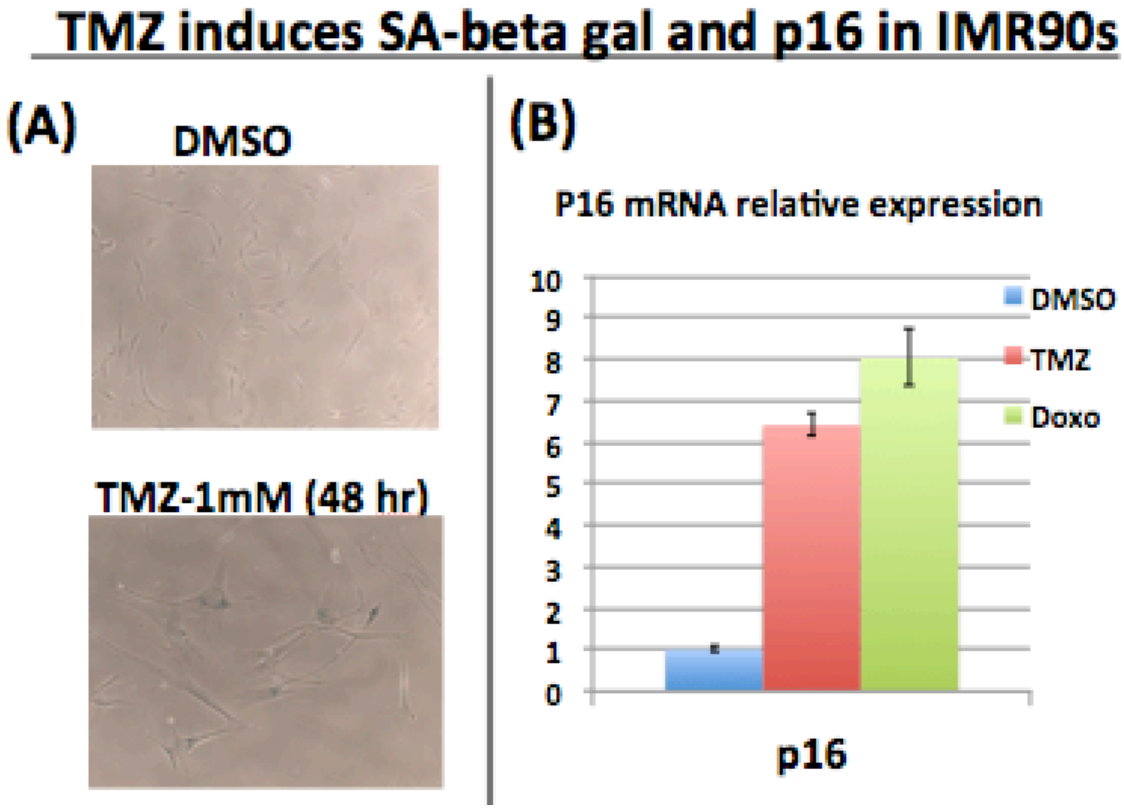

Figure 5.6 1 mM TMZ induces the expression of senescence markers in IMR90 fibroblasts after a 48-hour treatment. IMR90 cells were treated with 1 mM TMZ for 48 hours, then (A) cells were stained for SA-β-gal, and (B) RNA was isolated and p16 expression was tested using real-time PCR.

FDA-approved drugs

The U.S. Food and Drug Administration (FDA) has approved five medications (listed below) to treat the symptoms of Alzheimer's disease.

Drug name	Brand name	Approved For	FDA Approved
1. donepezil	Aricept	All stages	1996
2. galantamine	Razadyne	Mild to moderate	2001
3. memantine	Namenda	Moderate to severe	2003
4. rivastigmine	Exelon	All stages	2000
5. donepezil and memantine	Namzaric	Moderate to severe	2014

Table 5.1 List of FDA-approved drugs for AD treatment (Ref: http://www.alz.org/research/science/alzheimers_disease_treatments.asp).

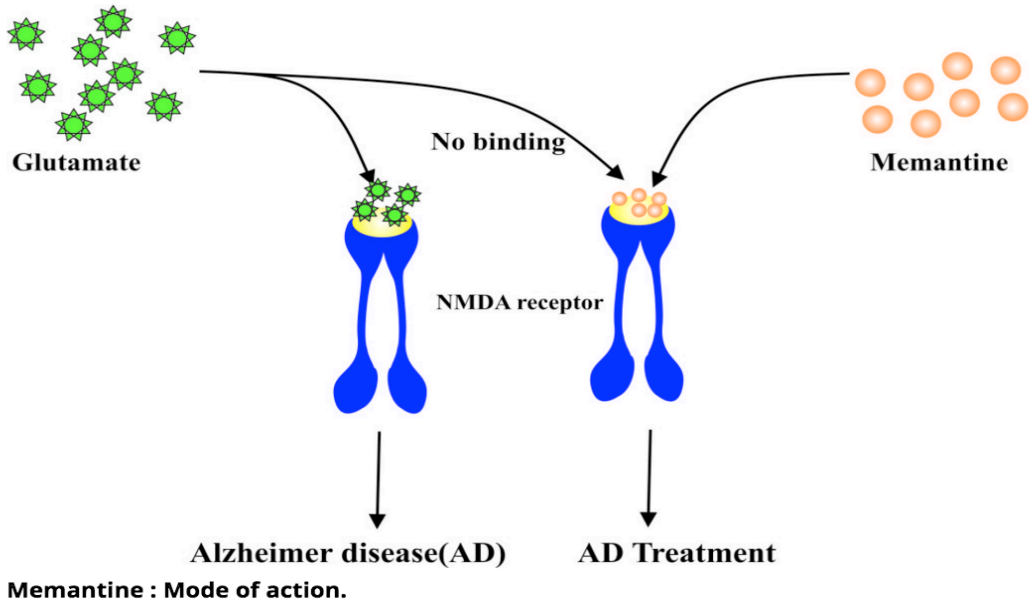

Figure 5.7 Mechanism of action for Memantine (FDA-approved drug to reduce Glu toxicity in AD patients) (Johnson and Kotermanski 2006).

Chapter 6: Discussion and Conclusion

Pro-inflammatory factors secreted by astrocytes not only could have a detrimental effect in brain cancer, but also in neurodegenerative diseases. Inflammation is an important part of various neurodegenerative diseases such as AD and PD (Morales et al. 2014; Tan et al. 2014). Moreover, cellular senescence in the brain has been observed, suggesting the presence of senescent astrocytes in AD patients or upon irradiation (Chinta et al. 2015; Tan et al. 2014; Bhat et al. 2012; Zou et al. 2012).

In addition to inflammatory factors, astrocytes play a critical role in neuronal survival (McGeer and McGeer 1998; Ransom, Behar, and Nedergaard 2003; Salminen et al. 2011; Sofroniew and Vinters 2010; Volterra and Meldolesi 2005). In this project, I showed that senescence affects astrocyte-specific functional pathways, i.e., glutamate and potassium transporters regulation in irradiated astrocytes. Glutamate and potassium transporters are important to maintain the appropriate amount of Glu in the brain (Anderson and Swanson 2000). If the amount of Glu is imbalanced, it causes neuronal cell death by inducing Glu toxicity. Glu toxicity has also been studied in various neurodegenerative diseases, including AD, PD, HD, ALS and epilepsy (Maragakis and Rothstein 2006; Caudle and Zhang 2009; Seifert, Schilling, and Steinhauser 2006). Glu binds to N-methyl-D-aspartate (NMDA) subtype of neuronal ionotropic L-glutamate receptors. Almost all neurons in the CNS have NMDA receptors, and excessive activation of NMDA receptors leads to excitotoxicity.

In AD, the amyloid β–related peptides increase Glu release and inhibit Glu uptake by astrocytes, leading to excitotoxicity (Revett et al. 2013; Hynd, Scott, and Dodd 2004; Caudle and Zhang 2009). My results on the hippocampus of AD mouse model (J20) indicate that senescence is induced in a mouse model of AD and creates an inflammatory environment in the brain. I also found that there was a correlation between the induction of senescence and the downregulation of glutamate and potassium transporters in the hippocampus, suggesting that senescence has a key role in inducing Glut toxicity in AD. Furthermore, I determined that glutamine synthetase was also downregulated in astrocytes undergoing senescence. Glutamine synthatase is an enzyme that is necessary to convert glutamate into glutamine. Glutamine is then released from astrocytes and is taken up by neurons for further signaling (Bak, Schousboe, and Waagepetersen 2006). More investigation will be needed to determine how the downregulation of glutamine synthetase in senescent astrocytes affects the glutamate-glutamine cycle.

Other than AD, there are additional neurodegenerative diseases in which excitotoxicity has been documented (Van Den Bosch et al. 2006; Kucheryavykh et al. 2007; Doble 1999). Downregulation of glutamate transporters and glutamine synthetase in astrocytes has also been reported in epilepsy and ALS (Seifert, Schilling, and Steinhauser 2006). Moreover, downregulation of glutamate transporters and glutamine synthetase results in a progressively disturbed Glu homeostasis in the brain of patients with HD (Tong et al. 2014; Behrens et al. 2002; Estrada Sanchez, Mejia-Toiber, and Massieu 2008). Interestingly, other than glutamate transporters, potassium transporters are also necessary for efficient Glu uptake by astrocytes and preventing excitotoxocity (Kucheryavykh et al. 2007). My data show that senescent astrocytes also display a strong downregulation of the potassium transporter, Kir4.1. It has previously been shown that Kir4.1 deficiency contributes to excitotoxicity and neuronal dysfunction

(Tong et al. 2014). Kir4.1 deficiency also triggers detrimental effects in HD (Tong et al. 2014). However, none of these disease conditions (other than AD) has previously been tested for the potential presence and role of senescent cells. Finally, my results also show that senescent astrocytes downregulate the water transport channel AQP4. Further experiments will be needed in order to investigate the effects of AQP4 deficiency in astrocytes.

For the treatment of neurodegenerative diseases such as AD and ALS, there are currently a few FDA-approved drugs that inhibit NMDA receptors and are anti-excitotoxic. Among these drugs are Memantine and Riluzole (Howard et al. 2015; Zoccolella et al. 2007; Lacomblez et al. 1996). Since my studies show that several transporters (as well as glutamine synthetase) are downregulated in senescent astrocytes, it would be critical to test for the presence of senescent cells in various neurodegenerative diseases. In case senescent cells are detected in neurodegenerative diseases and are found to contribute to excitotoxicity, targeted removal of these cells could open up new avenues for treatment. Senolytics are a new class of drugs used to remove senescent cells, and compounds such as ABT263 have been shown to clear senescent cells efficiently and to rejuvenate stem cells in aged mouse tissues (Chang et al. 2016).

In conclusion, astrocytes are capable of undergoing senescence and they express classical senescence markers. In addition, senescent astrocytes show a downregulation of the expression of astrocyte-specific transporters and enzymes. As a consequence of this downregulation, there is a disruption of the ability of astrocytes to maintain normal glutamate homeostasis, leading to excitotoxicity. In the case of various neurodegenerative diseases, clearance of senescent cells could be used to develop novel therapeutic approaches.

Chapter 7: Materials and Methods

Cell cultures

13.5-day old embryos were dissected and cultured to produce MEF. Primary mouse cells were expanded for no more than 10 doublings. Human IMR90 fibroblasts were bought from ATCC. Cells were not re-authenticated by the laboratory, but regularly monitored for Mycoplasma contaminations (once/2 weeks). All cells were cultured in 3% oxygen for at least 4 doublings prior to use. Primary astrocytes and their corresponding culture media were obtained from ScienCell (#1800 and #1801, respectively), and cultured as per instructions provided by ScienCell. Purity of the astrocytes was confirmed using GFAP staining (antibody obtained from Sigma-Aldrich, #C9205). All the human primary cells were seeded at 5,000 cells/cm^2 and grown into respective cell culture media. Doxorubicin (Doxo) and temozolomide (TMZ) (Sigma Aldrich) were dissolved in DMSO at 100 mmol/l and diluted in serum-containing medium.

X-irradiation of cells

Cells were seeded in 4-well chambers, 6-well plates or 100-mm plates, and irradiated at 320 kv and 10 mA to achieve a dose of 10 Gy. Mock-irradiated cells were placed in the irradiator without power for an equivalent interval. After IR, fresh media was added.

SA-β-Gal assay

SA-β-gal staining was performed using the Biovision kit (Prod# K320-250). Cells were plated at a density of 5,000 cells/cm^2. SA-β-gal staining was performed 24-48 hours after seeding, when cells are normally in log phase growth, and 60%–70% confluent, to minimize false-positive staining. Cells were then washed with PBS and fixed for 5 min with 2% formaldehyde–0.2% glutaraldehyde. After another wash with PBS, cells were incubated overnight at 37°C in staining solution containing 1 mg/ml 5-bromo-4-chloro-3-inolyl-β-D-galactoside, 40 mM citric acid/phosphate buffer (pH 6.0), 5 mM potassium ferricyanide, 5 mM sodiumferricyanide, 150 mM NaCl, and 2 mM $MgCl_2$. Cells were washed with PBS, and a minimum of 400 cells counted. Positive cells (blue cells) are expressed as a percentage of the total cell number.

Immunofluorescence

Cells were washed in PBS, fixed in 4% paraformaldehyde, permeabilized with 0.5% Triton-X 100, washed, incubated in 10% goat serum for 1 hour at RT, and then incubated with a GFAP-Cy3 antibody (Sigma-Aldrich, #C9205), or a HMGB1 antibody (Abcam, #ab18256) at 4°C overnight. After washing, slides were incubated with Alexa conjugated secondary antibodies for 30-45 min at RT. Nuclear DNA was stained with DAPI in mounting media (Vectasheild).

Enzyme-linked immunosorbent assays (ELISA)

ELISA kit to detect HMGB1 was from Neo Scientific (prod# HH0016) and used according to the manufacturer's protocols. Conditioned media were prepared by incubating NS and SEN astrocytes in serum-free astrocyte medium for 24 hours. Media were collected 14 days after irradiation, and ELISA results were normalized to cell numbers.

Real time-PCR

RNA was prepared using the Isolate II RNA mini kit (Bio-52073). RNA was reverse transcribed into cDNA using a kit from Applied Biosystems (Carlsbad CA, USA). qRT-PCR reactions were performed using the Universal Probe Library system (Roche, South San Francisco CA, USA). For quantification, the $2^{-\Delta\Delta Cp}$ method was used to determine relative expression level normalized against β-actin.

Primer/probe sets were:

	Human Primers	**UPL Probe**	**Forward Primer**	**Reverse Primer**
1	Actin-1	64	ccaaccgcgagaagatga	Tccatcacgatgccagtg
2	p16	67	gagcagcatggagccttc	Cgtaactattcggtgcgttg
3	LMNB1	3	gtgctgcgagcaggagac	Ccattaagatcagattccttcttagc
4	IL-6	45	gcccagctatgaactccttct	Gaaggcagcaggcaacac
5	IL-8	72	agacagcagagcacacaagc	Atggttccttccggtggt
6	IL-1b	78	tacctgtcctgcgtgttgaa	Tctttgggtaatttttgggatct
7	TGF-A	64	cattgtccatgcctcaggata	Gatttctagaagaaaaatccccaaa
8	CXCL1	52	tcctgcatcccccatagtta	Cttcaggaacagccaccagt
9	EAAT1	88	ggccaagaagaaagtgcaga	Ggtcggagggtaaatccaag
10	EAAT2	58	gcccaaatgaatggtgttgt	Gggtggctgtgaggctta
11	Kir4.1	39	cagctctgctcctaactcctg	Aatacaccttggcaactgacg
12	AQP4	17	gggaaattgggaaaaccatt	Gacatactcataaaggccaccag
13	GLUL(T1)	5	aagagggcaaccctaacgat	Ttgctgaggtggtcatggt
14	GLUL(T2)	55	aagagcggagcgtgtgag	Tcatggtggaaggtgttctg
15	GLUL(T3)	31	ttctggcgatggttgagac	Gtgggaacttgctgaggtg

	Mouse Primers	**UPL Probe**	**Forward Primer**	**Reverse Primer**
1	Actin-1	64	ctaaggccaaccgtgaaaag	Accagaggcatacagggaca
2	LMNB1	15	gggaagtttattcgcttgaaga	Atctcccagcctcccatt
3	IL-6	6	gctaccaaactggatataatcagga	ccaggtagctatggtactccagaa
4	CXCL1	75	ttttgtatgtattagggtgaggaca	Gcgtgttgaccatacaatatgaa
5	CXCL10	3	gctgccgtcattttctgc	Tctcactggcccgtcatc

6	MMP-3	7	ttgttctttgatgcagtcagc	Gatttgcgccaaaagtgc
7	IL-1b	38	agttgacggaccccaaaag	Agctggatgctctcatcagg
8	GLAST	89	gttccctggggagcttct	Ttactatctagggccgccatt
9	GLT-1a	58	cccaaatgaatggggtcat	Atactggctgcaccaatgc
10	Kir4.1	51	agtcttggccctgcctgt	Agcgaccgacgtcatctt

		Forward Primer	**Reverse Primer**
Mouse p16		aactctttcggtcgtacccc	Tcctcgcagttcgaatctg
IDT Probe: Mouse_p16_FAM:	5' /56-FAM/AGG TGA TGA /ZEN/TGA TGG GCA ACG TTC AC/3IABkFQ/ -3'		

Western blot analysis

Cells were washed with PBS, scraped in 200 µl of 5% sodium dodecyl sulfate, passed through a needle and centrifuged at 2,000 rpm for 5 min. Supernatants were assayed for protein concentration using the BCA protein assay kit (Pierce). Proteins were separated on 4-12% polyacrylamide gels (Biorad) and transferred to a PVDF membrane (Millipore). Membranes were blocked in 5% milk powder and incubated with primary antibody for 2 hour at room temperature or overnight at 4°C. Membranes were washed with 1X tris buffered saline tween-20 (TBS-T), incubated with HRP conjugated secondary antibodies (Invitrogen), washed with TBS-T, and detected using an Enhanced Electrochemoluminescence kit (GE Healthcare). The following primary antibodies were used: EAAT1 (Abcam, #ab416), Kir4.1 (Alomone Labs, #APC-035), AQP4 (Sigma-Aldrich, #HPA014784-100UL), GS (Abcam, #ab178422), and Actin (Sigma-Aldrich, #A2228-200UL).

Co-culture assays

On Day 1, 40,000 neurons were seeded in 24-well plates on L-Poly lysine-coated glass coverslips. On Day 3, SEN or NS astrocytes were labeled with CMPTX-red, and 40,000 SEN and NS astrocytes were seeded on top of the neurons. On Day 4, co-cultures were treated with media containing either 10 mM Glu or control media. On Day 5, co-culture glass coverslips were fixed and stained with DAPI. Fluorescence images were taken for the quantification of surviving cells.

RNA-seq experiment

Six different lot numbers of human primary astrocytes were bought from ScienCell (Cat #1800, Lot # 17320,17158,16091, 16492, 16700, 18709). Cells were seeded at

5,000/cm^2 as recommended by the company. The next day, cells were X-irradiated or mock-treated as described above. Mock cells were treated with serum-free media for 24 hours, and RNA was isolated. X-irradiated cells were treated with complete media for 13 days, and treated with serum-free media for 24 hours. 14 days after X-irradiation, RNA was isolated. RNA quality was tested using NanoDrop Spectrometer. RNA was reverse transcribed into cDNA using a kit from Applied Biosystems (Carlsbad CA, USA). qRT-PCR reactions were performed as described above for p16, IL-6, IL-8, EAAT1, EAAT2 and Kir4.1 before sending the samples to BGI Americas Corporation for RNA-seq.

IL-1beta neutralizing experiment

Astrocytes were X-irradiated to induce senescence. Right after irradiation, NS (mock-irradiated) and SEN (X-irradiated) cells were treated with an IL-1beta neutralizing antibody (R&D Systems, Prod# MAB201-500). NS samples were collected after 24 hours and SEN samples were collected after 14 days (medium was refreshed every 3 days for SEN cells). RNA was isolated from each sample and analyzed using real-time PCR methods.

Crystal violet assay

MEFs and IMR90 fibroblasts were seeded at 10,000/cm^2 in 12-well plates. The next day, cells were treated with either TMZ or DMSO control for 24 or 48 hours. Then, the cells were fixed with methanol and stained with crystal violet to analyze colony formation.

Mouse models

WT C57BL/6 mice were obtained from NIH. After arrival, mice were housed for 2 weeks at the Buck Institute. Then, the mice were euthanized and various parts of the brain were isolated for RNA analysis. p16-3MR mice were maintained in the AAALAC-accredited Buck Institute animal facility. All procedures were approved by the Institutional Animal Care and Use Committee. p16-3MR mice were bred in-house. For the in vivo luminescence and tissue extraction, both male and female mice were used. J20 mice brain samples were obtained from the Bredesen Laboratory at the Buck Institute. J20 is a widely used mouse model of AD, overexpressing the human amyloid precursor protein (APP) that harbors two mutations linked to familial AD (the Swedish and Indiana mutations). Mutant APP expression is driven by the human platelet-derived growth factor (PDGFb chain) promoter thus enabling high level of expression of human APP in neurons. Compared to mice expressing an equivalent level of WT human APP, J20 mice have higher levels of amyloid beta (Ab), which show a further increase between 6 and 9 months of age. Amyloid deposition is progressive in J20 mice, with Ab plaques typically appearing by 5-7 months of age and becoming widespread by 8-10 months of age. Importantly, hippocampal oligomeric Ab increases in an age-dependent

manner in J20 mice, with significant elevations evident by 8-10 weeks of age (Mucke et al. 2000). J20 mice also show an age-dependent loss in synapses, as measured by synaptophysin immunoreactivity in presynaptic terminals, by 8-10 months of age.

Bioluminescence

For in vivo luminescence using Renilla Luciferase, mice were injected i.p. with 15 μg of Xenolight RediJect Coelentarazine (Calipers/Perkin Elmer). Twenty-five minutes later, the mice were anesthetized using isofluorane, and luminescence was measured using the Xenogen IVIS-200 Optical Imaging System (Caliper Life Sciences; 5-minute medium binning). For in vivo luminescence using Firefly Luciferase, mice were injected i.p. with 150 mg/kg of Xenolight D-Luciferin (Calipers/Perkin Elmer). Five minutes later, the mice were anesthetized using isofluorane, and luminescence was measured using the Xenogen IVIS-200 Optical Imaging System (Caliper Life Sciences; 3-minute medium binning).

Statistical analyses

All data that show error bars are presented as mean ± s.e.m. The significance of difference in the mean values was determined using the two-tailed Student's t test unless otherwise mentioned, and normal distribution was assumed for all of these. $P<0.05$ was considered significant. Each cell culture experiment was reproduced at least twice independently. SA-β-gal quantification was performed blindly.

Bibliography

Acosta, J. C., A. O'Loghlen, A. Banito, M. V. Guijarro, A. Augert, S. Raguz, M. Fumagalli, M. Da Costa, C. Brown, N. Popov, Y. Takatsu, J. Melamed, F. d'Adda di Fagagna, D. Bernard, E. Hernando, and J. Gil. 2008. 'Chemokine signaling via the CXCR2 receptor reinforces senescence', *Cell*, 133: 1006-18.

Alcorta, D. A., Y. Xiong, D. Phelps, G. Hannon, D. Beach, and J. C. Barrett. 1996. 'Involvement of the cyclin-dependent kinase inhibitor p16 (INK4a) in replicative senescence of normal human fibroblasts', *Proc Natl Acad Sci U S A*, 93: 13742-7.

Alimonti, A., C. Nardella, Z. Chen, J. G. Clohessy, A. Carracedo, L. C. Trotman, K. Cheng, S. Varmeh, S. C. Kozma, G. Thomas, E. Rosivatz, R. Woscholski, F. Cognetti, H. I. Scher, and P. P. Pandolfi. 2010. 'A novel type of cellular senescence that can be enhanced in mouse models and human tumor xenografts to suppress prostate tumorigenesis', *J Clin Invest*, 120: 681-93.

Allavena, P., A. Sica, G. Solinas, C. Porta, and A. Mantovani. 2008. 'The inflammatory micro-environment in tumor progression: the role of tumor-associated macrophages', *Crit Rev Oncol Hematol*, 66: 1-9.

Anderson, C. M., and R. A. Swanson. 2000. 'Astrocyte glutamate transport: review of properties, regulation, and physiological functions', *Glia*, 32: 1-14.

Bak, L. K., A. Schousboe, and H. S. Waagepetersen. 2006. 'The glutamate/GABA-glutamine cycle: aspects of transport, neurotransmitter homeostasis and ammonia transfer', *J Neurochem*, 98: 641-53.

Baker, D. J., B. G. Childs, M. Durik, M. E. Wijers, C. J. Sieben, J. Zhong, R. A. Saltness, K. B. Jeganathan, G. C. Verzosa, A. Pezeshki, K. Khazaie, J. D. Miller, and J. M. van Deursen. 2016. 'Naturally occurring p16(Ink4a)-positive cells shorten healthy lifespan', *Nature*, 530: 184-9.

Baker, D. J., T. Wijshake, T. Tchkonia, N. K. LeBrasseur, B. G. Childs, B. van de Sluis, J. L. Kirkland, and J. M. van Deursen. 2011. 'Clearance of p16Ink4a-positive senescent cells delays ageing-associated disorders', *Nature*, 479: 232-6.

Bakkenist, C. J., and M. B. Kastan. 2003. 'DNA damage activates ATM through intermolecular autophosphorylation and dimer dissociation', *Nature*, 421: 499-506.

Bartkova, J., N. Rezaei, M. Liontos, P. Karakaidos, D. Kletsas, N. Issaeva, L. V. Vassiliou, E. Kolettas, K. Niforou, V. C. Zoumpourlis, M. Takaoka, H. Nakagawa, F. Tort, K. Fugger, F. Johansson, M. Sehested, C. L. Andersen, L. Dyrskjot, T. Orntoft, J. Lukas, C. Kittas, T. Helleday, T. D. Halazonetis, J. Bartek, and V. G. Gorgoulis. 2006. 'Oncogene-induced senescence is part of the tumorigenesis barrier imposed by DNA damage checkpoints', *Nature*, 444: 633-7.

Beausejour, C. M., A. Krtolica, F. Galimi, M. Narita, S. W. Lowe, P. Yaswen, and J. Campisi. 2003. 'Reversal of human cellular senescence: roles of the p53 and p16 pathways', *EMBO J*, 22: 4212-22.

Behrens, P. F., P. Franz, B. Woodman, K. S. Lindenberg, and G. B. Landwehrmeyer. 2002. 'Impaired glutamate transport and glutamate-glutamine cycling: downstream effects of the Huntington mutation', *Brain*, 125: 1908-22.

Bhat, R., E. P. Crowe, A. Bitto, M. Moh, C. D. Katsetos, F. U. Garcia, F. B. Johnson, J. Q. Trojanowski, C. Sell, and C. Torres. 2012. 'Astrocyte senescence as a component of Alzheimer's disease', *PLoS ONE*, 7: e45069.

Bitto, A., C. Sell, E. Crowe, A. Lorenzini, M. Malaguti, S. Hrelia, and C. Torres. 2010. 'Stress-induced senescence in human and rodent astrocytes', *Exp Cell Res*, 316: 2961-8.

Bodnar, A. G., M. Ouellette, M. Frolkis, S. E. Holt, C. P. Chiu, G. B. Morin, C. B. Harley, J. W. Shay, S. Lichtsteiner, and W. E. Wright. 1998. 'Extension of life-span by introduction of telomerase into normal human cells', *Science*, 279: 349-52.

Brenner, A. J., M. R. Stampfer, and C. M. Aldaz. 1998. 'Increased p16 expression with first senescence arrest in human mammary epithelial cells and extended growth capacity with p16 inactivation', *Oncogene*, 17: 199-205.

Bruijn, L. I., M. W. Becher, M. K. Lee, K. L. Anderson, N. A. Jenkins, N. G. Copeland, S. S. Sisodia, J. D. Rothstein, D. R. Borchelt, D. L. Price, and D. W. Cleveland. 1997. 'ALS-linked SOD1 mutant G85R mediates damage to astrocytes and promotes rapidly progressive disease with SOD1-containing inclusions', *Neuron*, 18: 327-38.

Campisi, J. 2005. 'Senescent cells, tumor suppression, and organismal aging: good citizens, bad neighbors', *Cell*, 120: 513-22.

Campisi, J., and F. d'Adda di Fagagna. 2007. 'Cellular senescence: when bad things happen to good cells', *Nat Rev Mol Cell Biol*, 8: 729-40.

Carlsson, S. K., S. P. Brothers, and C. Wahlestedt. 2014. 'Emerging treatment strategies for glioblastoma multiforme', *EMBO Mol Med*, 6: 1359-70.

Caudle, W. M., and J. Zhang. 2009. 'Glutamate, excitotoxicity, and programmed cell death in Parkinson disease', *Exp Neurol*, 220: 230-3.

Chang, J., Y. Wang, L. Shao, R. M. Laberge, M. Demaria, J. Campisi, K. Janakiraman, N. E. Sharpless, S. Ding, W. Feng, Y. Luo, X. Wang, N. Aykin-Burns, K. Krager, U. Ponnappan, M. Hauer-Jensen, A. Meng, and D. Zhou. 2016. 'Clearance of senescent cells by ABT263 rejuvenates aged hematopoietic stem cells in mice', *Nat Med*, 22: 78-83.

Chinta, S. J., G. Woods, A. Rane, M. Demaria, J. Campisi, and J. K. Andersen. 2015. 'Cellular senescence and the aging brain', *Exp Gerontol*, 68: 3-7.

Chung, H. Y., M. Cesari, S. Anton, E. Marzetti, S. Giovannini, A. Y. Seo, C. Carter, B. P. Yu, and C. Leeuwenburgh. 2009. 'Molecular inflammation: underpinnings of aging and age-related diseases', *Ageing Res Rev*, 8: 18-30.

Coppe, J. P., C. K. Patil, F. Rodier, A. Krtolica, C. M. Beausejour, S. Parrinello, J. G. Hodgson, K. Chin, P. Y. Desprez, and J. Campisi. 2010. 'A human-like senescence-associated secretory phenotype is conserved in mouse cells dependent on physiological oxygen', *PLoS ONE*, 5: e9188.

Coppe, J. P., C. K. Patil, F. Rodier, Y. Sun, D. P. Munoz, J. Goldstein, P. S. Nelson, P. Y. Desprez, and J. Campisi. 2008. 'Senescence-associated secretory phenotypes reveal cell-nonautonomous functions of oncogenic RAS and the p53 tumor suppressor', *PLoS Biol*, 6: 2853-68.

d'Adda di Fagagna, F., P. M. Reaper, L. Clay-Farrace, H. Fiegler, P. Carr, T. Von Zglinicki, G. Saretzki, N. P. Carter, and S. P. Jackson. 2003. 'A DNA damage checkpoint response in telomere-initiated senescence', *Nature*, 426: 194-8.

Davalos, A. R., J. P. Coppe, J. Campisi, and P. Y. Desprez. 2010. 'Senescent cells as a source of inflammatory factors for tumor progression', *Cancer Metastasis Rev*, 29: 273-83.

Davalos, A. R., M. Kawahara, G. K. Malhotra, N. Schaum, J. Huang, U. Ved, C. M. Beausejour, J. P. Coppe, F. Rodier, and J. Campisi. 2013. 'p53-dependent release of Alarmin HMGB1 is a central mediator of senescent phenotypes', *J Cell Biol*, 201: 613-29.

Demaria, M., M. N. O'Leary, J. Chang, L. Shao, S. Liu, F. Alimirah, K. Koenig, C. Le, N. Mitin, A. M. Deal, S. Alston, E. C. Academia, S. Kilmarx, A. Valdovinos, B. Wang, A. de Bruin, B. K. Kennedy, S. Melov, D. Zhou, N. E. Sharpless, H. Muss, and J. Campisi. 2017. 'Cellular Senescence Promotes Adverse Effects of Chemotherapy and Cancer Relapse', *Cancer Discov*, 7: 165-76.

Demaria, M., N. Ohtani, S. A. Youssef, F. Rodier, W. Toussaint, J. R. Mitchell, R. M. Laberge, J. Vijg, H. Van Steeg, M. E. Dolle, J. H. Hoeijmakers, A. de Bruin, E. Hara, and J. Campisi. 2014. 'An essential role for senescent cells in optimal wound healing through secretion of PDGF-AA', *Dev Cell*, 31: 722-33.

Devinsky, O., A. Vezzani, S. Najjar, N. C. De Lanerolle, and M. A. Rogawski. 2013. 'Glia and epilepsy: excitability and inflammation', *Trends Neurosci*, 36: 174-84.

DeWitt, D. A., G. Perry, M. Cohen, C. Doller, and J. Silver. 1998. 'Astrocytes regulate microglial phagocytosis of senile plaque cores of Alzheimer's disease', *Exp Neurol*, 149: 329-40.

Di Leonardo, A., S. P. Linke, K. Clarkin, and G. M. Wahl. 1994. 'DNA damage triggers a prolonged p53-dependent G1 arrest and long-term induction of Cip1 in normal human fibroblasts', *Genes Dev*, 8: 2540-51.

Di Micco, R., M. Fumagalli, A. Cicalese, S. Piccinin, P. Gasparini, C. Luise, C. Schurra, M. Garre, P. G. Nuciforo, A. Bensimon, R. Maestro, P. G. Pelicci, and F. d'Adda di Fagagna. 2006. 'Oncogene-induced senescence is a DNA damage response triggered by DNA hyper-replication', *Nature*, 444: 638-42.

Dimri, G. P., K. Itahana, M. Acosta, and J. Campisi. 2000. 'Regulation of a senescence checkpoint response by the E2F1 transcription factor and p14(ARF) tumor suppressor', *Mol Cell Biol*, 20: 273-85.

Dimri, G. P., X. Lee, G. Basile, M. Acosta, G. Scott, C. Roskelley, E. E. Medrano, M. Linskens, I. Rubelj, O. Pereira-Smith, and et al. 1995. 'A biomarker that identifies senescent human cells in culture and in aging skin in vivo', *Proc Natl Acad Sci U S A*, 92: 9363-7.

Djukic, B., K. B. Casper, B. D. Philpot, L. S. Chin, and K. D. McCarthy. 2007. 'Conditional knock-out of Kir4.1 leads to glial membrane depolarization, inhibition of potassium and glutamate uptake, and enhanced short-term synaptic potentiation', *J Neurosci*, 27: 11354-65.

Doble, A. 1999. 'The role of excitotoxicity in neurodegenerative disease: implications for therapy', *Pharmacol Ther*, 81: 163-221.

Drummond-Barbosa, D. 2008. 'Stem cells, their niches and the systemic environment: an aging network', *Genetics*, 180: 1787-97.

Estrada Sanchez, A. M., J. Mejia-Toiber, and L. Massieu. 2008. 'Excitotoxic neuronal death and the pathogenesis of Huntington's disease', *Arch Med Res*, 39: 265-76.

Franceschi, C., M. Capri, D. Monti, S. Giunta, F. Olivieri, F. Sevini, M. P. Panourgia, L. Invidia, L. Celani, M. Scurti, E. Cevenini, G. C. Castellani, and S. Salvioli. 2007. 'Inflammaging and anti-inflammaging: a systemic perspective on aging and longevity emerged from studies in humans', *Mech Ageing Dev*, 128: 92-105.

Freund, A., A. V. Orjalo, P. Y. Desprez, and J. Campisi. 2010. 'Inflammatory networks during cellular senescence: causes and consequences', *Trends Mol Med*, 16: 238-46.

Fusenig, N. E., and P. Boukamp. 1998. 'Multiple stages and genetic alterations in immortalization, malignant transformation, and tumor progression of human skin keratinocytes', *Mol Carcinog*, 23: 144-58.

Grivennikov, S. I., F. R. Greten, and M. Karin. 2010. 'Immunity, inflammation, and cancer', *Cell*, 140: 883-99.

Gunnarson, E., M. Zelenina, G. Axehult, Y. Song, A. Bondar, P. Krieger, H. Brismar, S. Zelenin, and A. Aperia. 2008. 'Identification of a molecular target for glutamate regulation of astrocyte water permeability', *Glia*, 56: 587-96.

Gurney, M. E., H. Pu, A. Y. Chiu, M. C. Dal Canto, C. Y. Polchow, D. D. Alexander, J. Caliendo, A. Hentati, Y. W. Kwon, H. X. Deng, and et al. 1994. 'Motor neuron degeneration in mice that express a human Cu,Zn superoxide dismutase mutation', *Science*, 264: 1772-5.

Hara, E., R. Smith, D. Parry, H. Tahara, S. Stone, and G. Peters. 1996. 'Regulation of p16CDKN2 expression and its implications for cell immortalization and senescence', *Mol Cell Biol*, 16: 859-67.

Harley, C. B., A. B. Futcher, and C. W. Greider. 1990. 'Telomeres shorten during ageing of human fibroblasts', *Nature*, 345: 458-60.

Hayflick, L. 1965. 'The Limited in Vitro Lifetime of Human Diploid Cell Strains', *Exp Cell Res*, 37: 614-36.

Herbig, U., W. A. Jobling, B. P. Chen, D. J. Chen, and J. M. Sedivy. 2004. 'Telomere shortening triggers senescence of human cells through a pathway involving ATM, p53, and p21(CIP1), but not p16(INK4a)', *Mol Cell*, 14: 501-13.

Howard, R., R. McShane, J. Lindesay, C. Ritchie, A. Baldwin, R. Barber, A. Burns, T. Dening, D. Findlay, C. Holmes, R. Jones, R. Jones, I. McKeith, A. Macharouthu, J. O'Brien, B. Sheehan, E. Juszczak, C. Katona, R. Hills, M. Knapp, C. Ballard, R. G. Brown, S. Banerjee, J. Adams, T. Johnson, P. Bentham, and P. P. Phillips. 2015. 'Nursing home placement in the Donepezil and Memantine in Moderate to Severe Alzheimer's Disease (DOMINO-AD) trial: secondary and post-hoc analyses', *Lancet Neurol*, 14: 1171-81.

Hynd, M. R., H. L. Scott, and P. R. Dodd. 2004. 'Glutamate-mediated excitotoxicity and neurodegeneration in Alzheimer's disease', *Neurochem Int*, 45: 583-95.

Iannello, A., T. W. Thompson, M. Ardolino, S. W. Lowe, and D. H. Raulet. 2013. 'p53-dependent chemokine production by senescent tumor cells supports NKG2D-dependent tumor elimination by natural killer cells', *J Exp Med*, 210: 2057-69.

Jacobs, J. J., and T. de Lange. 2004. 'Significant role for p16INK4a in p53-independent telomere-directed senescence', *Curr Biol*, 14: 2302-8.

Jakel, S., and L. Dimou. 2017. 'Glial Cells and Their Function in the Adult Brain: A Journey through the History of Their Ablation', *Front Cell Neurosci*, 11: 24.

Janzen, V., R. Forkert, H. E. Fleming, Y. Saito, M. T. Waring, D. M. Dombkowski, T. Cheng, R. A. DePinho, N. E. Sharpless, and D. T. Scadden. 2006. 'Stem-cell ageing modified by the cyclin-dependent kinase inhibitor p16INK4a', *Nature*, 443: 421-6.

Jeon, H. Y., J. K. Kim, S. W. Ham, S. Y. Oh, J. Kim, J. B. Park, J. Y. Lee, S. C. Kim, and H. Kim. 2016. 'Irradiation induces glioblastoma cell senescence and senescence-associated secretory phenotype', *Tumour Biol*, 37: 5857-67.

Johnson, J. W., and S. E. Kotermanski. 2006. 'Mechanism of action of memantine', *Curr Opin Pharmacol*, 6: 61-7.

Jun, J. I., and L. F. Lau. 2010. 'The matricellular protein CCN1 induces fibroblast senescence and restricts fibrosis in cutaneous wound healing', *Nat Cell Biol*, 12: 676-85.

Kang, T. W., T. Yevsa, N. Woller, L. Hoenicke, T. Wuestefeld, D. Dauch, A. Hohmeyer, M. Gereke, R. Rudalska, A. Potapova, M. Iken, M. Vucur, S. Weiss, M. Heikenwalder, S. Khan, J. Gil, D. Bruder, M. Manns, P. Schirmacher, F. Tacke, M. Ott, T. Luedde, T. Longerich, S. Kubicka, and L. Zender. 2011. 'Senescence surveillance of pre-malignant hepatocytes limits liver cancer development', *Nature*, 479: 547-51.

Kelly, J., A. Ali Khan, J. Yin, T. A. Ferguson, and R. S. Apte. 2007. 'Senescence regulates macrophage activation and angiogenic fate at sites of tissue injury in mice', *J Clin Invest*, 117: 3421-6.

Kim, S. H., C. Beausejour, A. R. Davalos, P. Kaminker, S. J. Heo, and J. Campisi. 2004. 'TIN2 mediates functions of TRF2 at human telomeres', *J Biol Chem*, 279: 43799-804.

Kirkpatrick, J. P., N. N. Laack, H. A. Shih, and V. Gondi. 2017. 'Management of GBM: a problem of local recurrence', *J Neurooncol*.

Krishnamurthy, J., M. R. Ramsey, K. L. Ligon, C. Torrice, A. Koh, S. Bonner-Weir, and N. E. Sharpless. 2006. 'p16INK4a induces an age-dependent decline in islet regenerative potential', *Nature*, 443: 453-7.

Krishnamurthy, J., C. Torrice, M. R. Ramsey, G. I. Kovalev, K. Al-Regaiey, L. Su, and N. E. Sharpless. 2004. 'Ink4a/Arf expression is a biomarker of aging', *J Clin Invest*, 114: 1299-307.

Krizhanovsky, V., M. Yon, R. A. Dickins, S. Hearn, J. Simon, C. Miething, H. Yee, L. Zender, and S. W. Lowe. 2008. 'Senescence of activated stellate cells limits liver fibrosis', *Cell*, 134: 657-67.

Krtolica, A., S. Parrinello, S. Lockett, P. Y. Desprez, and J. Campisi. 2001. 'Senescent fibroblasts promote epithelial cell growth and tumorigenesis: a link between cancer and aging', *Proc Natl Acad Sci U S A*, 98: 12072-7.

Kucheryavykh, Y. V., L. Y. Kucheryavykh, C. G. Nichols, H. M. Maldonado, K. Baksi, A. Reichenbach, S. N. Skatchkov, and M. J. Eaton. 2007. 'Downregulation of Kir4.1 inward rectifying potassium channel subunits by RNAi impairs potassium transfer and glutamate uptake by cultured cortical astrocytes', *Glia*, 55: 274-81.

Kuilman, T., C. Michaloglou, L. C. Vredeveld, S. Douma, R. van Doorn, C. J. Desmet, L. A. Aarden, W. J. Mooi, and D. S. Peeper. 2008. 'Oncogene-induced senescence relayed by an interleukin-dependent inflammatory network', *Cell*, 133: 1019-31.

Laberge, R. M., P. Awad, J. Campisi, and P. Y. Desprez. 2012. 'Epithelial-mesenchymal transition induced by senescent fibroblasts', *Cancer Microenviron*, 5: 39-44.

Lacomblez, L., G. Bensimon, P. N. Leigh, P. Guillet, and V. Meininger. 1996. 'Dose-ranging study of riluzole in amyotrophic lateral sclerosis. Amyotrophic Lateral Sclerosis/Riluzole Study Group II', *Lancet*, 347: 1425-31.

Le, O. N., F. Rodier, F. Fontaine, J. P. Coppe, J. Campisi, J. DeGregori, C. Laverdiere, V. Kokta, E. Haddad, and C. M. Beausejour. 2010. 'Ionizing radiation-induced long-term expression of senescence markers in mice is independent of p53 and immune status', *Aging Cell*, 9: 398-409.

Lecot, P., F. Alimirah, P. Y. Desprez, J. Campisi, and C. Wiley. 2016. 'Context-dependent effects of cellular senescence in cancer development', *Br J Cancer*, 114: 1180-4.

Lee, B. Y., J. A. Han, J. S. Im, A. Morrone, K. Johung, E. C. Goodwin, W. J. Kleijer, D. DiMaio, and E. S. Hwang. 2006. 'Senescence-associated beta-galactosidase is lysosomal beta-galactosidase', *Aging Cell*, 5: 187-95.

Lin, A. W., M. Barradas, J. C. Stone, L. van Aelst, M. Serrano, and S. W. Lowe. 1998. 'Premature senescence involving p53 and p16 is activated in response to constitutive MEK/MAPK mitogenic signaling', *Genes Dev*, 12: 3008-19.

Liu, D., and P. J. Hornsby. 2007. 'Senescent human fibroblasts increase the early growth of xenograft tumors via matrix metalloproteinase secretion', *Cancer Res*, 67: 3117-26.

Liu, H., M. M. Fergusson, R. M. Castilho, J. Liu, L. Cao, J. Chen, D. Malide, Rovira, II, D. Schimel, C. J. Kuo, J. S. Gutkind, P. M. Hwang, and T. Finkel. 2007. 'Augmented Wnt signaling in a mammalian model of accelerated aging', *Science*, 317: 803-6.

Liu, Y., H. K. Sanoff, H. Cho, C. E. Burd, C. Torrice, J. G. Ibrahim, N. E. Thomas, and N. E. Sharpless. 2009. 'Expression of p16(INK4a) in peripheral blood T-cells is a biomarker of human aging', *Aging Cell*, 8: 439-48.

Lujambio, A., L. Akkari, J. Simon, D. Grace, D. F. Tschaharganeh, J. E. Bolden, Z. Zhao, V. Thapar, J. A. Joyce, V. Krizhanovsky, and S. W. Lowe. 2013. 'Non-cell-autonomous tumor suppression by p53', *Cell*, 153: 449-60.

Mallette, F. A., M. F. Gaumont-Leclerc, and G. Ferbeyre. 2007. 'The DNA damage signaling pathway is a critical mediator of oncogene-induced senescence', *Genes Dev*, 21: 43-8.

Maragakis, N. J., and J. D. Rothstein. 2006. 'Mechanisms of Disease: astrocytes in neurodegenerative disease', *Nat Clin Pract Neurol*, 2: 679-89.

Marcu, J. P., R. T. Christian, D. Lau, A. J. Zielinski, M. P. Horowitz, J. Lee, A. Pakdel, J. Allison, C. Limbad, D. H. Moore, G. L. Yount, P. Y. Desprez, and S. D. McAllister. 2010. 'Cannabidiol enhances the inhibitory effects of delta9-tetrahydrocannabinol on human glioblastoma cell proliferation and survival', *Mol Cancer Ther*, 9: 180-9.

Mark, L. P., R. W. Prost, J. L. Ulmer, M. M. Smith, D. L. Daniels, J. M. Strottmann, W. D. Brown, and L. Hacein-Bey. 2001. 'Pictorial review of glutamate excitotoxicity: fundamental concepts for neuroimaging', *AJNR Am J Neuroradiol*, 22: 1813-24.

McConnell, B. B., M. Starborg, S. Brookes, and G. Peters. 1998. 'Inhibitors of cyclin-dependent kinases induce features of replicative senescence in early passage human diploid fibroblasts', *Curr Biol*, 8: 351-4.

McGeer, E. G., and P. L. McGeer. 1998. 'The importance of inflammatory mechanisms in Alzheimer disease', *Exp Gerontol*, 33: 371-8.

Minamino, T., H. Miyauchi, T. Yoshida, Y. Ishida, H. Yoshida, and I. Komuro. 2002. 'Endothelial cell senescence in human atherosclerosis: role of telomere in endothelial dysfunction', *Circulation*, 105: 1541-4.

Minamino, T., T. Yoshida, K. Tateno, H. Miyauchi, Y. Zou, H. Toko, and I. Komuro. 2003. 'Ras induces vascular smooth muscle cell senescence and inflammation in human atherosclerosis', *Circulation*, 108: 2264-9.

Miura, T., M. P. Mattson, and M. S. Rao. 2004. 'Cellular lifespan and senescence signaling in embryonic stem cells', *Aging Cell*, 3: 333-43.

Molofsky, A. V., S. G. Slutsky, N. M. Joseph, S. He, R. Pardal, J. Krishnamurthy, N. E. Sharpless, and S. J. Morrison. 2006. 'Increasing p16INK4a expression decreases forebrain progenitors and neurogenesis during ageing', *Nature*, 443: 448-52.

Mombach, J. C., B. Vendrusculo, and C. A. Bugs. 2015. 'A Model for p38MAPK-Induced Astrocyte Senescence', *PLoS ONE*, 10: e0125217.

Morales, I., L. Guzman-Martinez, C. Cerda-Troncoso, G. A. Farias, and R. B. Maccioni. 2014. 'Neuroinflammation in the pathogenesis of Alzheimer's disease. A rational framework for the search of novel therapeutic approaches', *Front Cell Neurosci*, 8: 112.

Mucke, L., E. Masliah, G. Q. Yu, M. Mallory, E. M. Rockenstein, G. Tatsuno, K. Hu, D. Kholodenko, K. Johnson-Wood, and L. McConlogue. 2000. 'High-level neuronal expression of abeta 1-42 in wild-type human amyloid protein precursor transgenic mice: synaptotoxicity without plaque formation', *J Neurosci*, 20: 4050-8.

Munoz-Espin, D., M. Canamero, A. Maraver, G. Gomez-Lopez, J. Contreras, S. Murillo-Cuesta, A. Rodriguez-Baeza, I. Varela-Nieto, J. Ruberte, M. Collado, and M. Serrano. 2013. 'Programmed cell senescence during mammalian embryonic development', *Cell*, 155: 1104-18.

Munro, J., N. I. Barr, H. Ireland, V. Morrison, and E. K. Parkinson. 2004. 'Histone deacetylase inhibitors induce a senescence-like state in human cells by a p16-dependent mechanism that is independent of a mitotic clock', *Exp Cell Res*, 295: 525-38.

Nakamura, A. J., Y. J. Chiang, K. S. Hathcock, I. Horikawa, O. A. Sedelnikova, R. J. Hodes, and W. M. Bonner. 2008. 'Both telomeric and non-telomeric DNA damage are determinants of mammalian cellular senescence', *Epigenetics Chromatin*, 1: 6.

Narita, M., S. Nunez, E. Heard, M. Narita, A. W. Lin, S. A. Hearn, D. L. Spector, G. J. Hannon, and S. W. Lowe. 2003. 'Rb-mediated heterochromatin formation and silencing of E2F target genes during cellular senescence', *Cell*, 113: 703-16.

Nielsen, G. P., A. O. Stemmer-Rachamimov, J. Shaw, J. E. Roy, J. Koh, and D. N. Louis. 1999. 'Immunohistochemical survey of p16INK4A expression in normal human adult and infant tissues', *Lab Invest*, 79: 1137-43.

Nikitina, A. S., E. I. Sharova, S. A. Danilenko, T. B. Butusova, A. O. Vasiliev, A. V. Govorov, E. A. Prilepskaya, D. Y. Pushkar, and E. S. Kostryukova. 2017. 'Novel RNA biomarkers of prostate cancer revealed by RNA-seq analysis of formalin-fixed samples obtained from Russian patients', *Oncotarget*.

Ogryzko, V. V., T. H. Hirai, V. R. Russanova, D. A. Barbie, and B. H. Howard. 1996. 'Human fibroblast commitment to a senescence-like state in response to histone deacetylase inhibitors is cell cycle dependent', *Mol Cell Biol*, 16: 5210-8.

Ouchi, R., S. Okabe, T. Migita, I. Nakano, and H. Seimiya. 2016. 'Senescence from glioma stem cell differentiation promotes tumor growth', *Biochem Biophys Res Commun*, 470: 275-81.

Parrinello, S., J. P. Coppe, A. Krtolica, and J. Campisi. 2005. 'Stromal-epithelial interactions in aging and cancer: senescent fibroblasts alter epithelial cell differentiation', *J Cell Sci*, 118: 485-96.

Parrinello, S., E. Samper, A. Krtolica, J. Goldstein, S. Melov, and J. Campisi. 2003. 'Oxygen sensitivity severely limits the replicative lifespan of murine fibroblasts', *Nat Cell Biol*, 5: 741-7.

Ramirez, R. D., C. P. Morales, B. S. Herbert, J. M. Rohde, C. Passons, J. W. Shay, and W. E. Wright. 2001. 'Putative telomere-independent mechanisms of replicative aging reflect inadequate growth conditions', *Genes Dev*, 15: 398-403.

Ransom, B., T. Behar, and M. Nedergaard. 2003. 'New roles for astrocytes (stars at last)', *Trends Neurosci*, 26: 520-2.

Rath, B. H., J. M. Fair, M. Jamal, K. Camphausen, and P. J. Tofilon. 2013. 'Astrocytes enhance the invasion potential of glioblastoma stem-like cells', *PLoS ONE*, 8: e54752.

Ressler, S., J. Bartkova, H. Niederegger, J. Bartek, K. Scharffetter-Kochanek, P. Jansen-Durr, and M. Wlaschek. 2006. 'p16INK4A is a robust in vivo biomarker of cellular aging in human skin', *Aging Cell*, 5: 379-89.

Revett, T. J., G. B. Baker, J. Jhamandas, and S. Kar. 2013. 'Glutamate system, amyloid ss peptides and tau protein: functional interrelationships and relevance to Alzheimer disease pathology', *J Psychiatry Neurosci*, 38: 6-23.

Riemenschneider, M. J., and G. Reifenberger. 2009. 'Astrocytic tumors', *Recent Results Cancer Res*, 171: 3-24.

Robles, S. J., and G. R. Adami. 1998. 'Agents that cause DNA double strand breaks lead to p16INK4a enrichment and the premature senescence of normal fibroblasts', *Oncogene*, 16: 1113-23.

Rodier, F., and J. Campisi. 2011. 'Four faces of cellular senescence', *J Cell Biol*, 192: 547-56.

Rodier, F., J. P. Coppe, C. K. Patil, W. A. Hoeijmakers, D. P. Munoz, S. R. Raza, A. Freund, E. Campeau, A. R. Davalos, and J. Campisi. 2009. 'Persistent DNA damage signalling triggers senescence-associated inflammatory cytokine secretion', *Nat Cell Biol*, 11: 973-9.

Salminen, A., J. Ojala, K. Kaarniranta, A. Haapasalo, M. Hiltunen, and H. Soininen. 2011. 'Astrocytes in the aging brain express characteristics of senescence-associated secretory phenotype', *Eur J Neurosci*, 34: 3-11.

Schnabl, B., C. A. Purbeck, Y. H. Choi, C. H. Hagedorn, and D. Brenner. 2003. 'Replicative senescence of activated human hepatic stellate cells is accompanied by a pronounced inflammatory but less fibrogenic phenotype', *Hepatology*, 37: 653-64.

Seifert, G., K. Schilling, and C. Steinhauser. 2006. 'Astrocyte dysfunction in neurological disorders: a molecular perspective', *Nat Rev Neurosci*, 7: 194-206.

Serrano, M., A. W. Lin, M. E. McCurrach, D. Beach, and S. W. Lowe. 1997. 'Oncogenic ras provokes premature cell senescence associated with accumulation of p53 and p16INK4a', *Cell*, 88: 593-602.

Shay, J. W., and I. B. Roninson. 2004. 'Hallmarks of senescence in carcinogenesis and cancer therapy', *Oncogene*, 23: 2919-33.

Sofroniew, M. V., and H. V. Vinters. 2010. 'Astrocytes: biology and pathology', *Acta Neuropathol*, 119: 7-35.

Soroceanu, L., R. Murase, C. Limbad, E. Singer, J. Allison, I. Adrados, R. Kawamura, A. Pakdel, Y. Fukuyo, D. Nguyen, S. Khan, R. Arauz, G. L. Yount, D. H. Moore, P. Y. Desprez, and S. D. McAllister. 2013. 'Id-1 is a key transcriptional regulator of glioblastoma aggressiveness and a novel therapeutic target', *Cancer Res*, 73: 1559-69.

Stein, G. H., L. F. Drullinger, A. Soulard, and V. Dulic. 1999. 'Differential roles for cyclin-dependent kinase inhibitors p21 and p16 in the mechanisms of senescence and differentiation in human fibroblasts', *Mol Cell Biol*, 19: 2109-17.

Stobart, J. L., and C. M. Anderson. 2013. 'Multifunctional role of astrocytes as gatekeepers of neuronal energy supply', *Front Cell Neurosci*, 7: 38.

Storer, M., A. Mas, A. Robert-Moreno, M. Pecoraro, M. C. Ortells, V. Di Giacomo, R. Yosef, N. Pilpel, V. Krizhanovsky, J. Sharpe, and W. M. Keyes. 2013. 'Senescence is a developmental mechanism that contributes to embryonic growth and patterning', *Cell*, 155: 1119-30.

Takai, H., A. Smogorzewska, and T. de Lange. 2003. 'DNA damage foci at dysfunctional telomeres', *Curr Biol*, 13: 1549-56.

Tan, F. C., E. R. Hutchison, E. Eitan, and M. P. Mattson. 2014. 'Are there roles for brain cell senescence in aging and neurodegenerative disorders?', *Biogerontology*, 15: 643-60.

Tasnim, M., S. Ma, E. W. Yang, T. Jiang, and W. Li. 2015. 'Accurate inference of isoforms from multiple sample RNA-Seq data', *BMC Genomics*, 16 Suppl 2: S15.

te Poele, R. H., A. L. Okorokov, L. Jardine, J. Cummings, and S. P. Joel. 2002. 'DNA damage is able to induce senescence in tumor cells in vitro and in vivo', *Cancer Res*, 62: 1876-83.

Teismann, P., and J. B. Schulz. 2004. 'Cellular pathology of Parkinson's disease: astrocytes, microglia and inflammation', *Cell Tissue Res*, 318: 149-61.

Thornton, P., E. Pinteaux, R. M. Gibson, S. M. Allan, and N. J. Rothwell. 2006. 'Interleukin-1-induced neurotoxicity is mediated by glia and requires caspase activation and free radical release', *J Neurochem*, 98: 258-66.

Tong, X., Y. Ao, G. C. Faas, S. E. Nwaobi, J. Xu, M. D. Haustein, M. A. Anderson, I. Mody, M. L. Olsen, M. V. Sofroniew, and B. S. Khakh. 2014. 'Astrocyte Kir4.1 ion channel deficits contribute to neuronal dysfunction in Huntington's disease model mice', *Nat Neurosci*, 17: 694-703.

Toso, A., A. Revandkar, D. Di Mitri, I. Guccini, M. Proietti, M. Sarti, S. Pinton, J. Zhang, M. Kalathur, G. Civenni, D. Jarrossay, E. Montani, C. Marini, R. Garcia-Escudero, E. Scanziani, F. Grassi, P. P. Pandolfi, C. V. Catapano, and A. Alimonti. 2014. 'Enhancing chemotherapy efficacy in Pten-deficient prostate tumors by activating the senescence-associated antitumor immunity', *Cell Rep*, 9: 75-89.

Van Den Bosch, L., P. Van Damme, E. Bogaert, and W. Robberecht. 2006. 'The role of excitotoxicity in the pathogenesis of amyotrophic lateral sclerosis', *Biochim Biophys Acta*, 1762: 1068-82.

van Deursen, J. M. 2014. 'The role of senescent cells in ageing', *Nature*, 509: 439-46.

Ventura, A., D. G. Kirsch, M. E. McLaughlin, D. A. Tuveson, J. Grimm, L. Lintault, J. Newman, E. E. Reczek, R. Weissleder, and T. Jacks. 2007. 'Restoration of p53 function leads to tumour regression in vivo', *Nature*, 445: 661-5.

Volterra, A., and J. Meldolesi. 2005. 'Astrocytes, from brain glue to communication elements: the revolution continues', *Nat Rev Neurosci*, 6: 626-40.

Wang, Z., M. Gerstein, and M. Snyder. 2009. 'RNA-Seq: a revolutionary tool for transcriptomics', *Nat Rev Genet*, 10: 57-63.

Wiley, C. D., M. C. Velarde, P. Lecot, S. Liu, E. A. Sarnoski, A. Freund, K. Shirakawa, H. W. Lim, S. S. Davis, A. Ramanathan, A. A. Gerencser, E. Verdin, and J. Campisi. 2016. 'Mitochondrial Dysfunction Induces Senescence with a Distinct Secretory Phenotype', *Cell Metab*, 23: 303-14.

Wisniewski, H. M., and J. Wegiel. 1991. 'Spatial relationships between astrocytes and classical plaque components', *Neurobiol Aging*, 12: 593-600.

Wong, P. C., C. A. Pardo, D. R. Borchelt, M. K. Lee, N. G. Copeland, N. A. Jenkins, S. S. Sisodia, D. W. Cleveland, and D. L. Price. 1995. 'An adverse property of a familial ALS-linked SOD1 mutation causes motor neuron disease characterized by vacuolar degeneration of mitochondria', *Neuron*, 14: 1105-16.

Xue, W., L. Zender, C. Miething, R. A. Dickins, E. Hernando, V. Krizhanovsky, C. Cordon-Cardo, and S. W. Lowe. 2007. 'Senescence and tumour clearance is triggered by p53 restoration in murine liver carcinomas', *Nature*, 445: 656-60.

Yamazaki, Y., D. J. Baker, M. Tachibana, C. C. Liu, J. M. van Deursen, T. G. Brott, G. Bu, and T. Kanekiyo. 2016. 'Vascular Cell Senescence Contributes to Blood-Brain Barrier Breakdown', *Stroke*, 47: 1068-77.

Yao, X., S. Hrabetova, C. Nicholson, and G. T. Manley. 2008. 'Aquaporin-4-deficient mice have increased extracellular space without tortuosity change', *J Neurosci*, 28: 5460-4.

Yaswen, P., and M. R. Stampfer. 2002. 'Molecular changes accompanying senescence and immortalization of cultured human mammary epithelial cells', *Int J Biochem Cell Biol*, 34: 1382-94.

Zhou, F., S. Onizawa, A. Nagai, and K. Aoshiba. 2011. 'Epithelial cell senescence impairs repair process and exacerbates inflammation after airway injury', *Respir Res*, 12: 78.

Zhu, J., D. Woods, M. McMahon, and J. M. Bishop. 1998. 'Senescence of human fibroblasts induced by oncogenic Raf', *Genes Dev*, 12: 2997-3007.

Zindy, F., D. E. Quelle, M. F. Roussel, and C. J. Sherr. 1997. 'Expression of the p16INK4a tumor suppressor versus other INK4 family members during mouse development and aging', *Oncogene*, 15: 203-11.

Zoccolella, S., E. Beghi, G. Palagano, A. Fraddosio, V. Guerra, V. Samarelli, V. Lepore, I. L. Simone, P. Lamberti, L. Serlenga, G. Logroscino, and Slap registry. 2007. 'Riluzole and amyotrophic lateral sclerosis survival: a population-based study in southern Italy', *Eur J Neurol*, 14: 262-8.

Zou, Y., N. Zhang, L. M. Ellerby, A. R. Davalos, X. Zeng, J. Campisi, and P. Y. Desprez. 2012. 'Responses of human embryonic stem cells and their differentiated progeny to ionizing radiation', *Biochem Biophys Res Commun*, 426: 100-5.